Title
THE BEHAVIOR OF CHLORELLA FYRENOIDOSA IN STEADY STATE CONTINUOUS CULTURE

Authors
Dabes, Joseph H.
Wilke, Charles R.
Sauer, Kenneth H.

Publication Date
1970-08-01

UCRL-19958
c.2

THE BEHAVIOR OF CHLORELLA PYRENOIDOSA IN STEADY STATE CONTINUOUS CULTURE

Joseph N. Dabes*, Charles R. Wilke,
and Kenneth H. Sauer

August 1970

AEC Contract No. W-7405-eng-48

*Filed as a Ph.D. Thesis

LAWRENCE RADIATION LABORATORY
UNIVERSITY of CALIFORNIA BERKELEY

UCRL-19958
c.2

DISCLAIMER

Contents

THE BEHAVIOR OF CHLORELLA PYRENOIDOSA IN STEADY STATE CONTINUOUS CULTURE

Joseph N. Dabes, Charles R. Wilke, and Kenneth H. Sauer

Lawrence Radiation Laboratory
University of California
Berkeley, California 94720

August 1970

ABSTRACT

Chlorella pyrenoidosa was grown in steady state continuous culture. Algal growth was never limited by CO_2, minerals, pH, or temperature. The effects of the two remaining independent variables, specific growth rate and incident light intensity, on algal biomass productivity and algal physiology were examined.

It was found that optimum algal biomass productivity was obtained at a specific growth rate of approximately 1.6 day^{-1}, when the incident light intensity was 8.05 mw/cm^2. This optimum specific growth rate is not expected to change significantly as a function of incident light intensity. This optimum specific growth rate for cell biomass production results primarily from a hight light saturated rate of photosynthesis and a low amount of light transmitted through the culture.

Total chlorophyll content, chlorophyll a/chlorophyll b ratio, light saturated rate of photosynthesis, dark respiration rate, and RNA content were found to be strong functions of specific growth rate. On the other hand, maximum quantum efficiency, light saturated rate and maximum quantum efficiency of the quinone Hill reaction, and DNA content changed little, if at all, as a function of specific growth rate. Physiological changes

in the cells as a function of incident light intensity were small.

A mathematical expression for the light response curve of photosynthesis was formulated, which is consistent with both experimental data and current knowledge of the chemical kinetics of photosynthesis.

A mathematical model for the performance of optically dense algal systems, which are of interest for the mass culture of algae, is presented. This model differs from previous models, since it uses the above-mentioned light response curve to describe the local rate of photosynthesis and also accounts for changes in the physiology of the algae. This model for optically dense cultures was found to give a reasonable fit of our continuous culture experimental data, and should be useful in designing and predicting the performance of algal systems.

ACKNOWLEDGMENTS

Contributions to this work have come from many persons, and it is unfortunately possible to mention only a few. The authors gratefully acknowledge the assistance of Mr. Michael Cahn with the RNA and DNA analyses and Mr. Edward Norberg and the Forestry Department for providing and helping in the use of their spectroradiometer. We also thank Mr. Jerry Babcock for assistance in obtaining absorption spectra on the Cary 14 spectrophotometer; Mrs. Moira Ralls for help on various phases of the experimental work; Professor Roderick Park and other members of the Botany Department for helpful suggestions and advice on portions of this research; and Mr. Steven Miller, Mr. Cambell Robinson, and Mr. William Wernau for stimulating discussions on various aspects of this research. We are grateful to Drs. A. Wild and K. Egle of the University of Frankfurt, Germany, for supplying the mutant strain of Chlorella pyrenoidosa used in portions of this work.

One of the authors, J. N. Dabes, is grateful for financial support in the form of a National Institutes of Health Predoctoral Fellowship (No. 5-F01-GM-39,269) from the National Institute of General Medical Sciences.

This work was performed under the auspices of the U. S. Atomic Energy Commission.

I. INTRODUCTION

A. RESEARCH GOALS

The general objective of this research was to develop an improved kinetic model for the growth of algae, allowing optimization of design and operating conditions of mass culture algal systems. The mass culture of algae is of interest not only as a source of food or fodder. A companion study to this work is now underway evaluating the use of algae as a potential adsorbant in a process for separating radioactive metal ions, such as strontium-90, from dilute aqueous solutions. Such a large scale process would require the development of mass culture production facilities.

A complete understanding of the basic fundamentals of algal physiology and growth characteristics was the objective of this research. An understanding of these fundamentals is essential for the rational design and operation of mass culture algal systems. The specific research goals were:

1. To examine how the independent variables, specific growth rate and incident light intensity, affect the physiology of Chlorella pyrenoidosa. The algae would be grown at steady state in continuous culture. Physiological parameters examined would be:

   a. cell concentration
   b. productivity of cell material
   c. chlorophyll content
   d. chlorophyll a/chlorophyll b ratio
   e. absorption spectrum
   f. light response curve of photosynthesis
   g. light response curve of the quinone Hill reaction
   h. respiration rate in darkness
   i. cell composition by elements
   j. RNA and DNA content

2. To examine how some of the above physiological parameters respond to transients in the feed rate to the continuous culture unit.

3. To develop a mathematical model for the light response curve of photosynthesis. This model would be based upon current knowledge of the kinetics of the reactions in photosynthesis and be consistent with experimental data for the light response curve.

4. To use the above light response model to predict cell productivity performance in optically dense cultures of Chlorella pyrenoidosa. This would permit optimization of growth conditions in the dense algal systems that would be encountered in the mass culture of algae.

5. To attempt to improve productivity performance by using plant hormones and by using an algal mutant.

6. To briefly discuss some economic considerations of the mass culture of algae.

B. A BRIEF HISTORY OF PHOTOSYNTHESIS

The Early Work: Pre-1960

Man's knowledge of photosynthesis is increasing exponentially with time. For 2000 years the views of Aristotle held forth that the earth served as the stomach for plants, and that plants drew all food from the soil with their roots. Caesalpinus, during the sixteenth century, defended these Aristotelian views and explained the existence of leaves as simply protective devices for buds or fruits (Sachs, 1890).

This view was questioned only after Von Helmont grew a willow tree in a pot of soil. He removed the willow tree after it had grown to a large size and found that the soil had decreased in weight approximately 2 grams, a small fraction of the dry weight of the willow tree.

It was less than 200 years ago, in 1779, when Joseph Priestly found that the green parts of plants give off oxygen gas, the element that he had discovered 5 years earlier. Jan Ingen-Hous, in 1796, found that CO_2 is the chief carbon source for plants and that light is necessary for the fixation of CO_2 into plant material. Ingen-Hous also found that plants respire in the dark, giving off CO_2. Building upon the work of Ingen-Hous were several workers in the nineteenth century whose work led to the now-familiar overall reaction for photosynthesis in algae and higher plants:

$$CO_2 + H_2O \xrightarrow{h\nu} (CH_2O)_n + O_2 \qquad (1\text{-}1)$$

where $(CH_2O)_n$ represents sugars or carbohydrates, which are the main immediate products of photosynthesis.

Workers in the nineteenth century suspected that the chlorophyll of green plants and algae was the main pigment responsible for the conversion of light into chemical energy. Yet it was not until 1894 that Englemann proved that the intracellular particles known as chloroplasts were involved in photosynthesis. Englemann (1894) used the filamentous alga Spirogyra, aerotactic bacteria, and a narrow beam of light in a microscope. When he illuminated the spiral shaped chloroplast of Spirogyra, the aerotactic bacteria swarmed to that region, showing that oxygen was being evolved. When the narrow beam of light was used to illuminate regions of the Spirogyra cell that did not contain the chloroplast, the aerotactic bacteria showed no response, since no oxygen was evolved.

Blackman (1905) was first to propose that there were two main steps in photosynthesis, a light (photochemical) reaction and a dark (chemical) reaction. Blackman based these conclusions on experiments that showed increases in light intensity would produce increases in the rate of photosynthesis only up to a certain point. Above this point, increases in light intensity were ineffective in increasing photosynthetic rate. Furthermore, changes in temperature produced no changes in photosynthetic rate at low light

intentsities, suggesting a photochemical reaction governed in this region. But at high light intensities, the light saturated rate was greatly dependent on temperature, a result typical of ordinary chemical reactions. Blackman also suggested that these light response curves should rise in a linear fashion, abruptly bending over to the light saturated plateau. Such a sharp transition in the light response curve has been questioned by some workers, but in Chapter VI a theoretical explanation for this type of behavior will be offered.

Photosynthetic bacteria do not evolve oxygen, but require a reduced chemical species and light in order to reduce CO_2 to carbohydrate:

$$CO_2 + 2H_2D \xrightarrow{h\nu} (CH_2O)_n + H_2O + 2D \qquad (1\text{-}2)$$

where H_2D denotes an electron donor such as H_2S, thiosulfate, reduced organic compounds, or even hydrogen gas. Van Niel (1931) suggested that photosynthesis in green land plants may be exactly analogous to the above Equation (1-2) and that Equation (1-1) should be written:

$$CO_2 + 2H_2O^* \xrightarrow{h\nu} (CH_2O)_n + H_2O + O_2^* \qquad (1\text{-}3)$$

where the oxygen gas is actually formed from the oxygen atoms of the water. Van Niel proposed that the primary reaction in photosynthesis is the same in all photosynthetic organisms: a photolysis of water producing an oxidizing species, {OH}, and a reducing species, {H}. Equation (1-3) can therefore be broken down into three component equations:

$$4H_2O \xrightarrow{h\nu} 4\{H\} + 4\{OH\} \qquad (1\text{-}4)$$

$$4\{OH\} \xrightarrow{\text{dark}} O_2 + 2H_2O \qquad (1\text{-}5)$$

$$4\{H\} + CO_2 \xrightarrow{\text{dark}} (CH_2O)_n + H_2O \qquad (1\text{-}6)$$

Experimental support for Van Niel's hypothesis came when Ruben et al. (1941) found that the oxygen evolved in photosynthesis came from water rather than CO_2. By carrying out photosynthesis using O^{18}-labeled water or CO_2 it was found, by means of mass spectroscopy, that the O^{18} was present in the oxygen liberated by photosynthesis, not when the CO_2 was labeled, but only when the water was labeled.

Emerson and Arnold (1931, 1932), using Chlorella pyrenoidosa in carbonate-bicarbonate buffer, investigated the effect of short (about 10^{-5} sec) intense flashes of light. Several of their findings are important. First, they found one oxygen molecule evolved per 2500 chlorophyll molecules per flash, if the dark time between flashes was sufficiently long. Second, in order to obtain the maximum oxygen yield, the dark time separating flashes must be at least 0.02 sec at 25° C. At lower temperatures the dark time had to be longer. A Q_{10} of about 2.9 was found, which is typical of an enzymatic reaction, whereas a photochemical reaction would be expected to have a Q_{10} of zero. By this clever experimental device the existence of a photochemical "light" reaction and a chemical "dark" reaction, both of which were proposed by Blackman, were experimentally confirmed and separated. Third, with Chlorella cells that varied in chlorophyll concentrations by as much as a factor of three, and even with other species of plants (Arnold and Kohn, 1934), this basic "photosynthetic unit" of one oxygen evolved per 2500 chlorophylls per flash of light remained nearly the same. This large number of chlorophyll molecule cooperating in the evolution of a single O_2 molecule implied that most chlorophyll molecules simply act as antennas, transferring harvested energy to a species capable of chemically trapping it.

In the late 1930's Hill (1937, 1939) showed that isolated chloroplasts from leaves are capable of evolving oxygen, when an artificial electron acceptor, such as ferric oxalate, is provided along with light. If only the natural electron acceptor, CO_2, was provided

to these chlorplasts, there was neither oxygen evolution nor fixation of the CO_2 to form carbohydrates. It was nearly 20 years before Arnon et al. (1954a, 1954b) demonstrated that isolated chloroplasts were capable of fixing CO_2.

It was also during the 1930's when a controversy began over the minimum quantum requirement in photosynthesis (number of quanta of light absorbed for an O_2 molecule to be evolved, measured at low light intensities). Using Chlorella pyrenoidosa and the respirometer techniques that he had developed earlier, Warburg and co-workers found a minimum quantum requirement of only 3 or 4.* In a series of papers, Emerson and Lewis (1939, 1941, 1943) questioned Warburg's experimental techniques and results. Using Warburg's techniques, Emerson and Lewis found that a burst of CO_2 occurred just after the onset of illumination. The low quantum requirements measured by Warburg could be duplicated only if the experiment were run for a short period of time, taking maximum advantage of this transient gas burst. Since only total pressure change was followed by Warburg, it seemed he was treating this CO_2 burst as part of the oxygen evolved. By eliminating this initial transient, Emerson and Lewis found a minimum quantum requirement of about 10 quanta absorbed per O_2 evolved. Virtually all workers outside of Warburg's laboratory now believe that the minimum quantum requirement cannot be smaller than 8, based on both experimental and theoretical considerations. For some recent measurements and a review of the work to date, see Ng and Bassham (1968).

Working with Chlorella pyrenoidosa and monochromatic light, Emerson and Lewis (1943) found that the quantum requirement remained more or less the same at all wavelengths of light absorbed by Chlorella, until the wavelength of the illuminating light was increased beyond 680 nm. Beyond this point the efficiency of light utilization decreased rapidly (quantum requirement increased), even though light is absorbed by the pigment system up to and beyond

*For a review of Warburg's work, see Warburg (1948).

725 nm. This drop in quantum efficiency, often called the red drop phenomenon, became an even bigger paradox when Emerson et al. (1957) found that full efficiency could be extended beyond 680 nm, if supplementary light of short wavelength were provided along with the long wavelength light. These results suggested the existence of more than one pigment system differing in absorption of various wavelengths of light, but which must cooperate in order to obtain maximum efficiency.

During the 1950's a great deal was learned about the fixation of CO_2 in that portion of photosynthesis often referred to as the carbon fixation cycle, the Calvin cycle, or simply the "dark reactions" of photosynthesis (the last term is misleading, since many dark reactions also occur in the photo-electron transport portion of photosynthesis). Using radioactive labeled $C^{14}O_2$ Calvin and co-workers followed the path of the labeled carbon as it traversed its way through a series of 3, 4, 5, 6, and 7 carbon sugar phosphates in a cyclic manner, with glucose and other possible products being produced by the cycle. The actual CO_2 fixation step is accomplished by the enzyme carboxydismutase, which catalyzes the addition of CO_2 to 1, 5-ribulose diphosphate, resulting in the formation of two 3-phosphoglyceric acid molecules. To drive this whole cycle with the formation of sugar or carbohydrate requires the input of reducing power in the form of two NADPH and energy in the form of three ATP for each CO_2 fixed. Bassham and Calvin (1957) should be consulted for further details.

The reduction of NADP in chloroplasts as a result of the absorption of light was demonstrated by several workers in the early 1950's (Vishniac and Ochoa, 1951, 1952, Tolmach, 1951, Arnon, 1951). The other ingredient needed for the carbon fixation cycle, ATP, was shown to be produced by isolated chloroplasts by Arnon et al. (1954a, 1954b). Arnon et al. (1957, 1959) found two types of photophosphorylation, cyclic and non-cyclic. The former type is not

accompanied by oxygen evolution and undoubtedly involves an internal cycling of electrons, while non-cyclic is accompanied by oxygen evolution and the formation of NADPH from NADP.

The first success of relating photosynthesis to the morphology of the chloroplast was provided by Trebst et al. (1958), who showed that ATP and NADPH are produced at the pigment-containing membranes (lamellae or grana) in the chloroplast, while CO_2 fixation occurs in the non-membrane regions (stroma) of the chloroplast.

The Two Light Reaction Hypothesis: Post-1960

Within the past decade the amount of research in photosynthesis has accelerated greatly, but much remains to be unveiled. The mechanism of phosphorylation is still unknown, and the chemical identities of many of the components associated with the photo-electron transport system remain to be determined. Nevertheless, knowledge of the photo-electron transport system today is much greater than previous to 1960, when little was known of the events in this "light reaction" portion of photosynthesis.

A great stride was taken in 1960, when Hill and Bendall (1960) proposed the existence of two light reactions joined in a series manner. In the lamallae of chloroplasts they found two cytochromes, f and b_6, which had mid-point redox potentials of +0.36 volts and -0.06 volts, respectively.* Yet cytochrome f became oxidized and cytochrome b_6 became reduced when illumination was provided. They felt this could be best explained if there were two light reactions connected by an electron transport system that ran "downhill" from cytochrome b_6 to cytochrome f as shown in Fig. 1. It would then be reasonable to expect that a slow step in this electron transport chain would cause cytochrome f to be oxidized and cytochrome b_6 to become reduced in the light. Duysens et al. (1961), using a

*Very recent work suggests that what Hill and Bendall thought was cytochrome b_6 may actually have been cytochrome b_3. This does not affect the above arguments.

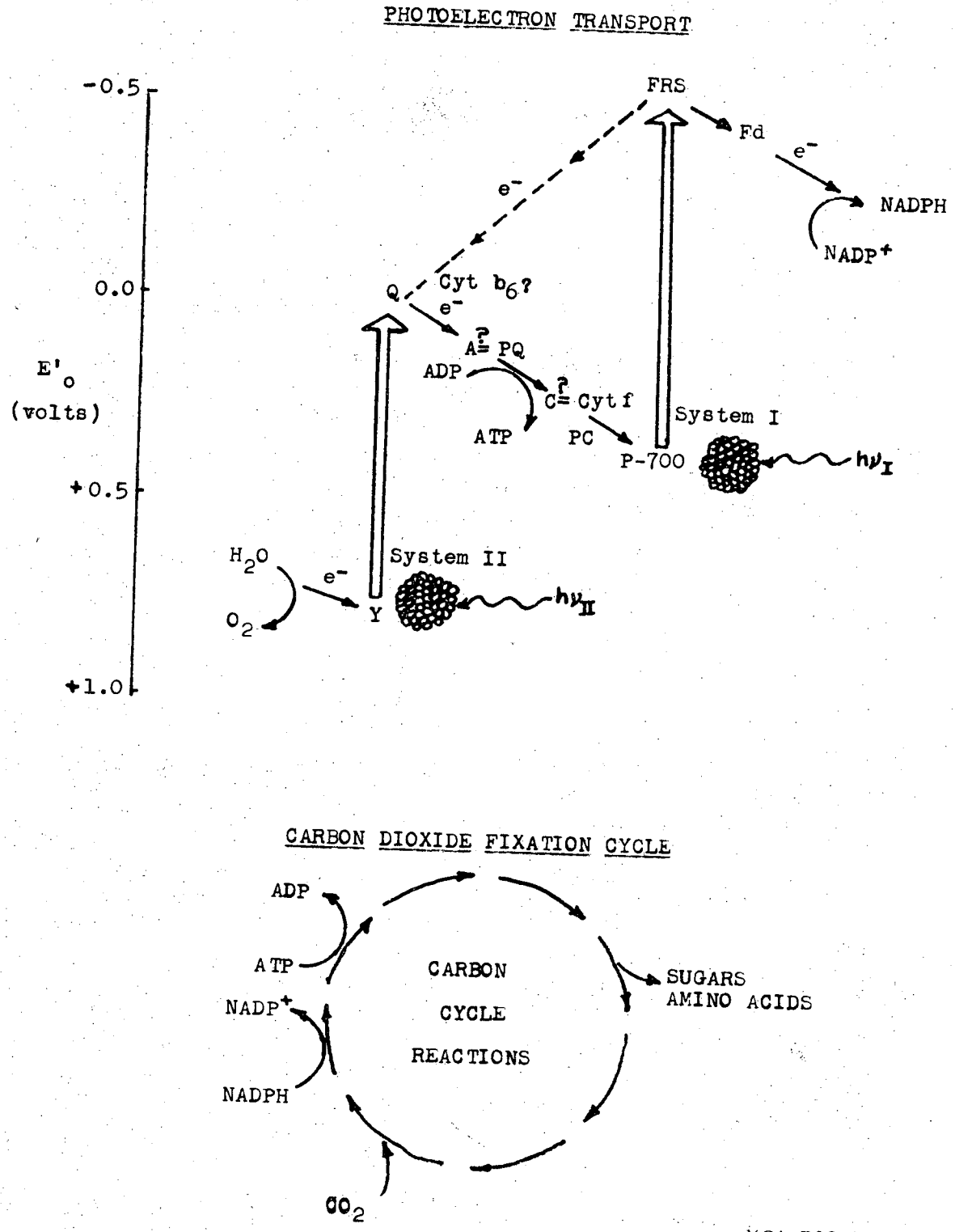

XBL 709-6504

Fig. 1. At the top of the diagram is shown the two light reaction scheme for photosynthetic electron transport. Some of the constituents are shown at their approximate mid-point redox potentials. At the bottom is a very diagrammatic representation of the carbon fixation cycle, where ATP, NADPH, and CO_2 are consumed, yielding sugars and amino acids as the main immediate products.

differential absorption spectrophotometer, found that a c-type cytochrome in the red alga Porphyridium cruentum was oxidized by long wavelength light and reduced by short wavelength light. This result was explained on the basis that this cytochrome is in the path of electron flow between two light reactions. These workers labeled the long wavelength absorbing system as System I and the short wavelength absorbing system as System II.

Figure 1 shows a generally accepted scheme for the electron transport reactions involved in photosynthesis (see, however, Knaff and Arnon (1969) for an alternative scheme involving three light reactions). The various components in the diagram are shown at their mid-point redox potentials. The energy necessary for boosting electrons against the electrochemical gradient is provided by photons absorbed by the two different photoreactions, as shown by the two heavy arrows. Light absorbed by System II results in the formation of an unknown strong oxidizing agent, Y, which is responsible for extracting electrons from water, and an unknown weak reducing agent, Q^-. Light absorbed by System I gives a strong reducing agent, FRS^-, which ultimately leads to the formation of reduced NADPH, and a weak oxidizing agent, chlorophyll P_{700}. The weak reducing agent of System II, Q^-, and the weak oxidizing agent of System I, P_{700}, are connected by a series of electron transport reactions, which give rise to ATP. All reactions are "downhill", electrochemically speaking, except for the two light reactions, which cannot proceed without energy in the form of light. The dashed line in Fig. 1 indicates the possibility of cyclic electron transport around System I, allowing the manufacture of ATP without the formation of NADPH.

Little is known of the reactions involving Y, the strong oxident produced by System II, and the evolution of oxygen, but these steps are currently being investigated by a large number of workers. Steps between the two photosystems are better known, even though the exact location of some of the cytochrome constituents is open to question. Relative pool sizes (or concentrations), equilibrium constants, and even kinetic rate constants for some of the intermediates

have been determined, mainly in the laboratories of Kok, Joliot, and Witt. Their findings are discussed in greater detail in Chapter VI, and here we will discuss only the probable identities of some of these inter-system components. Q is chemically unknown, but may, like P_{700}, be a chlorophyll *a* molecule in a special environment. Q and P_{700} appear to have similar pool sizes. A, which appears to be plastoquinone (PQ), is present at a concentration about an order of magnitude larger than P_{700} or Q. C, an intermediate just preceding P_{700} in the electron flow scheme, may well be cytochrome f or the copper-containing constituent known as plastocyanin (PC). The pool size of C is similar to the pool size of P_{700} according to Kok *et al.* (1969).

P_{700}, a special chlorophyll *a* molecule exhibiting reversible light induced absorbance changes at 700 nm, is undoubtedly the photochemical trap in the reaction center of System I. P_{700} harvests electronic excitation energy from the bulk "antenna" pigment molecules of System I. Kok (1961) discovered this pigment and showed that it is oxidized by light absorbed by System I and reduced by light absorbed by System II. Further evidence that P_{700} is located in the reaction center of System I was given by Witt *et al.* (1961), who showed that P_{700} is oxidized by System I light more rapidly than any other constituent in the photo-electron transport chain.

Recently Yocum and San Pietro (1969) have discovered what seems to be the electron acceptor for System I. This component has been given the name FRS (ferredoxin-reducing substance) and appears to consist of more than one uncharacterized molecular species.

Chlorophyll *a* is present in all oxygen-evolving photosynthetic organisms. Other pigments are also present depending on the species. For instance, chlorophyll *b* and carotenoids are present in green algae and plants, whereas blue-green and red algae contain phycocyanin and phycoerythrin. Duysens (1952) showed that these auxiliary pigments do not participate directly in photosynthesis. Duysens found that light absorbed by these accessory pigments never

shows up as fluorescence from the accessory pigments, but instead causes chlorophyll a to fluoresce. This suggests that the accessory pigments pass their harvested excitation energy to chlorophyll a. In green plants, Hind and Olson (1968) conclude that the accessory pigment chlorophyll b is either entirely or mainly associated with System II, based upon detergent fractionation studies of chloroplasts.

The morphological structures within the chloroplast lamellae have been extensively studied by Park and co-workers using the electron microscope. Park and Pon (1961) found particles of dimension 185 Å × 155 Å × 110 Å thick, appearing to be in the interior of chloroplast lamellae membranes, when the outer surface of the membrane was torn away by sonication. These particles, named quantasomes, each contain about 230 chlorophyll a and b molecules (Park and Biggins, 1964). Lamellar fragments consisting of about eight quantasomes have Hill reaction activity with DCPIP* and are able to reduce NADP. This information has led Park (1962) to suggest that the quantasome might be related to the photosynthetic unit first suggested by Emerson and Arnold (1932) on the basis of flashing light experiments. It should be recalled that about 8-10 quanta of light are needed to fix one CO_2 molecule (or release one O_2 molecule). Thus, in order to evolve one O_2 molecule in a single brief flash of light, the cooperation of 8-10 quantasomes, or approximately 2000 chlorophyll molecules, would be expected. This is similar to the 2500 chlorophylls per O_2 per flash actually obtained by Emerson and Arnold.

---

*2, 6-dichlorophenolindophenol

C. A BRIEF HISTORY OF THE WORK TOWARDS THE MASS CULTURE OF ALGAE

There is, at present, no large scale production of algae comparable to the agriculturally important land crops. Since it does not presently exist, the mass culture of algae for food or fodder cannot be discussed. We must instead direct our attention to efforts that have as their goal the mass culture of algae.

Within a few years after the end of World War II, interest developed in the possibility of culturing algae as a major food source. In the early 1950's researchers in photosynthesis, engineers, and food technologists from through-out the world were brought together at Stanford, California. These workers examined many problems associated with the mass culture of algae and the use of algae as food or a source of chemicals. The result of their work was a book edited by Burlew (1953), which even today remains the largest single treatise dealing with the cultivation and possible uses of algae.

These workers, however, found the need for more research. The mass culture of the unicellular alga Chlorella did not appear economically promising for the processes investigated by them. After this group disbanded in 1952, few of its members continued research on mass algal culture, and a period of relative inactivity in this field began. But several workers continued to be intrigued with the vast theoretical potential of algae as food, and particularly as a protein source. Tamiya (1959) presented actual performance data in the field for protein productivity. Chlorella pyrenoidosa can produce 14,000 lb of protein/acre/year, whereas the figure for a cereal such as wheat is only 269. This type of comparison is responsible for the accelerating interest today in mass algal culture. But in spite of this impressive productivity figure, the technological problems of cultivation and harvesting of unicellular algae remain formidable. These problems will be discussed in the next chapter.

Two developments since the 1950's have contributed to interest in this field. The first was the launching of the Sputnik satellite in 1957 and the resultant interest in space exploration. Here, interest has centered on using algae to set up closed ecological systems for extended manned space flights. Objectives have included using algae as both a source of oxygen and food, or as only a source of oxygen. Reviews on algae in life support systems are given by Oswald and Golueke (1964), Miller and Ward (1966), and Miller et al. (1968).

The second development was an interest in the cultivation of algae in conjunction with waste treatment, a process necessary to today's society. There are at least three ways algal culture can be tied in with waste treatment: in secondary treatment ponds fed by organic wastes, in tertiary treatment ponds for the removal of mineral nutrients such as nitrates and phosphates, or in a combined secondary-tertiary treatment process, where the objective would be to both reduce biological oxygen demand (BOD) and to remove nutrient minerals. The latter combined secondary-tertiary treatment is particularly attractive, since the bacterial degradation of the organic BOD enhances the concentration of CO_2 in the pond. Shelef et al. (1968) may be referred to for a further discussion of algal waste treatment systems.

Recent interest in the filamentous blue-green alga Spirulina has resulted from its ease of harvesting because of the mats it forms on the water's surface. Spirulina is also promising from several other stand-points. Its thin cell wall makes for good digestibility, and it has been used by natives of Lake Chad area of Africa as a protein source for an unknown number of years (Clement et al., 1967).

A recent review on the use of algae for food and fodder is given by Vincent (1969). Vincent argues that an economic process must be as simple as possible and not be concerned with such things as CO_2 enrichment and temperature control. He also points out that circulation equipment, needed to keep tiny non-floating algae such as

Chlorella in suspension, and most harvesting equipment, could be eliminated by cultivating floating filamentous algae such as Spirulina and Spirogyra.

Work in this field may be described as in the pilot plant stage. In addition to a pond of about 2/3 of an acre (10^6 liters) maintained by the Sanitary Engineering Department at the University of California at Berkeley, ponds are being designed or are operating in Czechoslovakia, Japan, and Formosa.

Much work remains to be done, both biological and technological in nature. Chlorella may not be the ideal alga; it has a low light saturated rate of photosynthesis, and its tiny size of about 5 microns leads to expensive harvesting problems. In addition to these problems, an understanding of the effect of growth conditions on the physiology and productivity of algal cultures has been largely lacking. It is hoped that this work will help to clarify this latter problem and lead to an optimization of culture conditions.

II. FACTORS AFFECTING PHOTOSYNTHETIC RATE IN ALGAE

A. A COMPARISON OF ALGAE TO THE GREEN LAND PLANTS

In this section the efficiency of converting solar energy into photosynthetic product will be considered. Also, algae will be compared with the present agricultural crops in regard to the variables that affect the efficiency of solar energy conversion. Efficiency is defined here as being equal to the heat of combustion of the plant material produced divided by the utilizable energy (380-720 nm) incident upon the plants.

Present crop production systems in agriculturally advanced areas obtain a maximum efficiency of solar energy conversion of only 2 - 2 1/2%, according to Bonner (1962). When the entire earth's surface is considered, the efficiency drops to about 0.4% (Valentyne, 1966). The conversion to edible foodstuffs is only a small fraction of this latter figure, since agriculturally important crops cover a minority of the earth's surface, and of the energy trapped by crops only a fraction is stored in the edible portions.

In contrast to the above low efficiencies, Kok (1952) found efficiencies as high as 20 - 25%* in Chlorella growing under optimum conditions in weak light. Efficiencies nearly as high have also been found in crops such as the sugar beet growing in optimum conditions. Discrepancies between these high maximum efficiences and the actual low efficiencies found in practical systems are caused by the following:

1. Lack (or oversupply) of minerals.
2. Improper pH.
3. Plant diseases or parasites.
4. Lack (or oversupply) of water.

---

*This is consistent with currently accepted figures for the quantum requirement. Assuming glucose is the product (ΔH_c = 112 kcal/mole), quanta at 600 nm, and a quantum requirement of 10 quanta/O_2 evolved, an energy conversion efficiency of 23.5% is calculated.

5. Temperature too high or too low.
6. Carbon dioxide content of the earth's atmosphere (0.03%) too low for the maximum growth of most plants.
7. Low photosynthetic efficiency at high light intensities (the light saturated rate of photosynthesis is reached at light intensities as low as 5 - 20% of direct overhead sunlight).
8. Solar energy stored in the inedible portions of plants such as roots, stems, and leaves.
9. The sun's energy striking the barren ground.

Modern agricultural techniques can control the first three items to near their optimum. Item 4 is, in many areas, a problem that requires irrigation. Items 5 and 6, temperature and CO_2 concentration, can be controlled only in enclosures such as greenhouses. No direct attempts have been made to do anything about Item 7, the light saturated rate of photosynthesis, but hopefully the recent basic research on tobacco mutants by Schmid and Gaffron (1967) will stimulate interest in this area. These workers have investigated tobacco mutants that have higher light saturated rates of photosynthesis. Item 8 deals with the inedible portions of plants; in crops such as corn this problem has been greatly reduced through plant breeding. Nevertheless, in any land crop this problem will always exist. Item 9, solar energy hitting barren ground, is a general problem with most crops before they reach full size.

Now let us examine these 9 problems as they concern the mass culture of algae. As in crops, the first 3 items are controllable. Item 4, water relations, is never a problem, except for evaporation and providing the ponds required by algae. Providing these ponds, however, is a major expense. Items 5 and 6, temperature and CO_2, may be at least partially controlled in open systems and completely controlled in closed systems. Item 7, the light saturated rate of photosynthesis, is a severe problem with Chlorella, since light saturation may be reached at light intensities as low as 5% of direct overhead sunlight. Hopefully algal strains

can be found that minimize this problem.

Item 8, dealing with inedible portions, is claimed to be one of the major advantages of algae, since they do not have roots, stems, etc. (however, some individuals, after experiencing the bitter choking taste of Chlorella, claim it to be completely inedible).

The greatest advantage of algae may be Item 9. With algal systems there is no need for solar energy to fall on barren ground during any portion of the year, except perhaps in freezing climates.

In spite of this rather promising outlook for the mass culture of algae, there has been no great rush to convert cornfields into algal ponds. There are some serious technological problems involved in algal culture; some of these problems are listed below:

1. CO_2 supply (a mass transfer problem).
2. Keeping algae in suspension.
3. Harvesting algae from dilute solution (approx. 200 ppm typical).
4. Drying algal product.
5. Large investiment cost.

The first problem involves getting CO_2 into the pond. If we rely on atmospheric CO_2, the liquid phase resistance at the pond's surface is a major barrier to CO_2 diffusing into the pond. Even if equilibrium between the concentrations of CO_2 in the atmosphere and in the pond could be maintained, many algae are limited in their growth rate by this concentration of CO_2.

The second problem is the settling of algae such as Chlorella and Scenedesmus in a stagnant pond. If there is no agitation, they will settle to the bottom and start to decay as conditions become anaerobic. In the 2/3 acre algae pond at the Sanitary Engineering Research Laboratory of the University of California at Berkeley large hydraulic pumps have been employed, usually agitating the pond twice a day, several hours at night and for a brief period just after noon. However, both the investment and operating costs of these pumps is large. Filamentous floating algae such as Spirulina would not have this problem.

The third problem, that of harvesting a very dilute suspension of tiny cells, is one of the most expensive. Both continuous centrifugation and chemical precipitation appeared to be promising to Golueke and Oswald (1965), although in terms of the economics, centrifugation appeared borderline because of power requirements and capitalization costs.

Drying the algal product is not as expensive as harvesting, but nevertheless involves difficulties stemming from the slurry-like consistency of the concentrated wet algae. This problem does not exist in agriculturally important crops such as cereals, where the crop is already dry when it is harvested.

The fifth problem is formidible. It is difficult to see how the high cost of lined ponds can be easily reduced. One approach that was mentioned in the last chapter is to combine algal culture with sewage treatment. The algae would be a by-product of sewage treatment, a process that must be carried out anyway. Also, the algae will remove some of the eutrification-causing nitrates and phosphates from the treated effluent. Since bacteria decomposing the sewage release CO_2 into the pond, the first problem listed above is to some extent solved.

B. LIMITING FACTORS

This work is concerned with the performance of the optically dense systems encountered in the steady state continuous culture of algae. Five independent variables influence the performance of such systems, CO_2 concentration, the concentrations of minerals, temperature, incident light intensity, and specific growth rate.

Carbon dioxide is, along with water, a raw material reactant in photosynthesis. It is the sole source of carbon in autotrophic photosynthetic organisms. Carbon dioxide enters photosynthesis in the carbon fixation cycle, where the enzyme ribulose-diphosphate carboxylase causes it to react with 1, 5-ribulose diphosphate yielding two molecules of 3-phosphoglyceric acid. Carbon dioxide may be a limiting factor at atmospheric levels because of the relatively

large Michaelis constant of the enzyme-CO_2 complex.

Various minerals are required for algal growth. Chlorella needs the elements nitrogen, phosphorus, potassium, magnesium, and sulfur. Also needed in trace quantities are the elements iron, calcium, boron, manganese, zinc, copper, molybdenum, and cobalt. Still in question are requirements for chlorine, sodium, and vanadium, which at least some species of algae appear to require.

These minerals are used in several possible ways by the cells. The elements nitrogen, phosphorus, and sulfur are incorporated into the building materials of the cell, proteins and nucleic acids. The other elements may be used as enzyme cofactors, in maintaining ion and osmotic balances, or bound into molecules such as hemes or coenzymes.

Some algae can grow only in a very narrow pH range, while others such as Chlorella tolerate a wide pH range. Emerson and Green (1938) examined the effect of pH on the rate of photosynthesis in Chlorella and found no detrimental effects over the pH range of 4.6 to 8.9.

Temperature has two effects. As one increases temperature, enzymes are capable of catalyzing biochemical reactions at a faster rate. This will result in a doubling or tripling of the maximum velocity of the enzyme for each 10° C increase. But in practice temperature cannot be increased without limit, since another phenomenon becomes important: enzymes usually start to become denatured and hence inactivated in the region of 30° C to 50° C. The activation energy for the inactivation of enzymes is usually much larger than the activation energy for the increase in catalysis rate.

The light incident upon photosynthetic organisms provides the energy required to drive the process of photosynthesis. The manner in which light enters into the mechanism of photosynthesis was discussed in Chapter I. Incident light intensity is one of the independent variables examined both experimentally and theoretically in later chapters.

The other major variable that this work directs itself to is specific growth rate. Specific growth rate has a profound effect on the physiology of algae i.e., how algae respond to the other four variables, CO_2, minerals, temperature, and light. The specific growth rate, μ, is simply the rate of growth of the algae: the rate of formation of new cell material per unit of cell material:

$$\mu \equiv \frac{1}{X} \frac{dX}{dt} \qquad (2\text{-}1)$$

where μ is the specific growth rate, time^{-1}; X is cell concentration, mass/volume; and t is time. In this report specific growth rate will be treated as an independent variable. As shown in the next section, the specific growth rate at steady state in continuous culture is equal to the feed rate to the culture unit divided by the culture volume:

$$\mu = \frac{F}{V} \qquad (2\text{-}2)$$

where F is feed rate, volume/time; and V is culture volume. In truth, F/V, not μ, is the independent variable, since only F or V can be physically set. But since the work in this report deals mainly with steady state continuous culture, we will treat μ as an independent variable.

C. THE KINETICS OF ALGAL GROWTH

Although this work is primarily concerned with steady state continuous culture, the batch growth of algae will be briefly considered. An inoculum of algae is placed in the culture vessel diagrammatically shown in Fig. 2. Light of constant intensity is used to illuminate one face of this rectangular culture vessel. The concentration of algae in the vessel will increase with time in a manner such as shown in Fig. 2. First, there is a lag phase when the algae are adapting to their new environment, gearing up their cellular machinery to be able to grow in this new environment.

Batch Growth: Exponential Phase

After the lag phase the cells begin to grow exponentially. Light is not limiting; in other words, the shading of cells near the back of the culture vessel by cells near the front of the vessel is negligible. A mass balance may be set up to describe the situation: the accumulation of cellular material is equal to the rate of generation of cellular material:

$$\frac{d(XV)}{dt} = \mu XV \qquad (2-3)$$

μ is proportional to the rate of photosynthesis. The rate of photosynthesis as a function of light intensity is given by a relationship such as shown in Fig. 2. This light response curve is measured on an optically thin suspension of algae where there is no appreciable shading of cells by other cells. If the incident light intensity is greater than that required to produce the light saturated rate of photosynthesis, then the algal cells are growing at their maximum specific growth rate, μ_{max}.

The definition for μ given by Equation (2-2) is obtained by rearranging Equation (2-3) applied to a constant volume of culture:

$$\mu \equiv \frac{1}{X} \frac{dX}{dt} . \qquad (2-2)$$

Since μ is constant, Equation (2-2) may be integrated. The cell concentration is found to increase exponentially with time:

$$X = X_0 \, e^{\mu t} \qquad (2-4)$$

where X_0 is the cell concentration at any arbitrary time zero during the exponential phase.

The total rate of production of new cell material, P, is simply the rate of accumulation of cellular material, mass/time:

$$P = \frac{d(XV)}{dt} = \mu XV. \qquad (2-5)$$

Note that P is directly proportional to μ, X, and V. But in the exponential phase there is an optically thin suspension, and most of

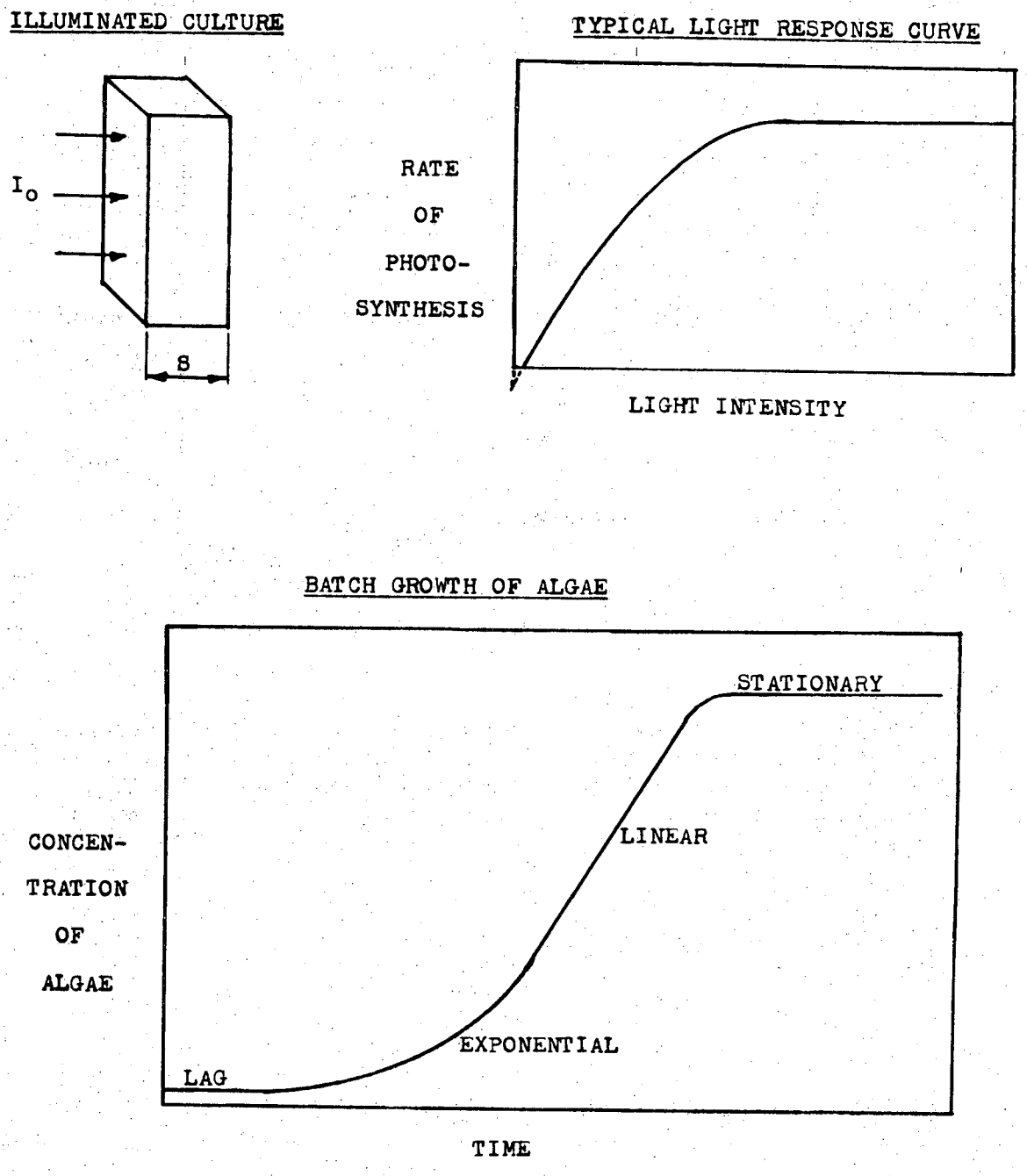

XBL 709-6505

Fig. 2. The batch culture of algae. Upper left, a diagrammatic representation of the batch culture discussed in the text. Upper right, a typical light response curve for the rate of photosynthesis as a function of light intensity for an optically thin suspension. Lower curve, the batch growth of algae as a function of time.

the light is transmitted through the culture and is wasted. It will be seen that the next phase, the linear phase, does not have this problem of wasting light.

Batch Growth: Linear Phase

The exponential phase lasts only as long as there is no appreciable shading of cells by other cells. When the suspension becomes so dense that negligible light is transmitted through the culture, a linear region of growth is entered. During this linear phase essentially all light is absorbed by the culture. The rate of increase of cell concentration is virtually independent of X, since absorption of light is virtually independent of X. A material balance gives:

$$\frac{d(XV)}{dt} = WA \qquad (2-6)$$

in which A is the illuminated surface area of the culture unit, and W is the rate of conversion of light into cell material, mass/time/area. W is approximately constant for a given incident light intensity, changing only if physiological parameters, such as the light saturated rate of photosynthesis or chlorophyll content, change. An average specific growth rate may be defined, based upon Equation (2-6):

$$\frac{d(XV)}{dt} = WA = \mu_{ave} XV \qquad (2-7)$$

$$\mu_{ave} = \frac{WA}{XV} . \qquad (2-8)$$

μ_{ave} is inversely proportional to the cell concentration, X, if W is constant. Since the cells in the culture flask are agitated, they are slowly moving around in the culture vessel. Therefore, a cell is photosynthesizing at a faster rate when near the highly illuminated front surface than when near the poorly illuminated back regions. But over a period of time, all algal cells in the vessel see approximately the same average illumination.

The production rate of cell material in the linear phase is found from Equation (2-6):

$$P = \frac{d(XV)}{dt} = WA \qquad (2-9)$$

Equation (2-9) states that P is directly proportional to the surface area, A, but is independent of V/A = S, the culture thickness. There is no analogy to this linear phase in fermentation systems, where P is always proportional to culture volume.

Batch Growth: Stationary Phase

When some essential nutrient that is required for growth has been entirely consumed, growth ceases. This essential component could be an element such as nitrogen. If more of this component were added to the culture medium, growth would resume once again.

Continuous Culture

The equations derived above for batch growth may be used for steady state continuous culture, if the accumulation term, $\frac{d(XV)}{dt}$, is replaced by the term, FX, which accounts for the algae leaving in the effluent. The steady state continuous culture situation is outlined in the diagram and equations given below:

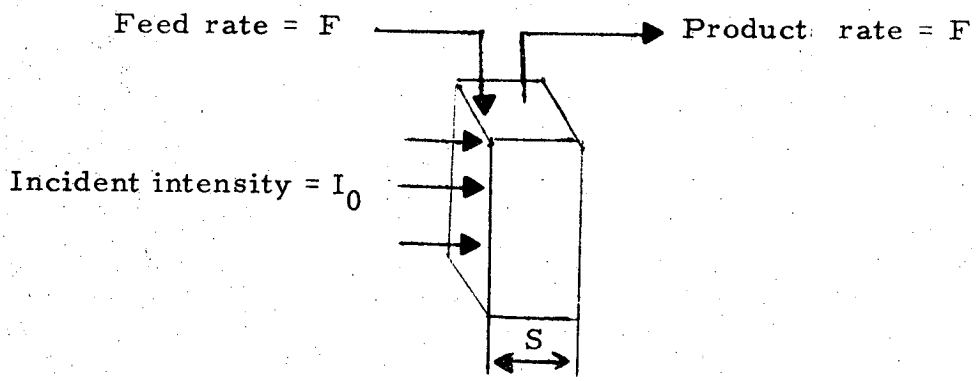

In + generation = out + accumulation

$$0 + \mu_{ave} XV = FX + 0 \qquad (2-10)$$

$$\mu_{ave} = \frac{F}{V} \text{ at steady state} \qquad (2-11)$$

where F is the feed rate to the culture unit, volume/time. Thus, μ_{ave} can be set simply by setting the feed rate to the culture unit.

At steady state the rate of production of cell material, P, is equal to the amount of cell material leaving in the effluent:

$$P = FX \tag{2-12}$$

whereas the productivity, p, is:

$$p = \frac{FX}{A} = \mu_{ave} XS \tag{2-13}$$

where S is the thickness of the culture vessel.

D. PREVIOUS WORK IN THE MATHEMATICAL MODELING OF ALGAL SYSTEMS

The effect of light intensity on dense algal systems has been examined by many workers; however, an understanding of how specific growth rate, μ*, affects algal systems is largely lacking. But before examining these two variables, a brief description of attempts at mathematically modeling the effects of CO_2, minerals, and temperature will be given.

The rate of photosynthesis as a function of carbon dioxide concentration was examined theoretically by Rabinowitch (1945, 1951, 1956), but little recent work has been reported. Using the current knowledge of the carbon fixing cycle, a re-examination of this important variable needs to be undertaken. Many workers claim that Chlorella is limited in its growth rate by the atmospheric level of CO_2. Steeman Nielsen (1955), however, claims the growth rate of Chlorella is CO_2-saturated, or nearly so, at an aqueous phase CO_2 concentration in equilibrium with that of air. The problem is complicated by the difficulty of obtaining equilibrium between gas and aqueous phases, which results from the large mass transfer resistance between the two phases.

Eyster (1967) examined the growth rate of Chlorella with respect to the concentrations of virtually all its known mineral

*Henceforth μ_{ave} will be referred to as μ; the subscript is dropped.

requirements. Shelef et al. (1968) investigated the growth rate of Chlorella as a function of nitrate concentration; a model that fell off exponentially to the maximum growth rate appeared to fit their data the best.

The effect of temperature on the growth rate of microbial systems is treated mathematically by Aiba et al. (1965). But the effect of temperature on photosynthetic systems is more complicated. Temperature has no effect on the rate of photosynthesis at low light intensities, while its effect on the light saturated rate of photosynthesis is typical of enzymatic systems. Blackman (1905) noticed this and postulated that photosynthesis consists of two separate types of reactions. At low light intensities a non-temperature dependent photochemical reaction limits the rate of photosynthesis. But at light saturation the rate of photosynthesis is limited by a temperature dependent enzymatic reaction.

Modeling the Effect of Light Intensity

Blackman (1905) suggested that the light response curve of photosynthesis could be modeled by the two straight lines shown in Fig. 3, which can be expressed mathematically as:

$$R_{O_2} = \Phi \epsilon I, \text{ when } I < \frac{S_A}{\Phi \epsilon} \qquad (2\text{-}14)$$

$$R_{O_2} = S_A, \quad \text{when } I > \frac{S_A}{\Phi \epsilon} \qquad (2\text{-}15)$$

where R_{O_2} is the rate of oxygen evolution, moles O_2/time/mass chlorophyll; Φ is the quantum yield, moles O_2/einstein of quanta; I is incident light intensity, einsteins/area/time; ϵ is the extinction coefficient of the pigments, area/mass chlorophyll; and S_A is the light saturated rate of photosynthesis, moles O_2/time/mass chlorophyll. With polychromatic light Φ, I, and ϵ are functions of wavelength.

All equations in this section, including Equations (2-14) and (2-15), apply only to optically thin suspensions of cells where there is no shading of cells by other cells. A light response curve is the

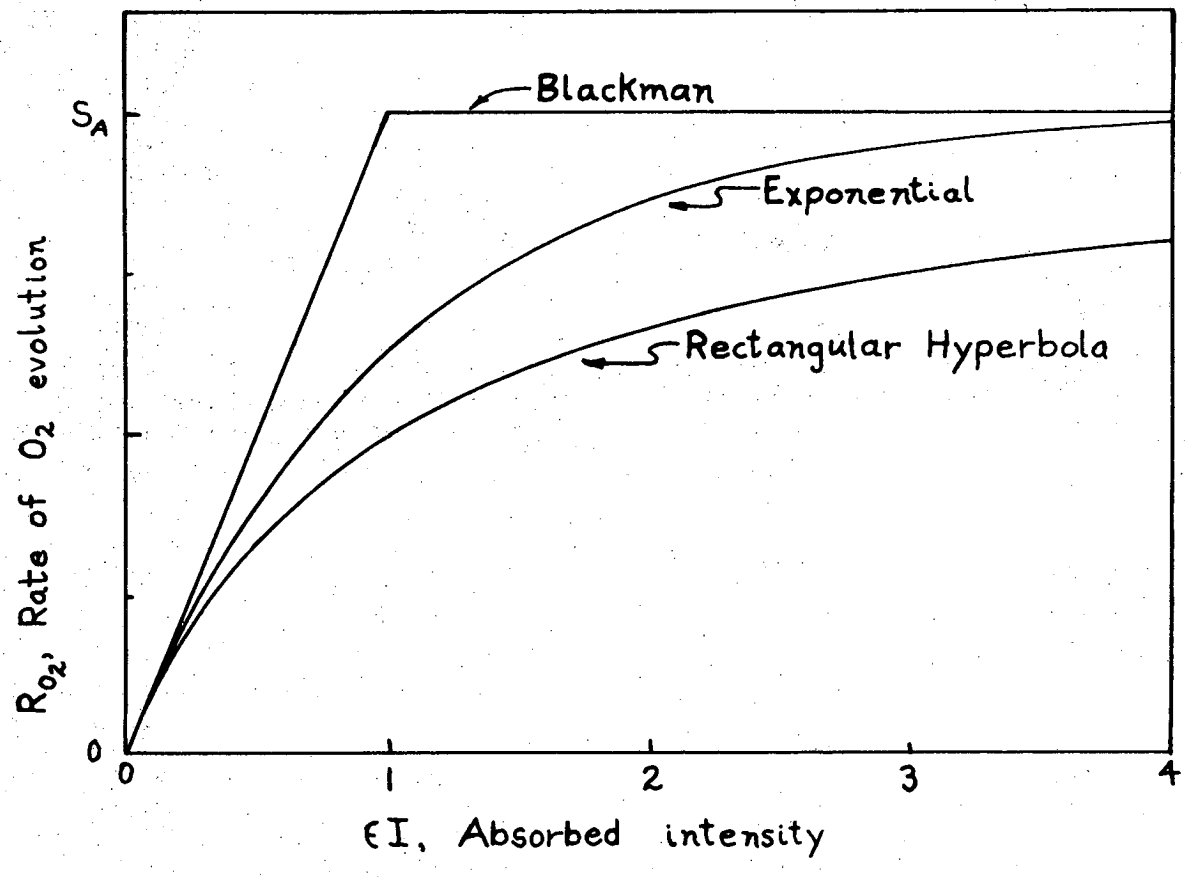

XBL 709-6506

Fig. 3. Three types of light response curves for optically thin suspensions that have been treated mathematically by the workers discussed in the text. All three models have the same initial slope, Φ, and the same saturated rate, S_A.

rate of photosynthesis as a function of light intensity and should not be measured using a dense suspension of cells, since the light intensity varies across the suspension.

Tamiya et al. (1953a) suggested that the light response curve in Chlorella could be fit by a rectangular hyperbola of the form:

$$R_{O_2} = \frac{\Phi \epsilon I S_A}{\Phi \epsilon I + S_A} . \qquad (2\text{-}16)$$

This equation is also plotted in Fig. 3. In their treatment, Tamiya et al. also examined the important case of the integrated performance of a dense suspension of Chlorella. They used the above equation for the local rate of photosynthesis and Beer's law to describe light intensity, I, as a function of distance into the culture, and then performed an integration with respect to distance into the culture. In using Beer's law, they assumed that polychromatic white light could be described by an average extinction coefficient. Even though this assumption simplifies the mathematics and is a convenient practical way of dealing with the problem in the field, it is not theoretically sound. Each wavelength of light may obey Beer's law with its own extinction coefficient, but all wavelengths cannot be described by an average extinction coefficient (the sum of a series of exponentials cannot be described by a single exponential).

The shape of the light response curve has been extensively discussed in Chapter 28 of the treatise by Rabinowitch (1951), but this work suffers from being written in an era when much less was known about photosynthesis.

Kok (1956), using Chlorella, obtained experimental data for the light response curve that could not be fit by the rectangular hyperbola of Equation (2-16), but did fit quite well an exponential function of the form:

$$R_{O_2} = S_A[1 - \exp(-\frac{\Phi \epsilon I}{S_A})] \qquad (2\text{-}17)$$

Equation (2-17) is also plotted in Fig. 3. Unlike the Blackman and hyperbolic forms, however, there is no theoretical mechanism that

can account for the form of this equation.

The performance of dense suspensions of algae was considered by van Oorschot (1955), who carried out the necessary integration for Blackman, hyperbolic, and exponential light response curves. Like Tamiya et al. (1953a), van Oorschot assumed that the attenuation of polychromatic light in a dense culture could be described by using Beer's law with an average extinction coefficient.

Lumry et al. (1959) noticed that ferricyanide Hill reaction data could be fit by the rectangular hyperbola function, as given by Equation (2-16), and developed a theoretical explanation based upon a one light reaction mechanism. It has recently been suggested by Lumry and co-workers (Muller et al., 1969) that the rectangular hyperbola function might be used to model the light response curve of overall photosynthesis. But the rectangular hyperbola function does not seem to fit most available experimental data (see Chapter VI), and its theoretical basis as derived by Lumry et al. (1959) considers only one light reaction. Today most workers believe that at least two light reactions are implicated in photosynthesis.

Fredrickson et al. (1961) used the rectangular hyperbola function for a mathematical analysis of the performance of optically dense cultures of algae. The case of a "completely stirred" culture was also considered. A "completely stirred" culture takes advantage of the so-called flashing light effect, and results in the rate of photosynthesis not being a function of distance into the culture. In a follow-up of this theoretical work, Miller et al. (1964) experimentally demonstrated an increase in photosynthetic efficiency in a highly turbulent system. Unfortunately, the enormous amount of power needed to maintain such high turbulence seems to make such a system uneconomical.

Shelef et al. (1968) obtained productivity data on Chlorella growing in steady state continuous culture at various specific growth rates. They then attempted to model this data mathematically. They assumed that respiration rate, chlorophyll content, and the light response curve did not change as a function of specific growth rate, and

did not measure these quantities experimentally. Their productivity data was then checked against theoretical predictions derived from integrating the Blackman, hyperbolic, and exponential light response curves. They concluded that the exponential function gave the best fit of their experimental data. Although Beer's law was used, an interesting innovation of these workers was to take into account the variation of extinction coefficient with wavelength of light. However, as shown by Myers and Graham (1959) and also in Chapter III, the respiration rate, the chlorophyll content, and the light response curve all change with specific growth rate, rather than remaining constant as Shelef and co-workers assumed.

A few words should be mentioned about the relationship between the dark respiration rate and the true rate of photosynthesis. Most workers assume that the true rate of photosynthesis may be found by adding the dark respiration rate to the net rate of photosynthesis, which is normally experimentally measured. This is not an entirely valid procedure, since the rate of respiration itself is a function of light intensity (Myers and Graham, 1963b, Brown and Weis, 1959, Weis and Brown, 1959, Hoch et al., 1963). But in Chlorella the assumption of a constant respiration rate does not lead to serious error, since the dark respiration rate is only about 1/20 to 1/80 of the light saturated rate of photosynthesis according to Myers and Graham (1963a) and confirmed by our own measurements in Chapter III.

Modeling the Effect of Specific Growth Rate on Algal Physiology

Algal cells growing at steady state in a chemostatically controlled system do not see the light intensity incident upon the culture vessel. Instead, as they drift around in the culture vessel, they see an average light intensity that has been determined by the specific growth rate. The higher the specific growth rate is set, the higher is the average light intensity that the cells in the culture vessel see. The algal cells respond to such changes in their environment; such

physiological quantities as chlorophyll content, dark respiration rate, and the light response curve are dependent upon the specific growth rate.

No previous work has been done on mathematically modeling the effect of specific growth rate on algal physiology. Thus such changes have not been taken into account in the mathematical modeling of the performance of algal systems. However, Myers and Graham (1959) used a chemostat to vary specific growth rate and measured chlorophyll content, dark respiration rate, and light response curves in Chlorella ellipsoidea. All of these quantities showed drastic changes. Their light response curves, which have been replotted on a per mg chlorphyll basis, are shown in Fig. 4. The advantages of plotting such data on a chlorophyll basis are discussed in Chapter IV.

It is unfortunate that many researchers in the field of photosynthesis do not precisely control the growth conditions of their plant or algal material. This undoubtedly confuses the comparison of photosynthetic data taken in different laboratories, or even between data taken on different days within a single laboratory. The usual practice is to grow algae in batch culture, taking sample suspensions as they are needed. Specific growth rate changes with time in a batch culture; the physiology of the algae is therefore changing with time. Continuous culture is the only way that one can hope to attain a constant, reproducible, unchanging supply of algae.

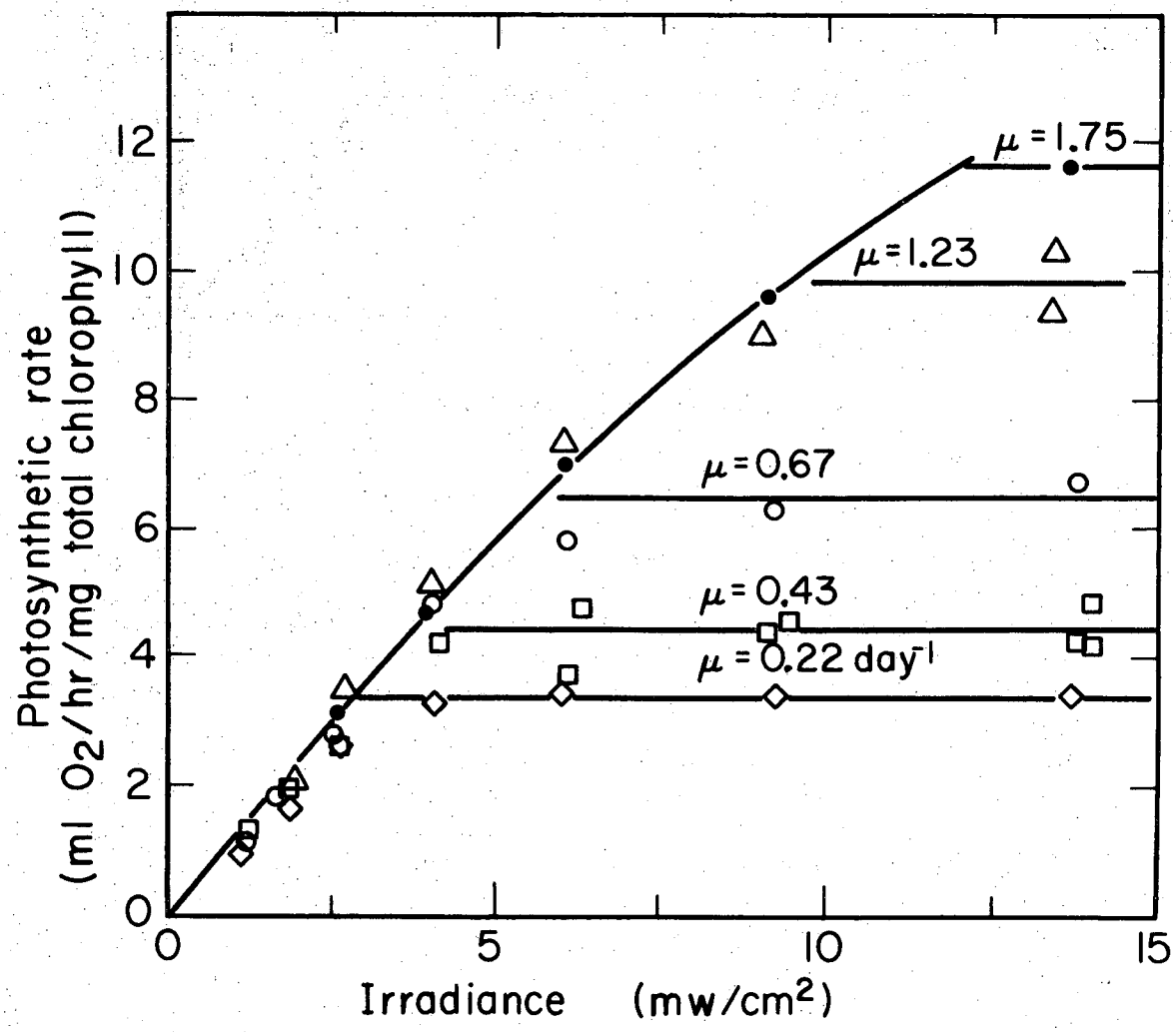

XBL698-3636

Fig. 4. Light response curves of Myers and Graham (1959). Chlorella ellipsoidea were grown in continuous culture at 25° C at the steady state specific growth rates, μ, as shown in the figure. The points shown were not directly given by Myers and Graham, but were calculated using Fig. 8 and Table II of their paper.

NOMENCLATURE

A	=	Illuminated surface area
F	=	Feed rate, volume/time
I	=	Light intensity, einsteins/area/time
p	=	Productivity of cell material, mass/area/time
P	=	Production of cell material, mass/time
R_{O_2}	=	Rate of oxygen evolution, moles O_2/time/mass chlorophyll
Q_{10}	=	The ratio of process rates at temperatures 10° C apart
S	=	Thickness of an algal culture
S_A	=	The light saturated rate of photosynthesis, moles O_2/Time/mass chlorophyll
t	=	Time
V	=	Volume of algal culture
W	=	Rate of formation of cell biomass, mass/area/time
X	=	Cellular biomass concentration, mass/volume
X_0	=	Cellular biomass concentration at time zero, mass/volume
ΔH_c	=	Heat of combustion, kcal/mole
ϵ	=	Extinction coefficient of the pigments, area/mass chlorophyll
μ	=	Specific growth rate, $time^{-1}$
μ_{ave}	=	Average specific growth rate, $time^{-1}$
μ_{max}	=	Maximum specific growth rate, $time^{-1}$
Φ	=	Maximum quantum yield, moles O_2/einstein

III. EXPERIMENTAL WORK

A. CONTINUOUS CULTURE UNIT

All experimental data were taken using bacteria-free algae grown in the continuous culture unit described below.

Equipment

A schematic flow diagram of the equipment is given in Fig. 5. None of the equipment that needed to be sterilized was fixed in place, and all such equipment was sterilized by autoclaving or dry heat. Heat resistant silicone tubing was used for all flexible connections.

The 20 liter feed bottle was devised to be a constant head device as shown on the flow diagram. A vacuum continuously withdrew a small bleed of air from the air space at the top of the feed bottle. This air was replaced through another line, which was open to the atmosphere. Because this latter line had negligible pressure drop from one end to the other, both ends were at atmospheric pressure. When a time switch opened the valve between the feed tank and burette, the liquid level in the burette eventually reached exactly the same level as the point where air was released into the feed bottle. Thus, the level to which the burette filled always remained the same, being completely independent of the nutrient level in the feed bottle.

When the burette was dumped by the time switch, the nutrient level in the burette declined into the capillary tubing beneath the burette. The level within the capillary was approximately the same as the level in the culture vessel, but fluctuations were not important, since the capillary contained negligible volume. Thus, an exact volume of nutrient was released at regular intervals, yielding an extremely stable feed rate, which could be maintained constant for many weeks.

Air containing 4% CO_2 flowed into the culture unit at a rate of 0.4 standard cubic feet/hour. It was sterilized by passing it through

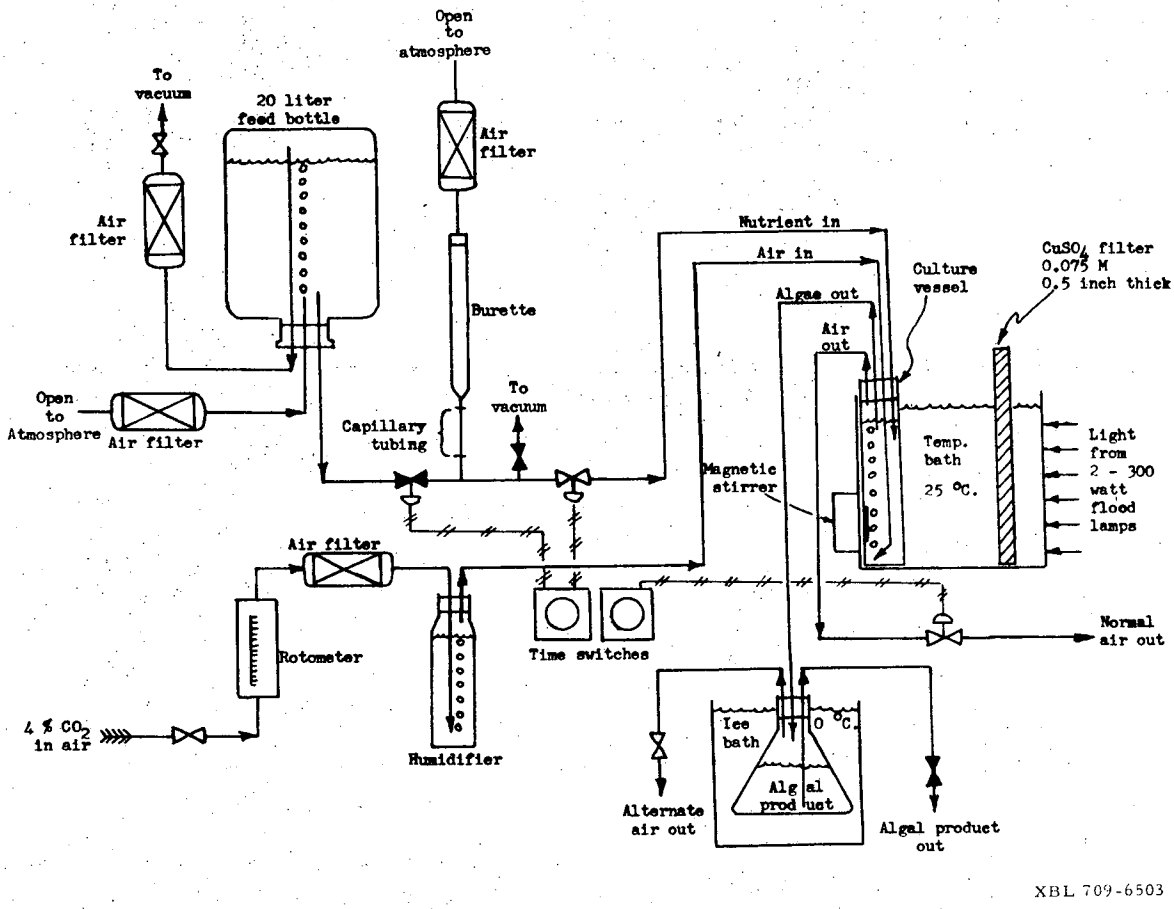

Fig. 5. Flow diagram of the continuous culture unit used to grow the algae for the experiment described in this chapter.

a packed glass wool filter and humidified by bubbling through water.

The culture vessel itself was rectangular (9.1 cm wide × 19.9 cm high × 2.8 cm thick) and held about 500 ml of liquid culture. The sides and bottom of the flask were platinum plated to prevent scattered light from escaping at the edges. The front and the back of the vessel were completely transparent. A magnetic stirrer at the back of the vessel helped to break up air bubbles and provided agitation. The culture vessel was suspended in a 25° C constant temperature bath.

Illumination was normally provided by two 300 watt reflector flood lamps connected to a rheostat and a constant voltage transformer. The light passed through 1.28 cm of a 0.075 M $CuSO_4$ solution as well as 28 cm of temperature bath water. These filters absorbed most of the infrared radiation. The amount of radiation reaching the culture vessel was checked daily with a Model 65 YSI-Kettering radiometer. If necessary, the rheostat was adjusted to keep incident radiation constant.

There were two exit streams from the culture vessel. Normally, air would leave from near the top of the culture vessel. However, at intervals determined by a time switch, a solenoid valve would close this line, forcing algae suspension out the line that is labelled "algae out" in Fig. 5. Once the algae suspension level fell below the entrance of the take-off line, air would start leaving through this line, purging the line of all liquid. After a fixed time the solenoid valve would open, and air would exit in the normal fashion. This type of algal take-off system had two advantages. First, settling of algal cells in the liquid take-off line was never a problem, since the line was purged with air after the algal product was collected. Second, since air and liquid were not continuously withdrawn through a single line, the problem of foaming was greatly minimized. Foaming can cause an increase in the concentration of cells in the effluent liquid as compared to the concentration in the

culture vessel. An anti-foam agent was also used to combat this latter problem.

The algal product was collected in a darkened ice bath. Here algae were sometimes maintained for short periods (as long as 8 hours) before they were used in the various analyses and experiments described later in this chapter.

Growth Conditions

Growth conditions insured the temperature, minerals, pH, or CO_2 never limited growth. Only light intensity ever limited the growth rate of, and determined physiological changes in, the algal cells. But in the optically dense cultures considered here, the algal cells receive varying intensities of illumination as they move around in the culture vessel. Thus, light intensity received by the algal cells is not a variable that can be independently specified for dense systems. In fact, even average light intensity cannot be specified. Instead, this limitation by light is determined at steady state by specific growth rate and incident light intensity, which are independent variables. Examination of the effects of these two variables on the physiology of Chlorella pyrenoidosa is the purpose of the experiments described in this chapter.

The temperature of the culture unit was maintained at 25° C by the constant temperature water bath. This is the optimum temperature of growth for Chlorella pyrenoidosa.

No attempt was made to control pH in the culture vessel. Nevertheless, the pH remained in the fairly narrow range of 6.6 to 7.4. Emerson and Green (1938) found that pH, over the range of 4.6 to 8.9, had no effect upon the rate of photosynthesis in Chlorella pyrenoidosa.

The composition of the nutrient medium is given in Table 1. The nutrient medium is from Myers (1963) with three changes: the addition of an anti-foam agent, the addition of vanadium to the trace

Table I. Chlorella Nutrient Medium*

The following components are mixed with distilled water without adjusting pH;

KNO_3	5.0 gm/l
$MgSO_4 \cdot 7H_2O$	2.5 gm/l
KH_2PO_4	1.25 gm/l
Trace solution	5.0 ml/l
Antifoam-Union Carbide Y-4988	0.2 ml/l

The trace solution is made as follows:

EDTA	100.0 gm/l
$CaCl_2$	16.8 gm/l
H_3BO_3	22.8 gm/l
$FeSO_4 \cdot 7H_2O$	10.6 gm/l
$ZnSO_4 \cdot 7H_2O$	17.6 gm/l
$MnCl_2 \cdot 4H_2O$	2.8 gm/l
MoO_3 (as ammonium molybdate)	1.4 gm/l
$CuSO_4 \cdot 5H_2O$	3.2 gm/l
$Co(NO_3)_2 \cdot 6H_2O$	1.0 gm/l
V_2O_5 (dissolved in HCl)	0.6 gm/l

After adding all trace components, the pH of the trace solution is adjusted with KOH pellets to the range of 6.5-6.7.

*Modified from Myers (1963).

solution, and an increase in the nitrate concentration. This composition should support growth up to about 10 grams dry weight/liter before nitrogen becomes limiting.

CO_2 was provided at a level of 4% in air. This concentration was more than sufficient to insure that CO_2 never limited.

Illumination was continuous, 24 hours per day. The spectral distribution of the light incident on the culture flask is given in Fig. 6. as measured by an ISCO Model SR spectroradiometer. The incident light intensity was maintained at 8.05 mw/cm^2 (from 380-720 nm) unless otherwise stated. 8.05 mw/cm^2 is roughly equivalent to 20% of overhead solar radiation between 380 and 720 nm.

B. RESULTS AT STEADY STATE: EFFECT OF SPECIFIC GROWTH RATE ON THE PHYSIOLOGY OF CHLORELLA PYRENOIDOSA

In this section algae that have adapted to a particular specific growth rate, μ, are examined with respect to a number of characteristics. Measurements were performed as rapidly as possible to insure that negligible re-adaptation took place. The transient data taken in Section D of this chapter show how slowly the cells re-adapt to a new environment.

After changing feed rate to the culture vessel, one week was sufficient to reach physiological steady state at the higher specific growth rates, but as long as four weeks was needed at the lower specific growth rates.

Productivity

At steady state Equation (2-13) gives the productivity, p:

$$p = \frac{FX}{A} \qquad (2\text{-}13)$$

where F is the nutrient feed rate, X is the cell concentration, and A is the illuminated surface area. Figure 7 shows productivity plotted as a function of specific growth rate, μ. The cell concentration

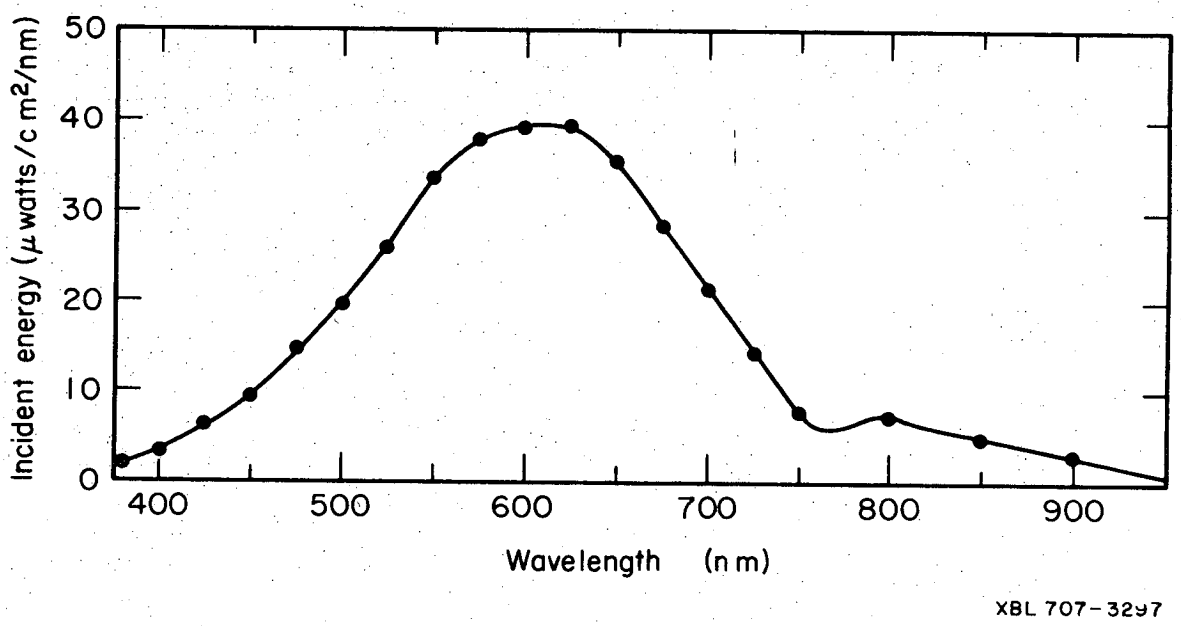

Fig. 6. The spectral energy distribution of the light reaching the front face of the culture vessel. The total energy in the region active in photosynthesis (380-720 nm) equals 8.05 mw/cm^2.

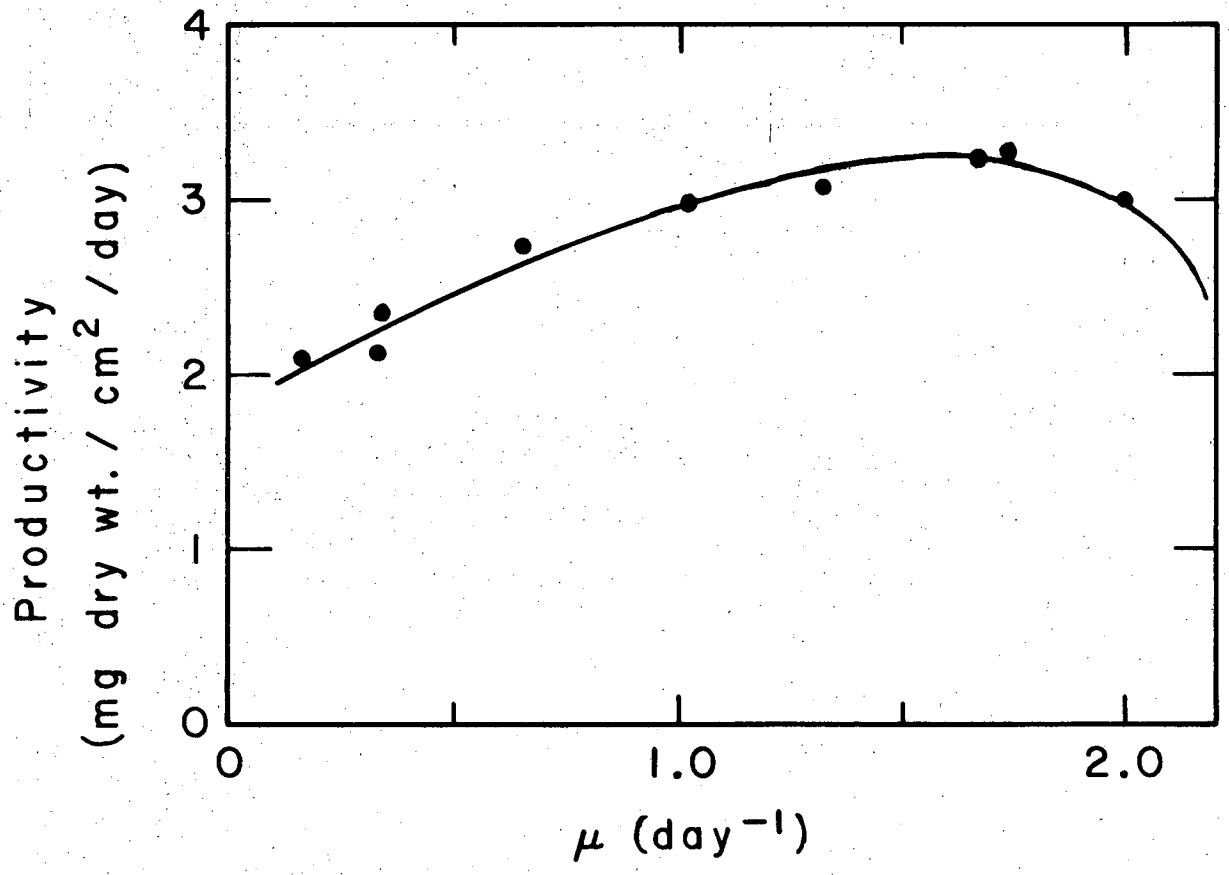

XBL695-2710

Fig. 7. Productivity of Chlorella pyrenoidosa in continuous culture as a function of the steady state specific growth rate, μ. Data were taken at 25°C. Incident intensity was 8.05 mw/cm^2. Washout occurs when $\mu = 2.3$ day^{-1}.

data used to calculate productivity are plotted in Fig. 8.

Figure 7 shows that productivity is optimum when $\mu = 1.6\,day^{-1}$. Productivity falls off at higher values of μ because of the increase in transmitted light shown in Fig. 9. Light not absorbed cannot be converted into cell material. In fact, when $\mu = 2.3\ day^{-1}$, washout is reached, since F/V has exceeded the maximum growth rate of the cells. At washout, cell concentration and productivity drop to zero. Productivity also falls off at values of μ smaller than $1.6\ day^{-1}$. This fall-off cannot be explained by light transmission since Fig. 9 shows there is none in this region. This drop in productivity, however, can be explained as caused by a decrease in the light saturated rate of photosynthesis. This point will be discussed more extensively later.

But even at the optimum productivity of 3.25 mg dry weight/cm^2/day, which occurs at $\mu = 1.6\ day^{-1}$, inefficiencies result from light saturation of the highly illuminated cells near the front of the culture vessel. At this optimum μ the quantum requirement is 18.3 quanta absorbed per O_2 evolved, and the efficiency of converting light energy into cell material is approximately 10.7%. These numbers are calculated and discussed more extensively in Chapter VIII.

Total Chlorophyll Content

Figure 10 shows how the steady state chlorophyll content varies with μ. The change is quite drastic and is of great importance to the physiology of the cells, since chlorophyll is the main light harvesting pigment. Considering an optically thin layer of cells, light absorption is directly proportional to chlorophyll content.

The trend of chlorophyll content shown in Fig. 10 has been found by other workers working both with batch and continuous cultures (Tamiya et al., 1953b, Myers and Graham, 1959, Belyanin and Kovrov, 1968). The chlorophyll assay was based upon the procedure of Arnon (1949), but added a hot methanol extraction of the cells to insure complete removal of chlorophyll. The procedure is completely

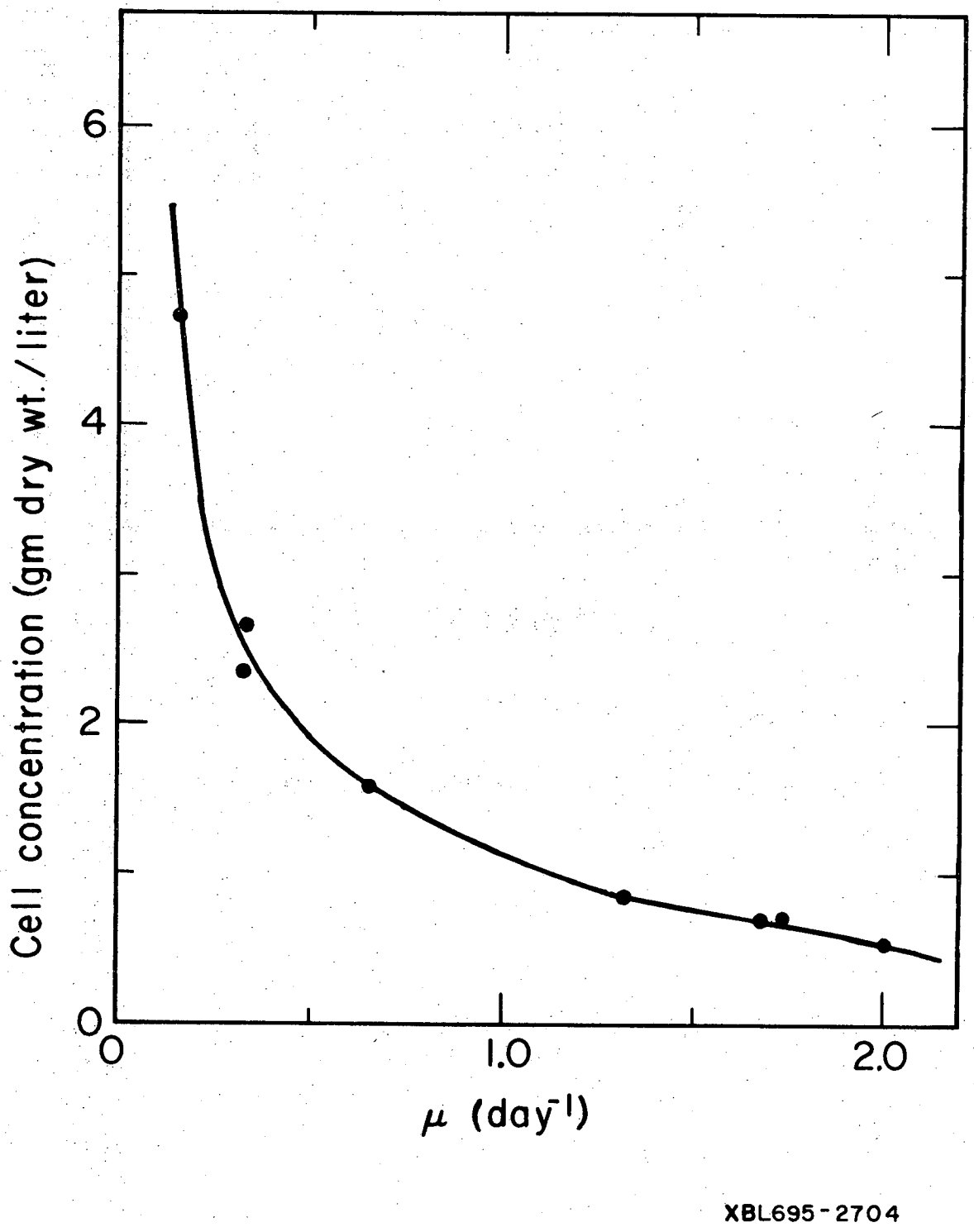

Fig. 8. Cell concentration as a function of steady state specific growth rate.

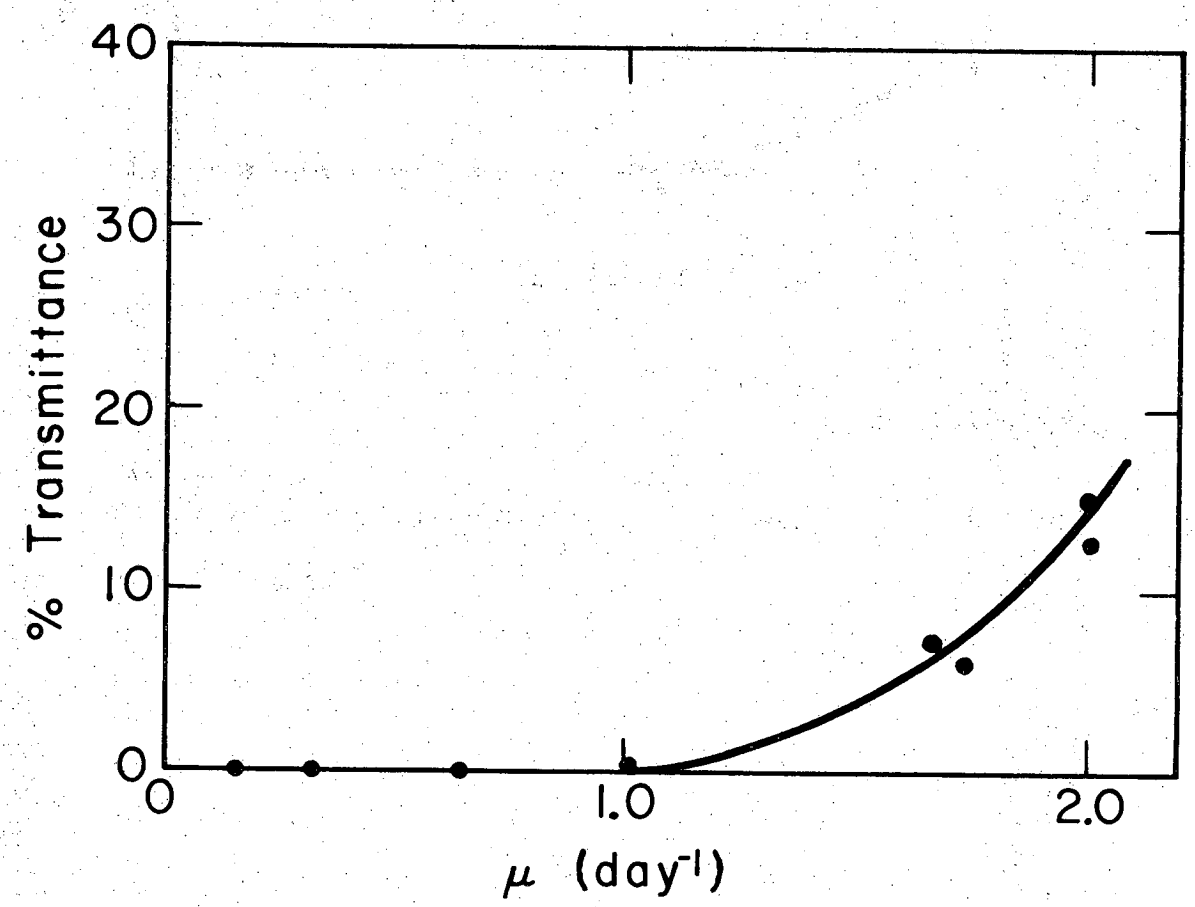

XBL695-2702

Fig. 9. % transmittance versus specific growth rate.

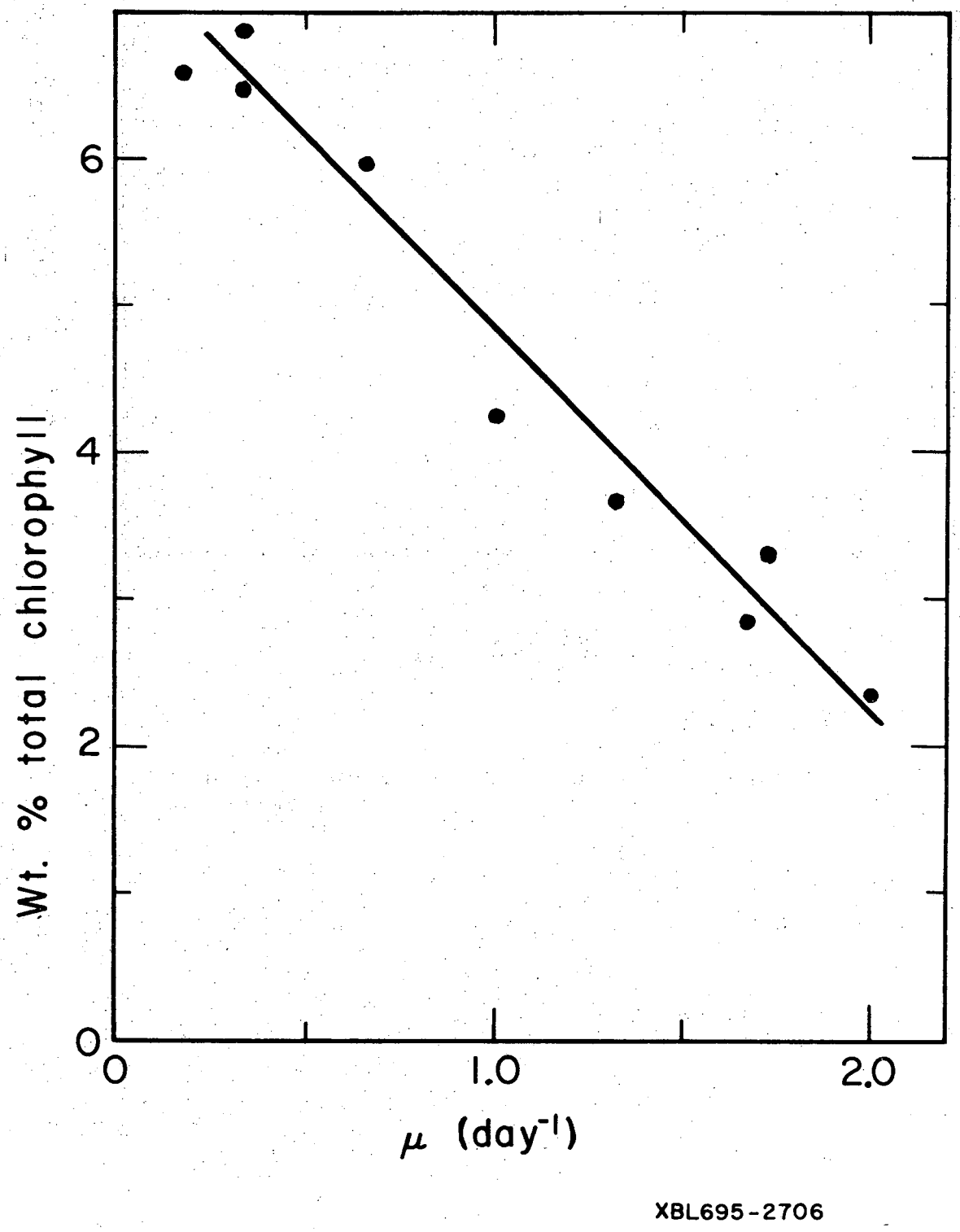

Fig. 10. Total chlorophyll content versus specific growth rate.

described in Appendix IV.

Chlorophyll a/Chlorophyll b Ratio

Although the chlorphyll a/chlorophyll b ratio does not change as drastically as total chlorophyll content, there is a definite trend in this ratio, as shown in Fig. 11.

Absorption Spectra

Figure 12 shows the absorption spectra for two types of cells, one grown at a high specific growth rate, and the other at a low specific growth rate. The curves were measured in a Cary 14 spectrophotometer with a Model 1462 scattered-transmission accessory. The curves were then adjusted in two ways to give Fig. 12. First, the absorbance measured at 750 nm was uniformly subtracted from the measured absorbance at all other wavelengths. This was done in an attempt to subtract light scattering; there is no absorption by any pigments at 750 nm. Second, the curves were adjusted to give the same absorbance at 680 nm, the chlorphyll a peak.

The high μ cells have a lower shoulder at 650 nm, the chlorophyll b peak, than the low μ cells. This agrees with the change in chlorophyll a/chlorophyll b ratio.

Light Response Curves

A light response curve is simply the rate of photosynthesis, with dark respiration rate added, plotted as a function of light intensity for optically thin suspensions of algae. All data presented here were taken in an illuminated respirometer using the procedure outlined in Appendix IV. The respirometer flasks contained a suspension of algal cells that had 4.2 μg total chlorophyll per cm^2 of illuminated area. The spectral distribution of the respirometer light source is shown in Fig. 13. It is very similar to the spectral distribution of the light source used to illuminate the culture vessel, which was given in Fig. 6. Both light sources used tungsten lamps

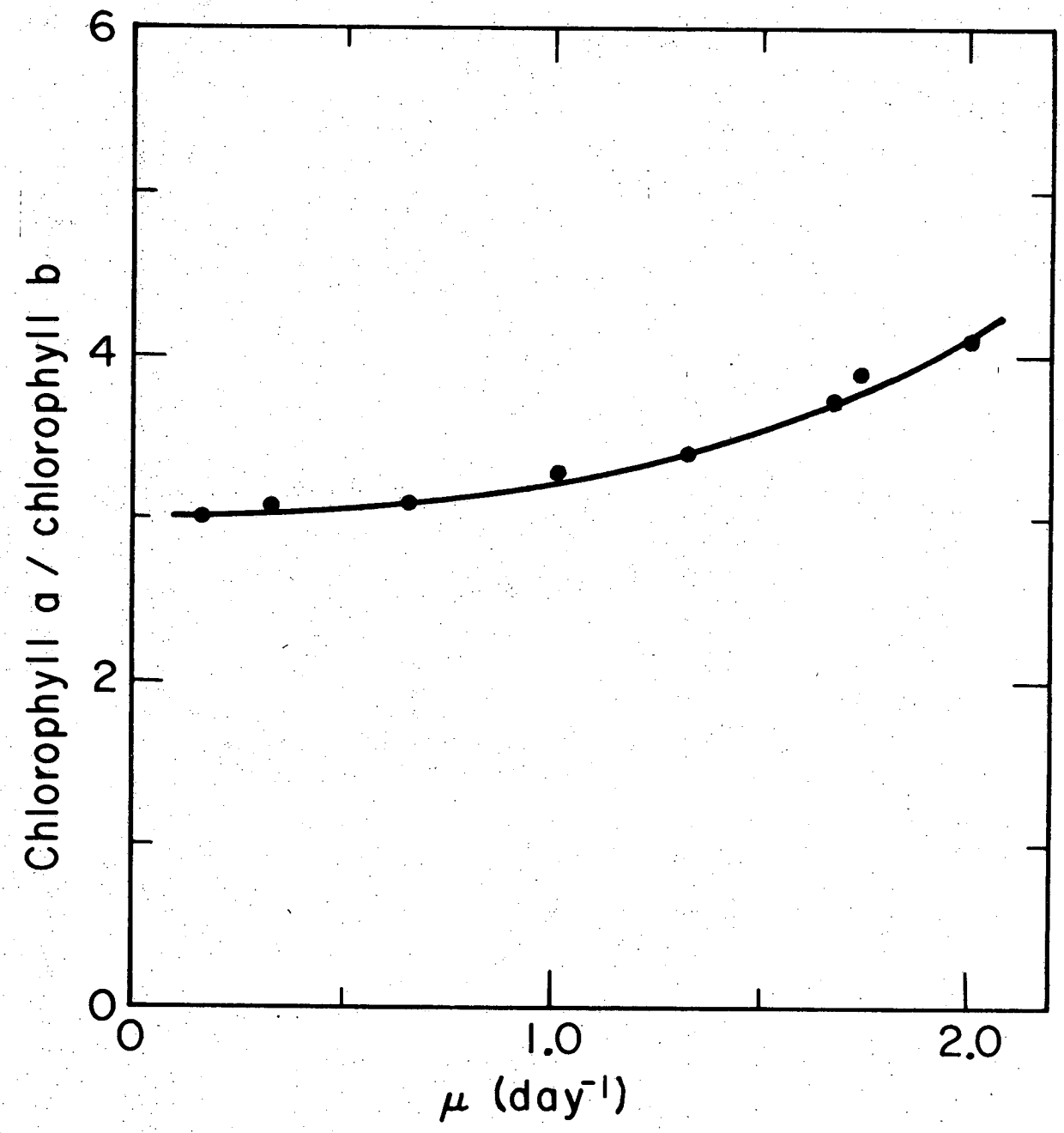

XBL695-2705

Fig. 11. Chlorophyll a/chlorphyll b ratio versus specific growth rate.

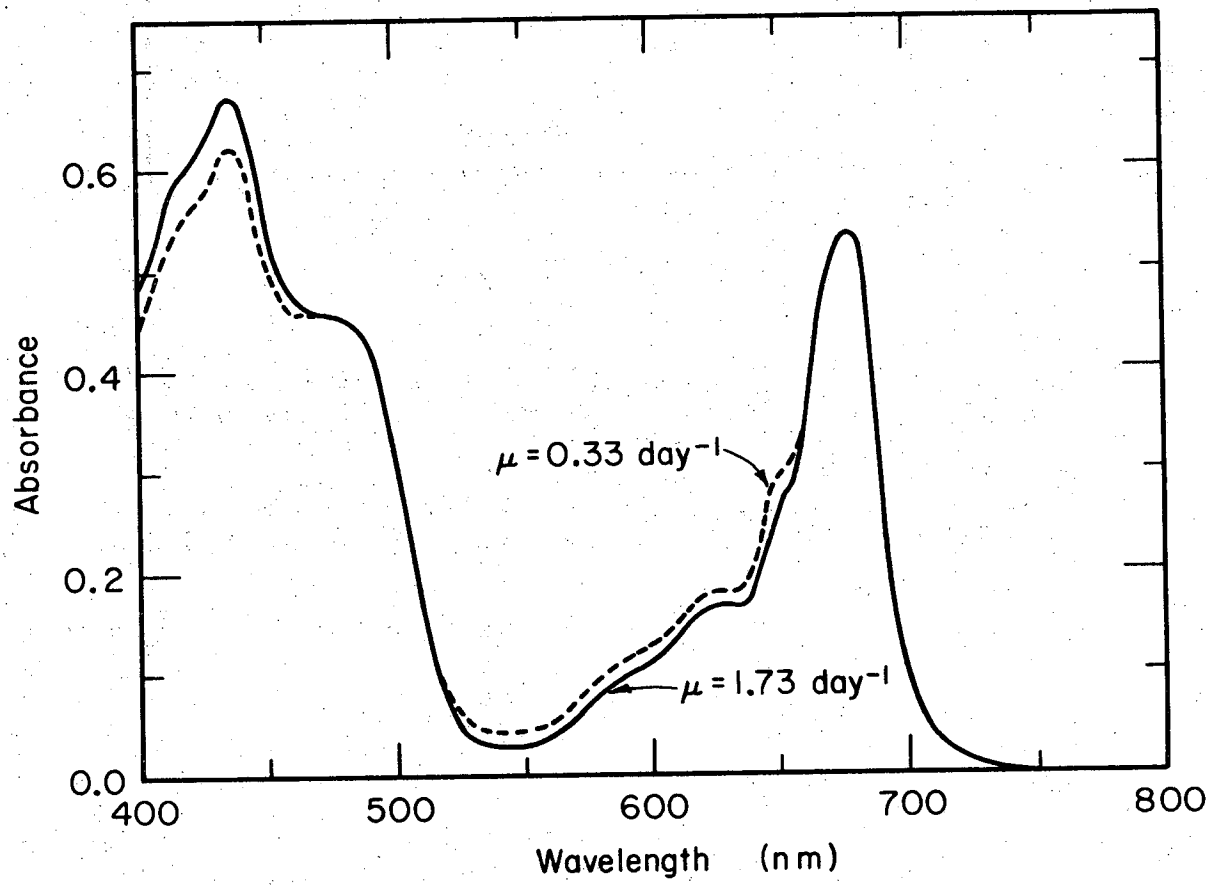

Fig. 12. Absorbance for algae grown at two different specific growth rates as a function of wavelength. The curves were adjusted to subtract out light scattering at 750 nm and to give the same absorbance at 680 nm, the chlorophyll a peak. For the curves as given: $\mu = 0.33\ day^{-1}$ has $14.4\ \mu g/cm^2$ of total chlorophyll, while $\mu = 1.73\ day^{-1}$ has $13.6\ \mu g/cm^2$ of total chlorophyll.

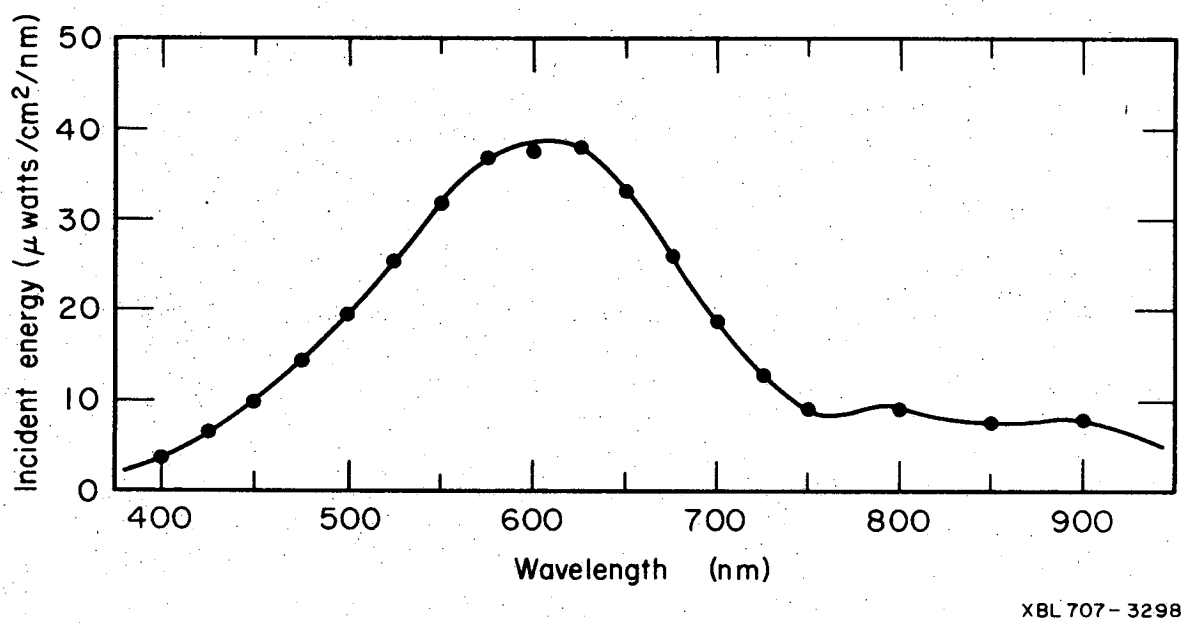

Fig. 13. The spectral distribution of the light reaching the bottom of the respirometer flasks.

and identical $CuSO_4$ solutions for removal of infrared radiation.

Light response curves are here plotted on a chlorophyll basis, since on a chlorophyll basis the quantum efficiencies of different types of algae may be directly compared. Quantum efficiency may be generally defined as the ratio of the rate of photosynthesis to the rate of light absorption. For optically thin suspensions the rate of light absorption is directly proportional to light intensity and nearly directly proportional to total amount of chlorophyll. At any given light intensity, the ratio of photosynthetic rates is also the ratio of quantum efficiencies, if the chlorophyll contents are the same.

In Fig. 14, light response curves for algae grown at two widely different specific growth rates are plotted. The experimental procedure, as outlined in Appendix IV, was to take algae from the steady state culture unit and run the light response curves in the respirometer as quickly as possible so that little re-adaptation of the algal cells could occur. The results shown in Fig. 14 are typical of those obtained at other specific growth rates in that:

1. The rates of photosynthesis at low light intensities were not a function of the specific rate of growth, μ.

2. The rates of photosynthesis at high light intensities were strong functions of the specific rate of growth, μ. The manner in which the light saturated rate changes as a function of μ is shown in Fig. 15. Note that the light saturated rate seems to increase linearly with μ.

3. The approach to light saturation occurred relatively sharply. The rectangular hyperbola function, as given by Equation (2-17), has been used by many workers to model light response curves. This function gives a straight line on a double reciprocal plot, such as Fig. 16, where the data given in Fig. 14 have been replotted. Our data do not give such a straight line, therefore, cannot be fit by the rectangular hyperbola function. Equations (6-17) and (6-18), which are derived in Chapter VI, are the solid lines shown in Figs. 14 and 16, and do fit the data quite well.

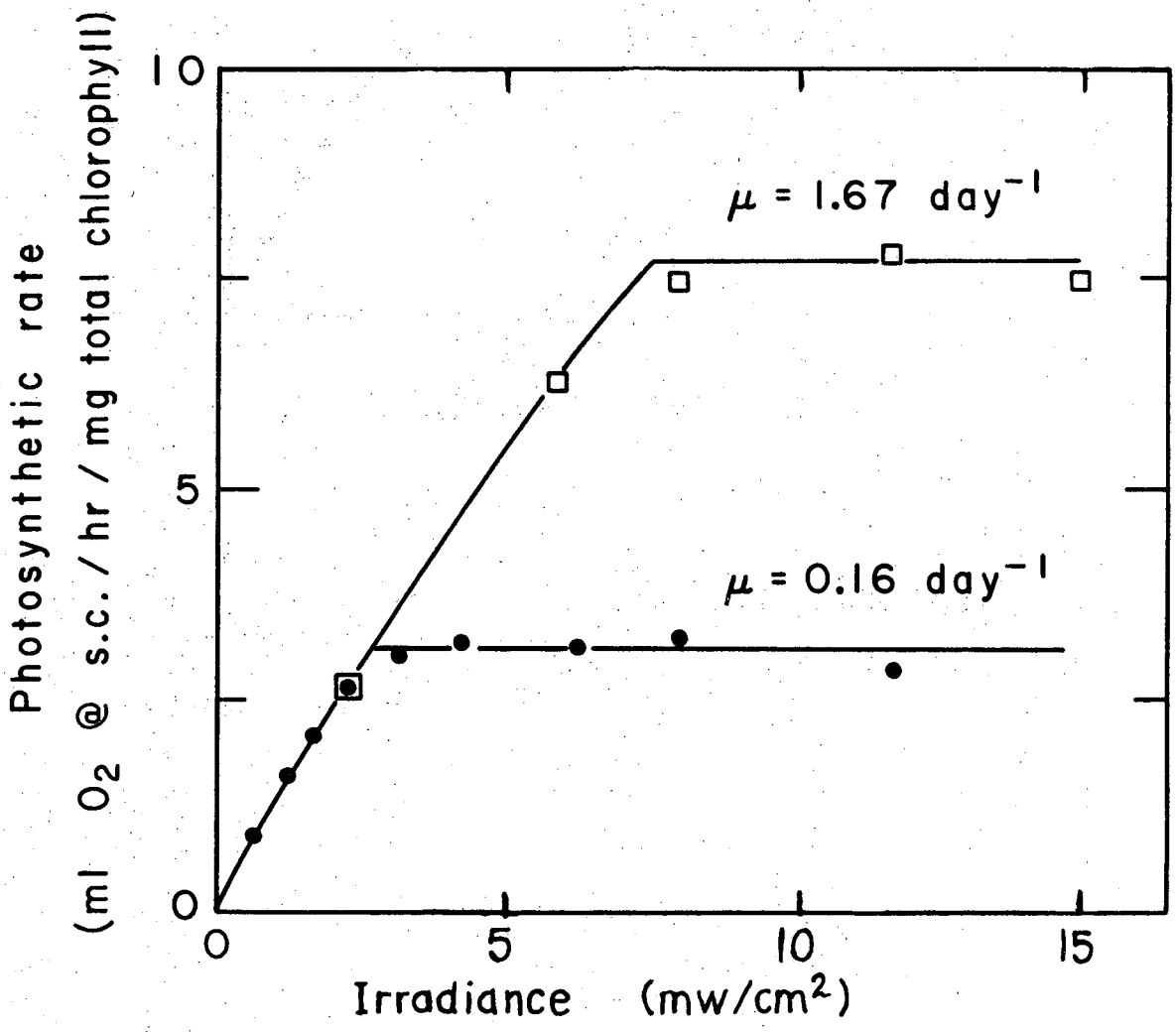

XBL695-2709

Fig. 14. Light response curves at 25° C for algae grown at the specific growth rates designated. ● = Run C-1 and □ = Run C-25. The curves drawn through the data are from Equations (6-17) and (6-18).

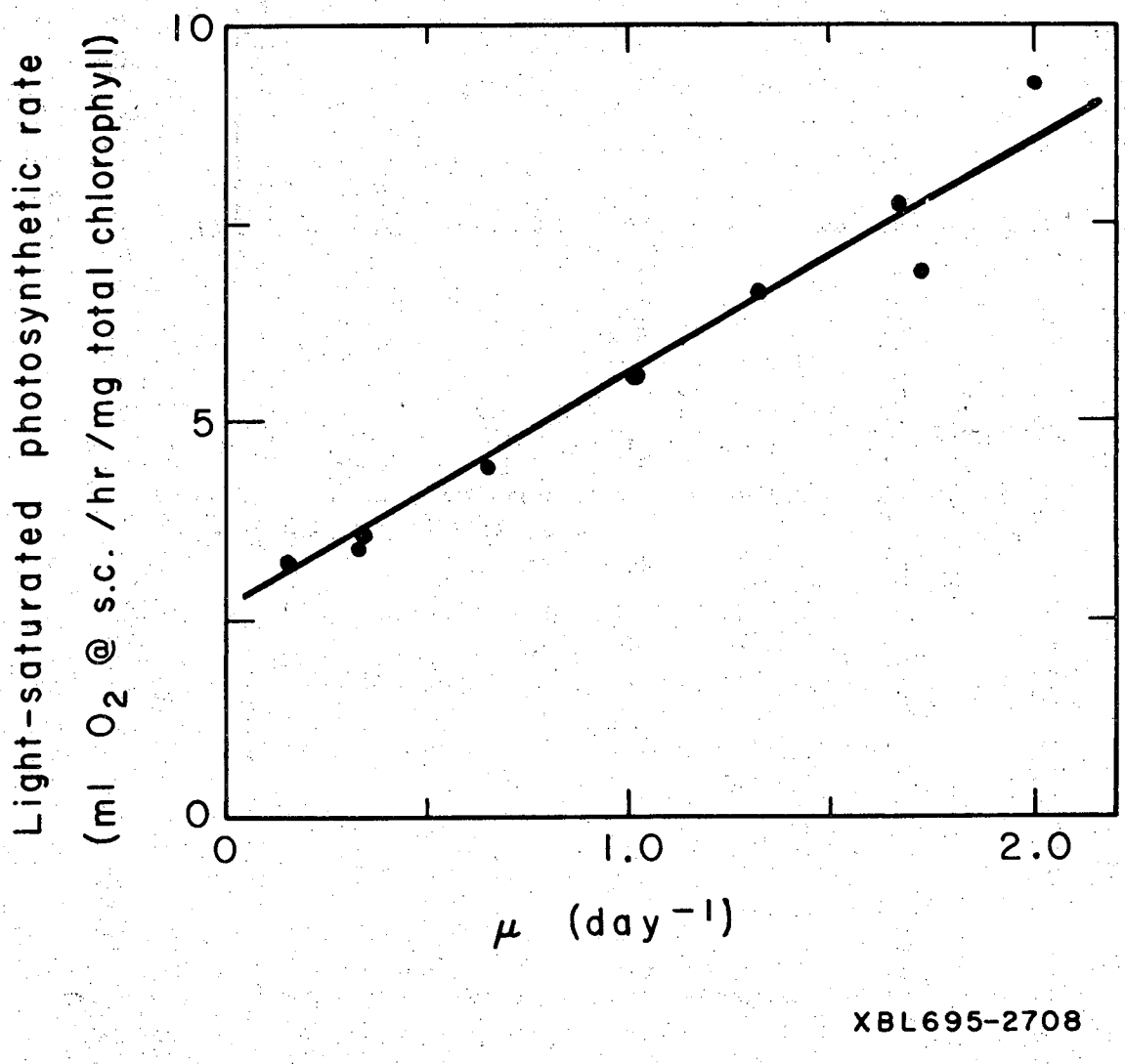

Fig. 15. Light saturated rate of photosynthesis at 25°C versus specific growth rate.

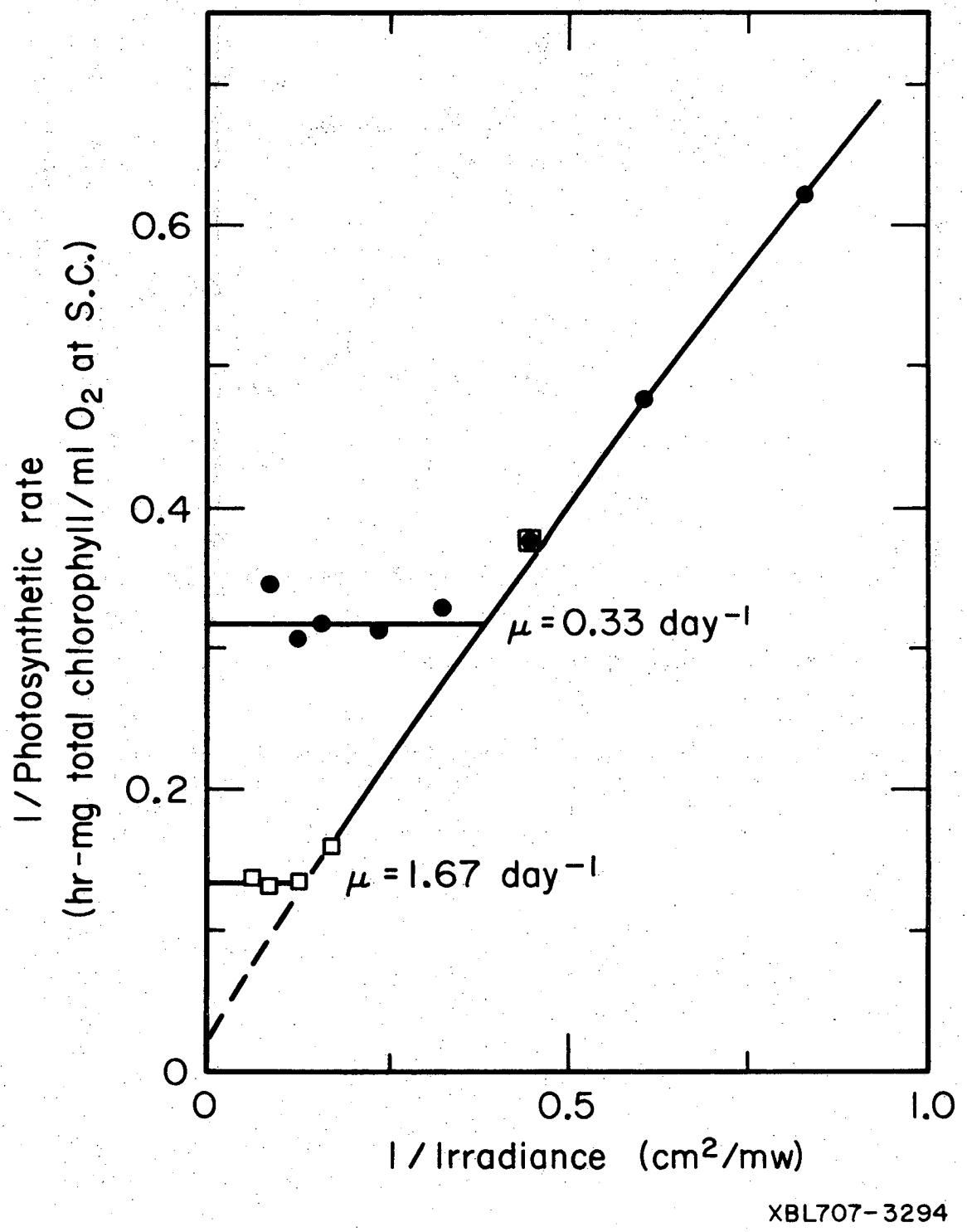

XBL707-3294

Fig. 16. A double reciprocal plot of the data shown in Fig. 14. The strong deviations of the data from the rectangular hyperbola function can be readily seen here. The lines drawn through the data are Equations (6-17) and (6-18).

Data from two other steady states of the culture unit are shown in Fig. 17. In addition to light response curves obtained in the respirometer at 25 °C, light response curves were obtained at 10° C for the same two types of algae. The 10° C curves will be of particular interest when the light response curves for the quinone Hill reaction are discussed.

Maximum Quantum Efficiency

The maximum quantum efficiency occurs at low light intensities. Figure 18 shows data from 16 different respirometer runs. The algae used were grown at specific growth rates ranging from 0.16 day^{-1} to 2.00 day^{-1}. Only data were plotted that were below light saturation, and it can be seen that that growth conditions exert no influence on this portion of the light response curve, since all data can be fit by a single curve. The curve is Equation (6-17), and was fit to the data by LSQVMT, a Lawrence Radiation Laboratory Computer Library program that may be used to fit non-linear equations by a least squares procedure. The best fit of the data was obtained when the two parameters in Equation (6-17), $\Phi\epsilon$ and S_M, had values of 1.316 cm^2. ml O_2* /mw/mg chlorophyll/hr and 49.6 ml O_2/ hr/mg chlorophyll, respectively. $\Phi\epsilon$ is the initial slope, and from it the maximum quantum efficiency was calculated. But to do this, three additional things were needed, the spectral distribution of the light incident upon the respirometer flasks (Fig. 13). the extinction coefficients of the algal cells as a function of wavelength (the average of the curves shown in Fig. 12 was used), and the quantity of chlorophyll in the respirometer flasks (4.2 μg chlorophyll/cm^2). The maximum quantum absorbed, or conversely, the minumum quantum requirement was 8.8 quanta absorbed/O_2 molecule evolved. Our number for the minimum quantum requirement is somewhat lower than

*Unless otherwise stated, all quantities of evolved O_2 are given at standard temperature and pressure (O° C, 1 atmosphere).

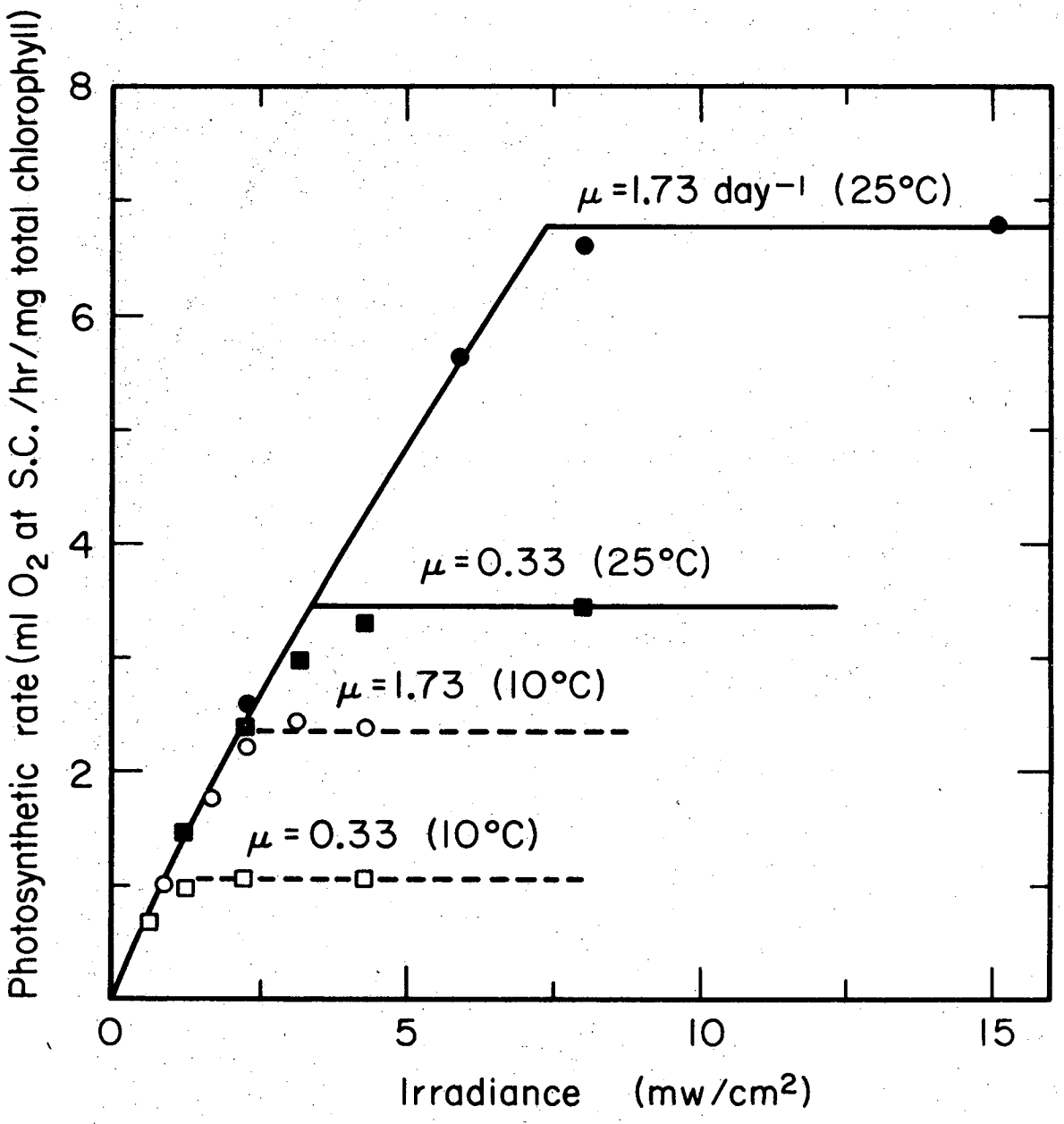

Fig. 17. Light response curves at 25° C and 10° C for algae grown at two different specific growth rates. ■ = Run D-10 □ = Run D-11, ● = Run D-31, and O = Run D-32.

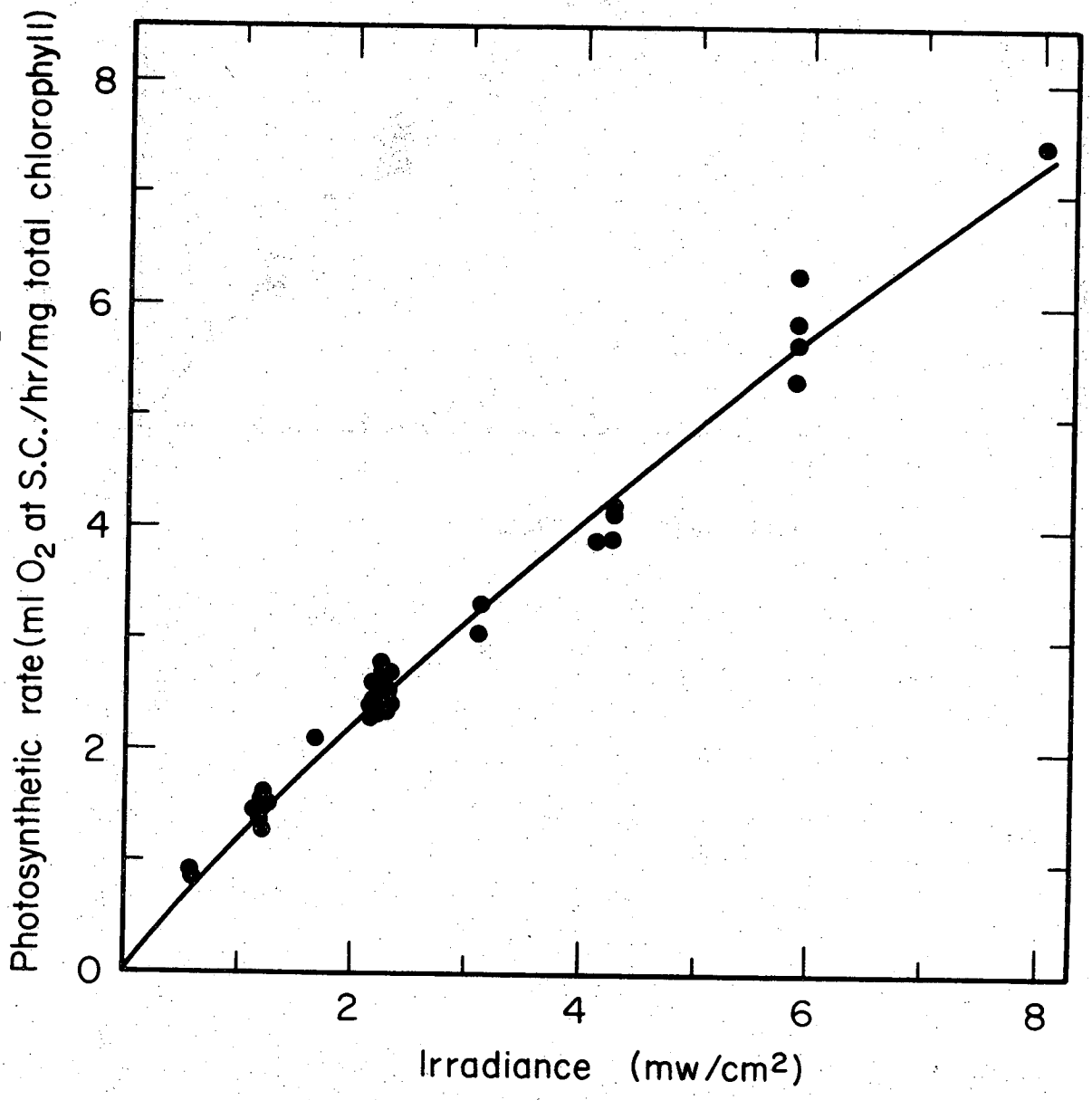

XBL 707-3293

Fig. 18. Light response curve data from 16 different respirometer runs. Only data are plotted that show no signs of approaching light saturation. Equation (6-17) was fitted to the data by a non-linear least squares procedure.

the recent results of Schwartz (1967) and Ng and Bassham (1968). Because of the round-about way our number was calculated, we question its absolute accuracy.

Dark Respiration Rate

Figure 19 shows how the respiration rate in the dark changes as a function of specific growth rate. The data shown were taken after the algal cells had been in the dark for approximately one hour, as described by the procedure given in Appendix IV. Note that the respiration rate is almost directly proportional to μ. These results are almost identical to those found by Myers and Graham (1959) for Chlorella ellipsoidea.

Light Response Curve of the Quinone Hill Reaction

Para-benzoquinone is a unique Hill oxidant, since besides being an artificial electron acceptor for the photo-electron transport system, it is also permeable to whole algal cells. This permeability is a necessity for obtaining the Hill reaction in whole cells. The quinone Hill reaction in whole algal cells was first investigated by Clendenning and Ehrmantraut (1950) and later was studied by Ehrmantraut and Rabinowitch (1952) and Bradley (1953). The experimental procedure employed here is similar to that used by the above workers and is completely described in Appendix IV.

The rate of oxygen evolution during the quinone Hill reaction was found to decrease with time in what appeared to be a first-order manner with respect to remaining activity. The rate of this inactivation was found to increase with increasing light intensity and increasing temperature. Also complicating the raw data was the lag in the appearance of evolved oxygen in the vapor phase of the respirometer flask. This was caused by the large diffusional resistance at the liquid-vapor interphase. In Appendix V we have given the method of mathematically correcting for these two complicating factors so that the true initial rates of the quinone Hill reaction might be obtained.

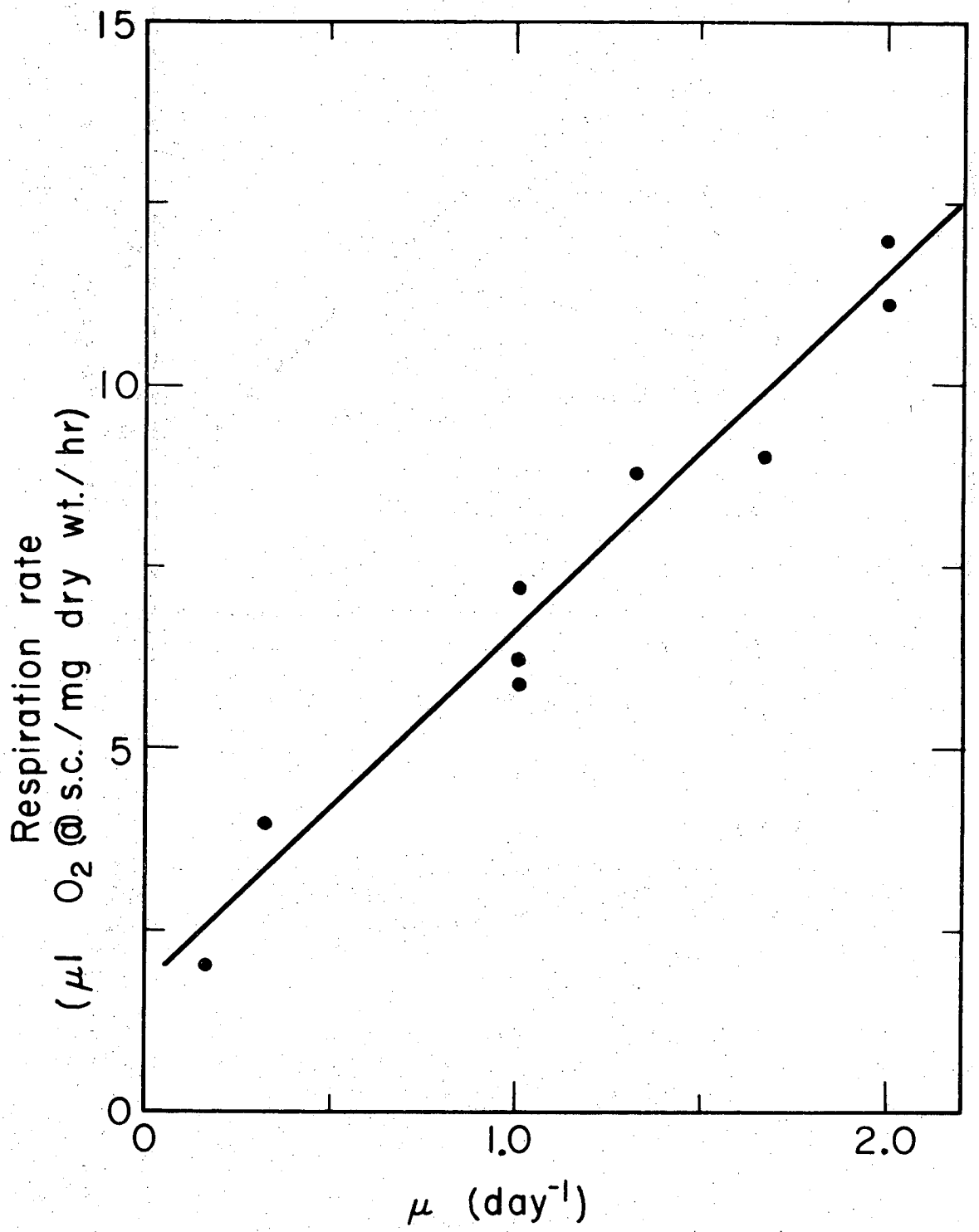

XBL695-2703

Fig. 19. Dark respiration rate versus specific growth rate. Data were taken at 25° C using phosphate buffer at pH = 7.4 as described in Appendix IV.

Figure 20 shows the initial rates of the quinone Hill reaction as a function of light intensity for algae grown at two different specific growth rates, $\mu = 0.33\ day^{-1}$ and $1.73\ day^{-1}$. These same algae were used for the rates of overall photosynthesis shown in Fig. 17. There are several things to be noticed in comparing Figs. 17 and 20.

Comparing the 10° C data, for the algae grown at $\mu = 0.33\ day^{-1}$ the maximum quinone Hill reaction rate is nearly three times higher than the maximum rate of overall photosynthesis. Even for the cells grown at $\mu = 1.73\ day^{-1}$, the maximum Hill reaction rate exceeds the maximum overall photosynthesis rate at 10° C. For the 25° C data the maximum Hill reaction rate again exceeds the maximum rate of overall photosynthesis for the $0.33\ day^{-1}$ cells, but not for the $1.73\ day^{-1}$ cells (although the quinone Hill reaction may not have reached light saturation).

The above results are particularly impressive because of the low maximum quantum efficiency obtained for the quinone Hill reaction. The maximum quantum efficiency for the quinone Hill reaction may be directly compared to the maximum quantum efficiency for overall photosynthesis by comparing the initial slope in Fig. 20 to the initial slope in Fig. 17. The initial slope of the quinone Hill reaction data is only about half the overall photosynthesis slope.

Unlike the results obtained for overall photosynthesis, there is no difference between the quinone Hill reaction results for the algae grown at the two different specific growth rates.

One can draw on important conclusion for at least three of the four sets of data shown in Figs. 17 and 20 where the maximum quinone Hill reaction rate exceeds the corresponding rate for overall photosynthesis. No reaction between oxygen evolution and System II sets, or has any influence upon, the light saturated rate of photosynthesis. For the data taken, it is not known whether quinone accepts electrons at the top of System II or at the top of System I.

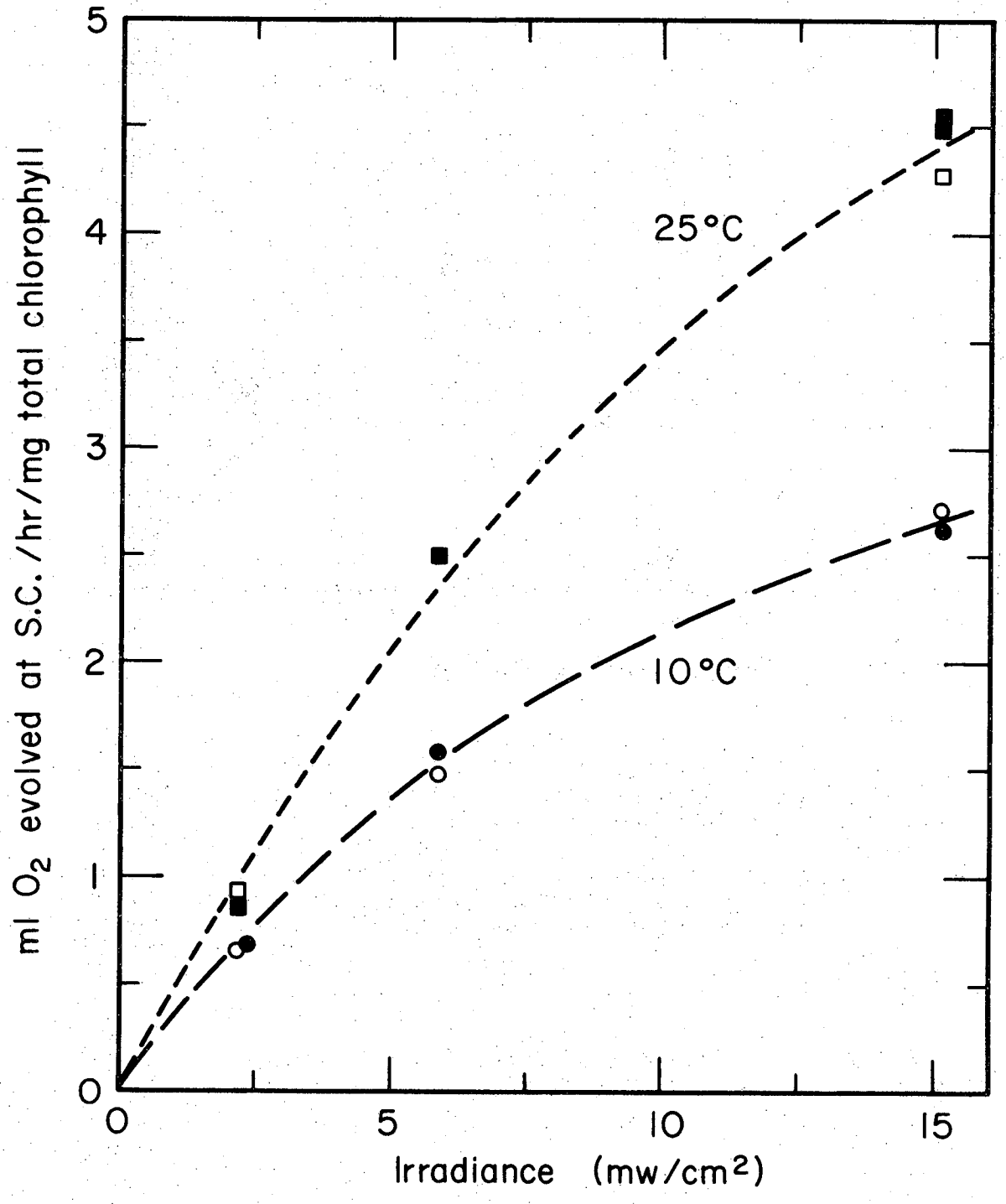

XBL707-3295

Fig. 20. Light response curves for the quinone Hill reaction at 25° C and 10° C. The overall photosynthesis light response curves for these algae are shown in Fig. 17. Squares denote data taken at 25° C, whereas circles denote data taken at 10° C. Filled symbols are data taken on algae grown at $\mu = 0.33\ day^{-1}$, while open symbols denote data taken on algae grown at $\mu = 1.73\ day^{-1}$. Rates of oxygen evolution plotted here are initial rates, calculated according to the procedure given in Appendix V. The reaction mix and experimental conditions are described in Appendix IV.

In either case all electrons donated to quinone must pass through the steps between oxygen evolution and System II. As shown in Chapter V, only one enzymatic reaction sets the light saturated rate of photosynthesis. Thus, no reaction between oxygen evolution and System II has any influence on the light saturated rate of photosynthesis.

Cell Composition by Elements

The effect of specific growth rate on the elemental composition of Chlorella pyrenoidosa is shown in Figs. 21, 22, and 23. Carbon, nitrogen, hydrogen, and ash were directly determined by analysis, and oxygen was obtained by difference. From these data the exact stoichiometric relationship between the production of cell material and the rate of photosynthesis can be determined. Taking into account the change of nitrate into cellular nitrogen, but neglecting any other valence changes of minerals in the nutrient medium, the following material balance equation is obtained for calls grown at a specific growth rate of 2.0 day^{-1}:

$$5.95\ H_2O + 5.92\ CO_2 + 1.00\ NO_3^- \rightarrow C_{5.92}H_{10.90}O_{2.69}N_{1.00} + 1.00\ OH^- + 8.55\ O_2 \qquad (3\text{-}1)$$

The first term on the right side of the equation is equivalent to 151.5 g of dry cells, when the ash content is added in. Similar equations may be generated for other specific growth rates. The relation between cell production and oxygen evolution at any specific growth rate is:

$$B = 1.64 \times 10^4 + 0.065 \times 10^4\ \mu \qquad (3\text{-}2)$$

where the units of B are mg dry weight/mole O_2.

RNA and DNA Content

Figure 24 shows how specific growth rate affects RNA and DNA content. The analyses were carried out using a modified Schmidt-Taunhauser technique as described by Cahn (1970). DNA

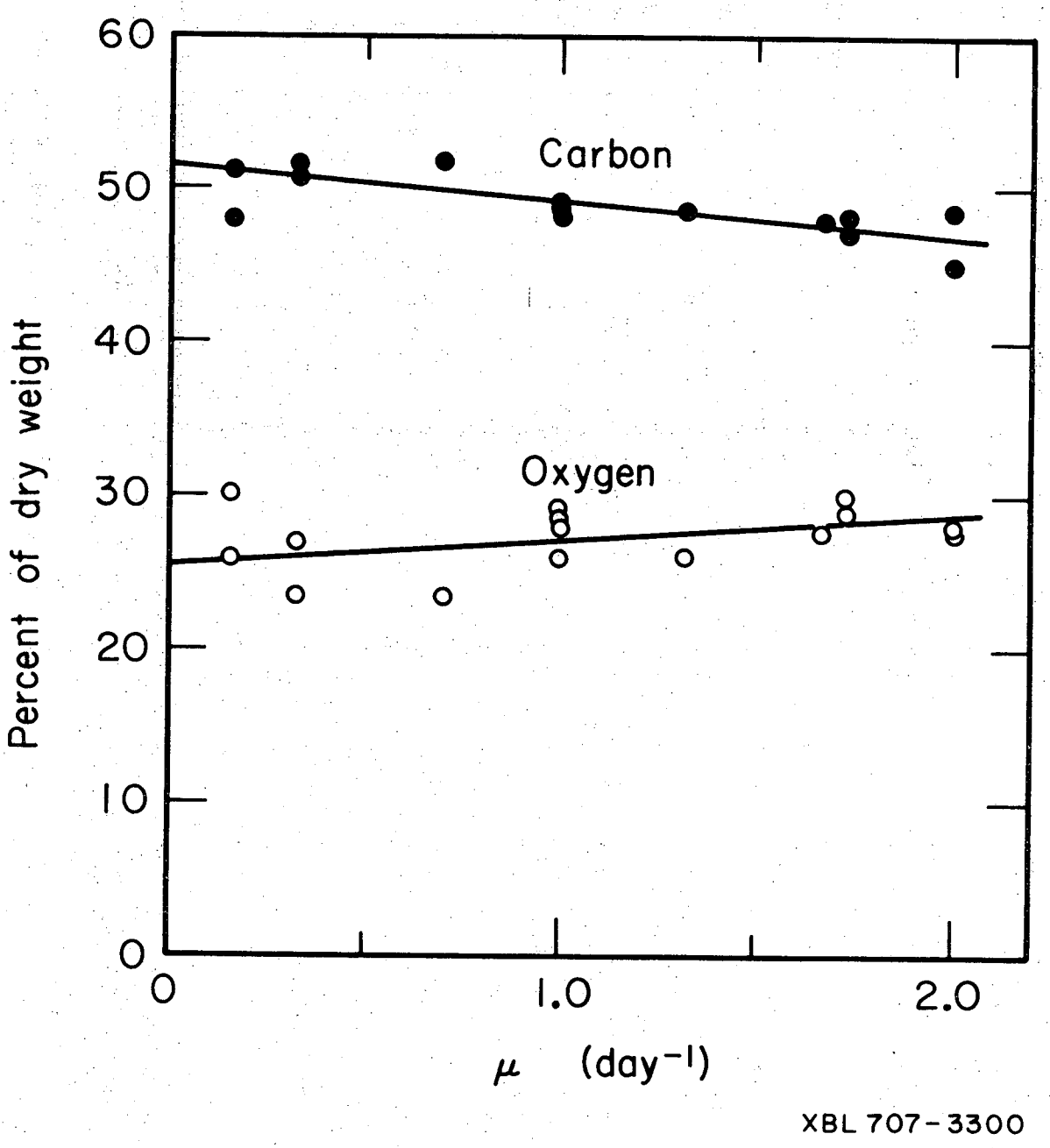

Fig. 21. Carbon and oxygen content versus specific growth rate.

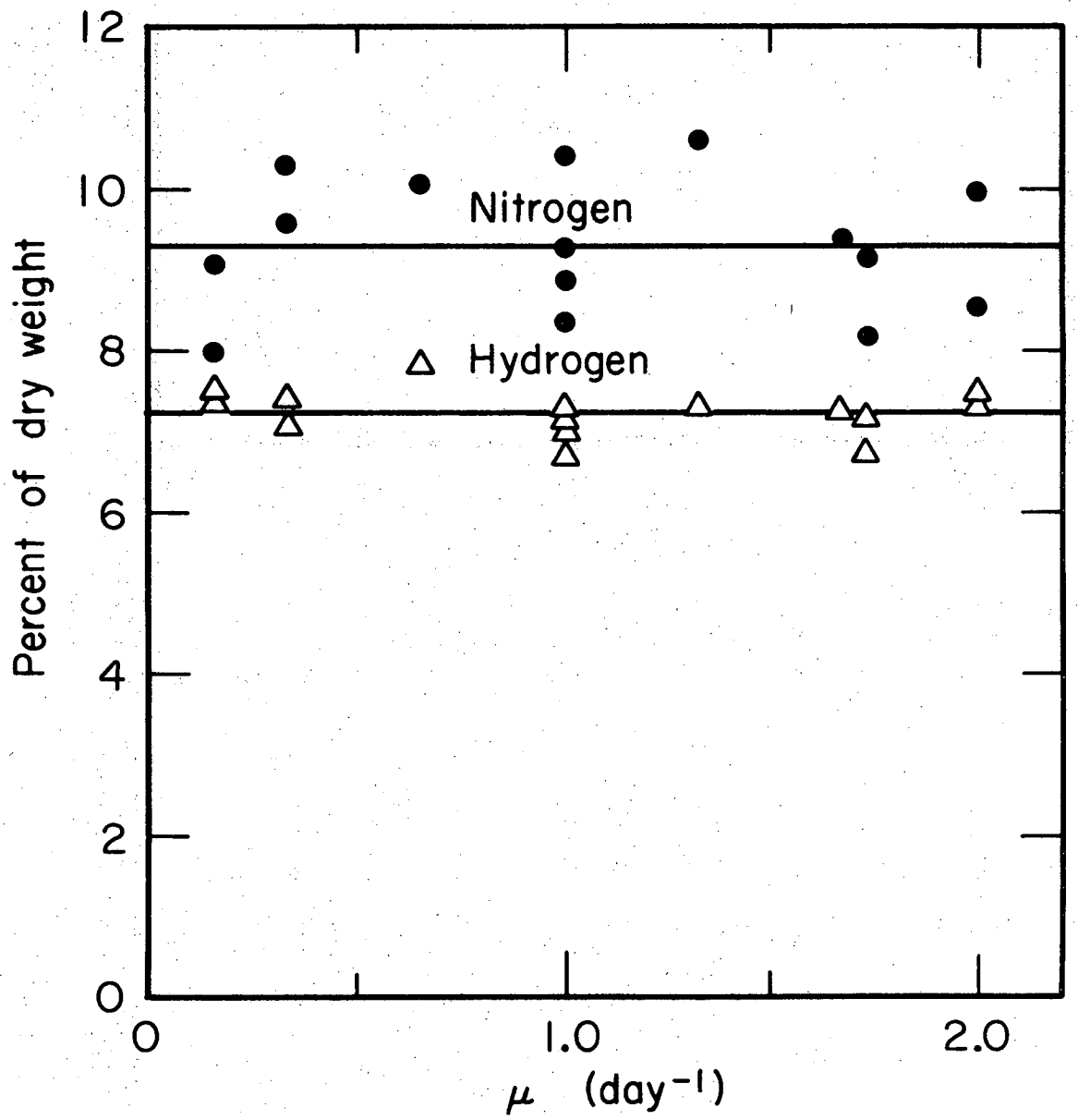

Fig. 22. Nitrogen and hydrogen content versus specific growth rate.

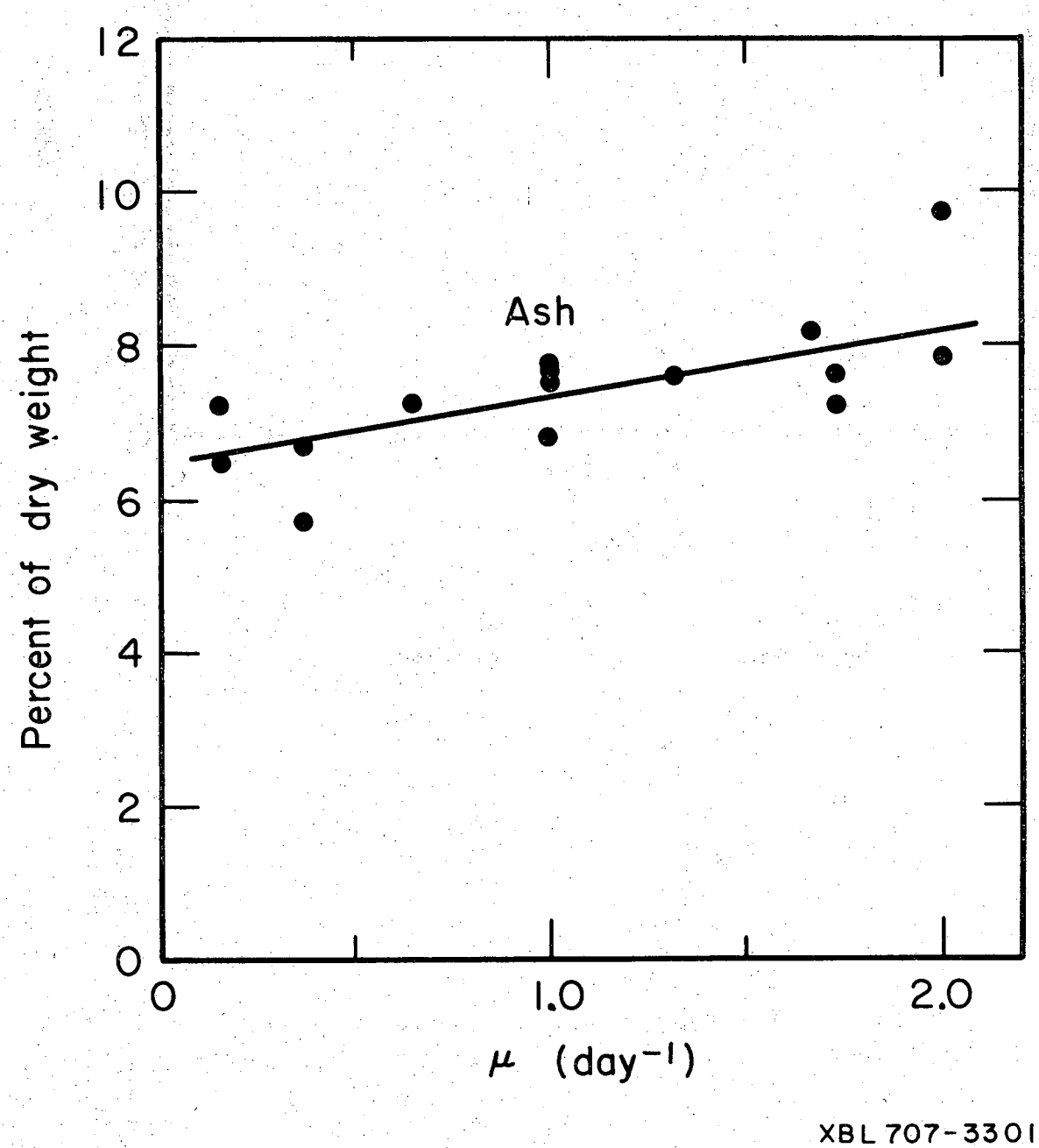

Fig. 23. Non-combustibles (ash) content versus specific growth rate.

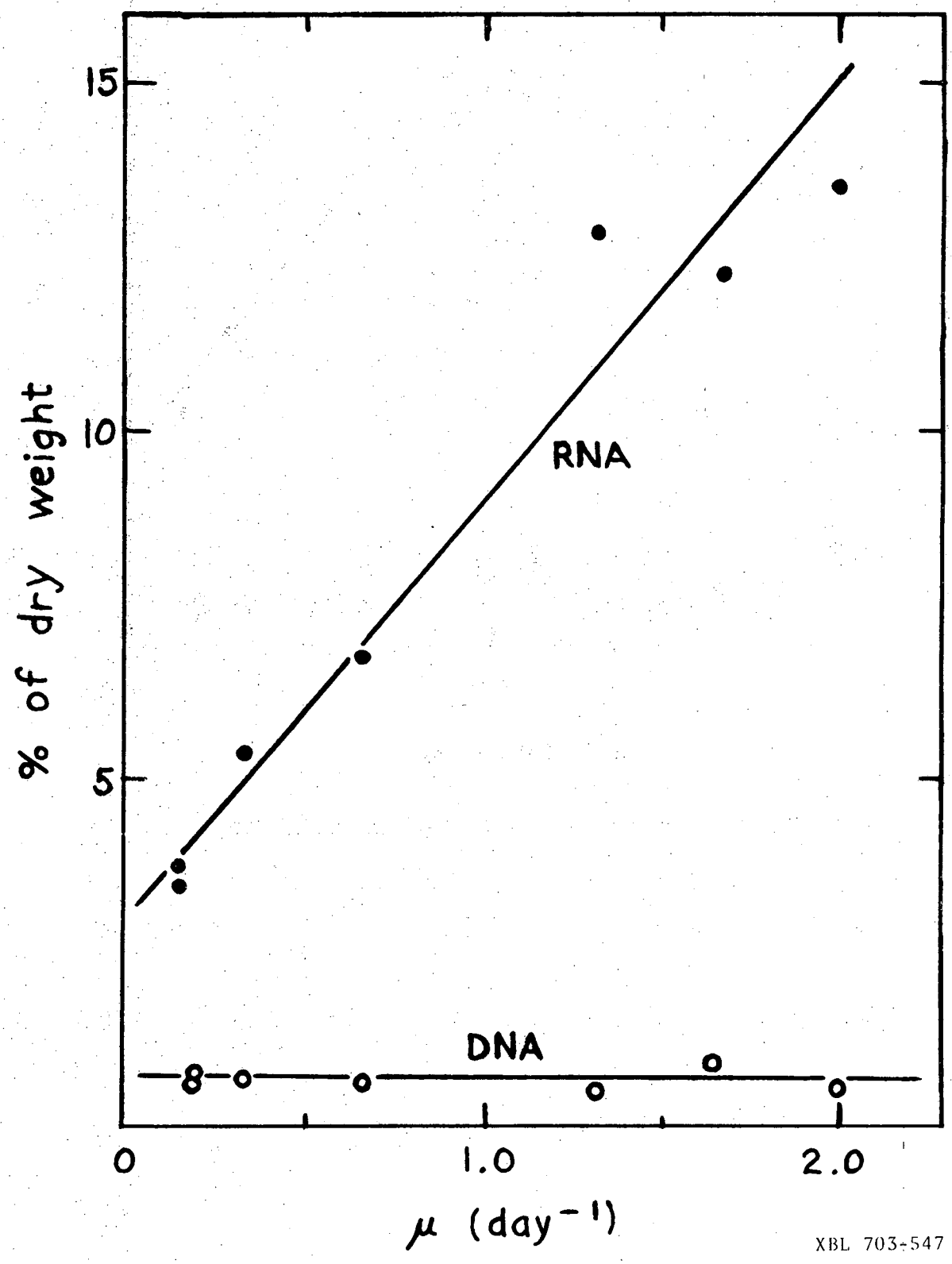

Fig. 24. RNA and DNA content versus specific growth rate.

content does not appear to vary, at least not significantly. But RNA content changes drastically, almost in direct proportion to specific growth rate. Why this should be so is explained as follows. Most RNA is present in the ribosomes, which are the protein manufacturing factories of the cell. Since most of the cell consists of protein or the products of protein enzymes, it is logical to expect more RNA (in the form of ribosomes) in cells that are growing at a more rapid rate. Similar results have been found for bacteria (see Maaloe and Kjeldgaard, 1966).

C. RESULTS AT STEADY STATE: EFFECT OF INCIDENT LIGHT INTENSITY ON THE PHYSIOLOGY OF CHLORELLA PYRENOIDOSA

In this section, the effect of varying the light intensity incident upon the culture vessel is examined. The steady state specific growth rate was held constant at 1.01 day^{-1}. The spectral distribution of all three light sources was virtually identical to Fig. 6. The results are summarized in Table II and in Fig. 25. Note that the data were all taken at a specific growth rate that is not optimum in terms of productivity.

Even though the incident light intensity was varied by more than a factor of five, there was little change in any of the physiological parameters examined. Indeed, expected scattering of the data makes uncertain the direction of any changes in chlorophyll content, chlorophyll a/chlorophyll b ratio, or cellular composition. These results show that it is mainly the growth rate of the cells, not the incident light intensity, that determines the physiology of Chlorella pyrenoidosa growing in dense culture.

D. UNSTEADY STATE RESULTS: TRANSIENTS IN CONTINUOUS CULTURE

Here the effects of a step change in the feed rate to the continuous culture unit will be examined. The slowness with which the physiology of the algal cells adapts to this change in environment will be demonstrated, reconfirming the work of Myers and Graham

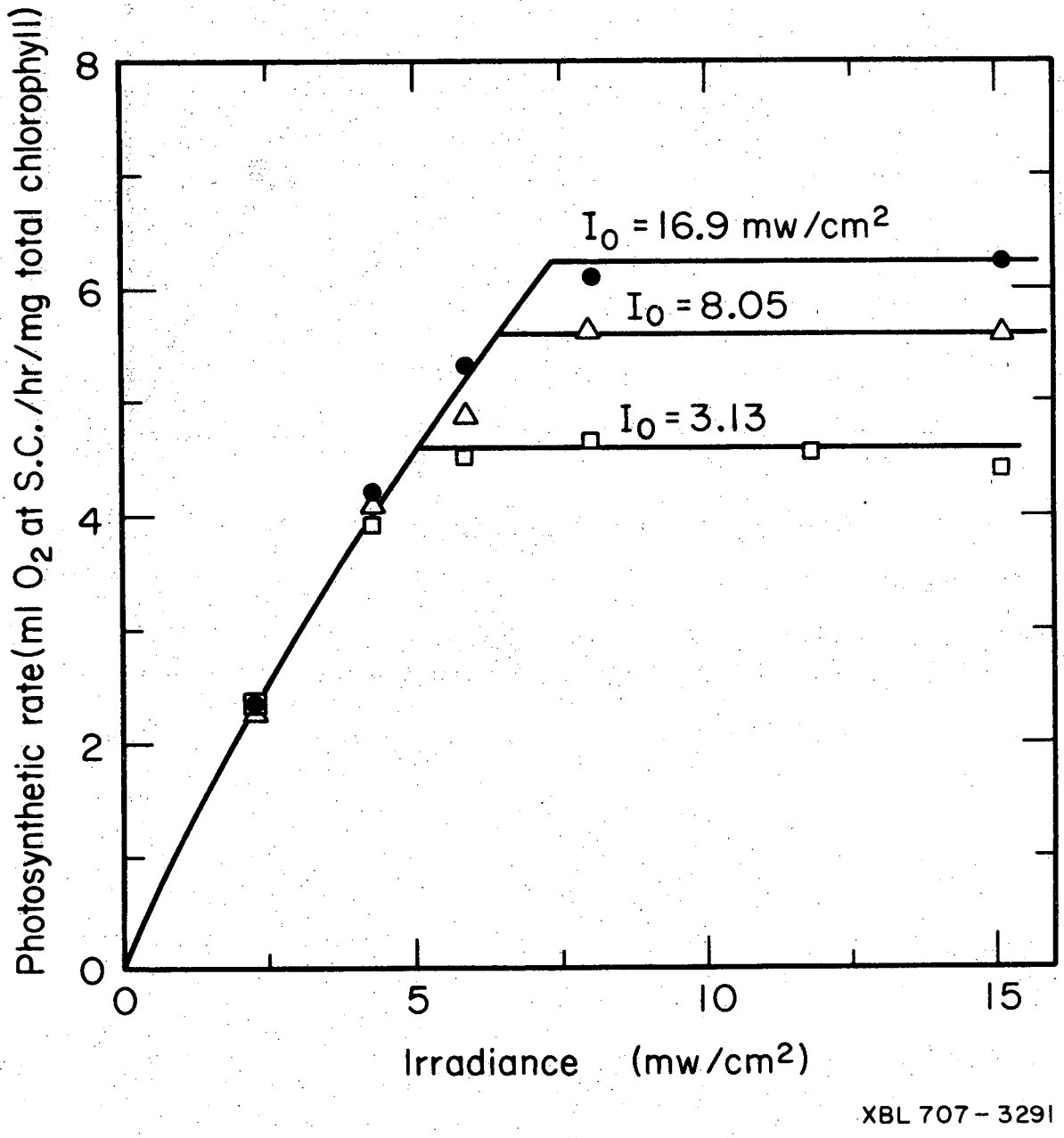

Fig. 25. Effect of incident light intensity on the light response curve. Data were taken at 25° C on algae grown at $\mu = 1.01\,day^{-1}$.

Table II. Effect of Incident Light Intensity on the Physiology of Chlorella pyrenoidosa.

Temperature = 25° C, μ = 1.01 day^{-1}

Incident light intensity, mw/cm^2	3.13	8.05	16.9
Run number	D-27	D-29	D-30
Cell concentration, mg dry wt./ml	0.56	1.11	1.76
Productivity, mg dry wt./cm^3/day	1.50	2.97	4.73
Efficiency of converting light energy into cell material, %	12.7	9.8	7.4
Total chlorophyll, %	4.60	4.25	4.38
Chlorophyll a/chlorophyll b ratio	3.69	3.10	3.38
Cell composition, %			
Carbon	48.4	48.8	49.1
Hydrogen	7.0	6.7	7.1
Nitrogen	9.3	8.9	10.4
Oxygen	28.5	27.9	25.9
Ash	6.8	7.7	7.5

(1959), which showed that batch culture cannot be compared with continuous culture.

Figure 26 shows how a number of physiological parameters changed as a result of changing the feed rate to a culture that had previously reached steady state at $\mu = F/V = 0.325\ day^{-1}$. At time = 0 on the figure, F/V was changed to $2.00\ day^{-1}$. Resultant changes in experimentally measured parameters are shown by the data points, which have been fit by the solid lines. For instance, curve A shows the manner in which cell concentration changes.

The dashed lines, B' and D', show how chlorophyll content and the light saturated rate of photosynthesis would change if the Chlorella cells adapted instantaneously to their changing environment. The dashed lines were calculated in the following fashion:

1. From curve A the cell concentration corresponding to any particular time may be obtained.
2. This cell concentration corresponds to a certain steady state specific growth rate, which may be found from Fig. 8.
3. Using this steady state specific growth rate, the chlorophyll content and the light saturated rate of photosynthesis may be predicted from Figs. 10 and 15.

Thus, the dashed lines represent the steady state results corresponding to the cell concentrations of line A.

Comparing the actual results to the predicted shows that adaptation is not instantaneous; instead, the actual data lag 10-20 hours behind the predicted changes. By comparison, a steady state value of $\mu = 2.00\ day^{-1}$ is equivalent to a doubling time of about 8 hours. The generation time of Chlorella pyrenoidosa is about 3 doubling times since one mother cell generally gives rise to 8 daughters. Does the size of this lag mean that physiological changes are mainly manifested in the daughter cells, and not in the mother cell? Perhaps the use of synchronous cultures could answer this question.

Figure 27 shows similar data, but with a downward step change in the feed rate to the culture unit.

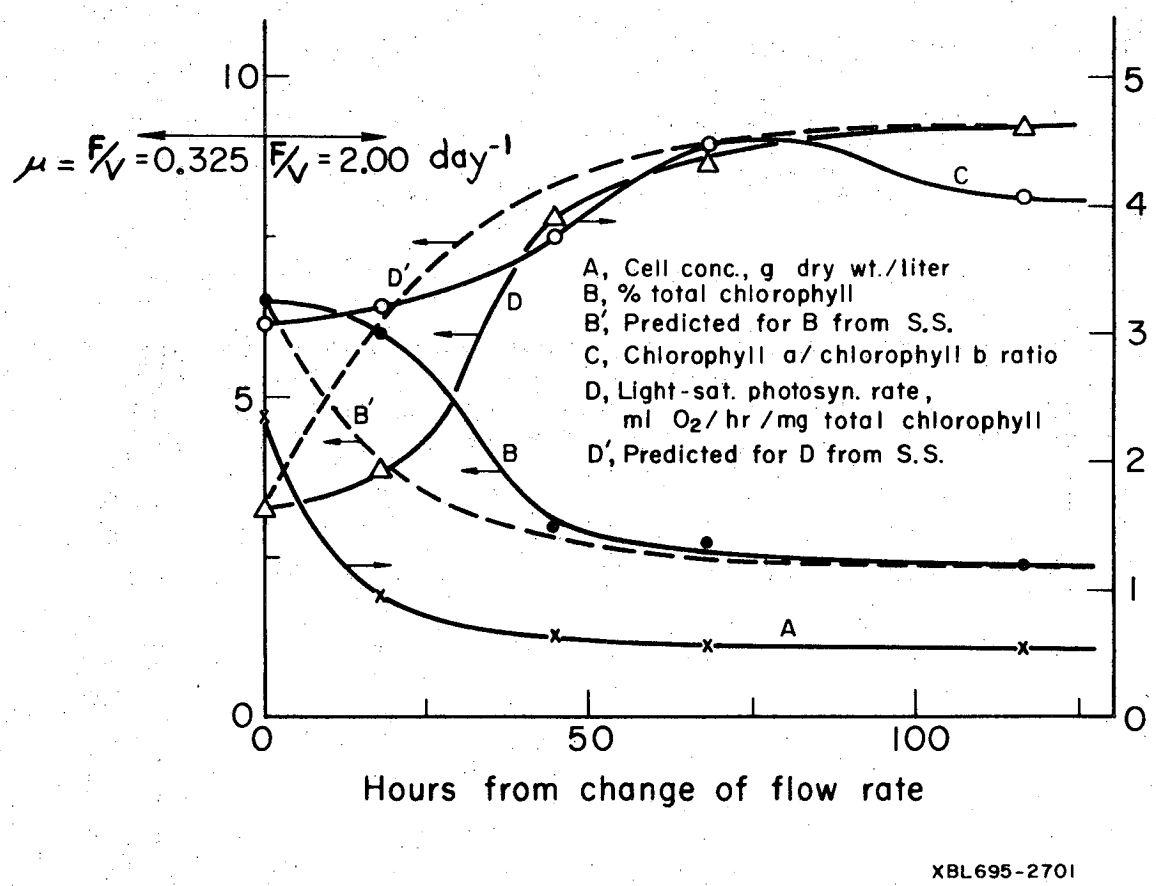

Fig. 26. Transients resulting from changing the feed rate to the continuous culture unit. At time zero the feed rate to the culture unit was increased. The dashed lines show expected changes if adaptation by the cells were instantaneous.

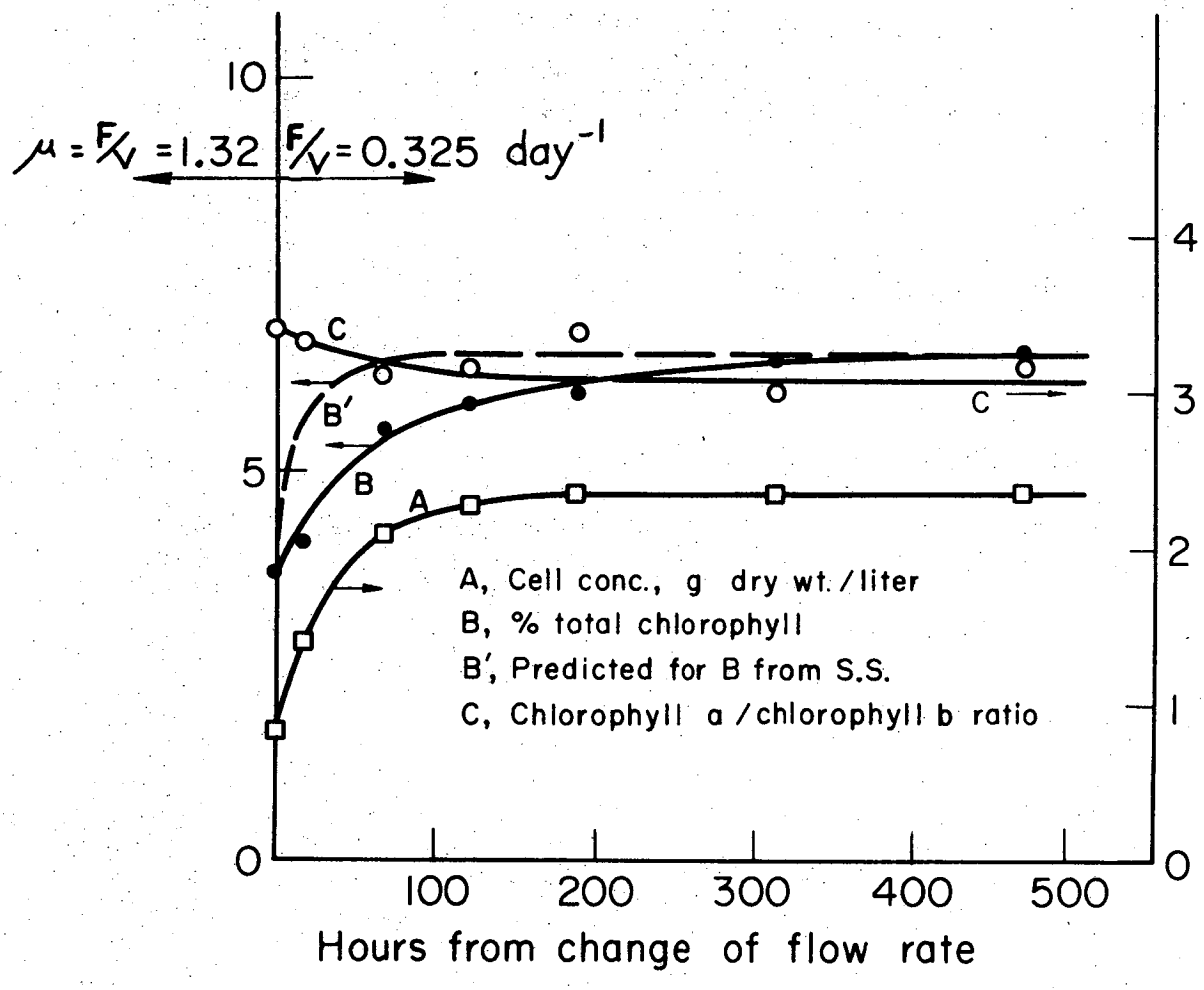

XBL695-2700

Fig. 27. Transients resulting from decreasing the feed rate to the continuous culture unit. Previous to time zero, the culture had reached steady state at $\mu = 1.32\ day^{-1}$.

E. ATTEMPTS AT INCREASING PRODUCTIVITY

Two attempts were made to increase the productivity of Chlorella in continuous culture, use of plant hormones and use of a pale green mutant. Both attempts failed to increase productivity.

Plant Hormones Added to the Nutrient Medium

Wareing et al. (1968) have shown that the plant hormones kinetin and gibberellic acid increase the light saturated rate of photosynthesis in maize. Treharne and Stoddart (1968) have shown a similar effect in red clover leaves when gibberellic acid is applied. These workers explain their results on the basis of the increased levels of carboxylating enzymes that result from the application of these hormones.

As far as algae are concerned, the literature is contradictory as to the effects of plant hormones (see the review of Conrad and Saltman, 1962). All such work has apparently been done in batch culture. With Chlorella vulgaris, Yin (1937) claimed that 3-indoleacetic acid increased cell size, but not the rate of cell division. However, Pratt (1937) in a similar experiment found no effect of indoleacetic acid. In similar work, Brannon and Bartsch (1939) found that this plant hormone had no effect on the cell size of Chlorella pyrenoidosa, but did result in a higher rate of growth. But Bach and Fellig (1958) questioned the results of these latter workers, since the indoleacetic acid added to the nutrient medium was first dissolved in ethanol, which is known to be directly utilizable by Chlorella.

In order to resolve the above contradictory results and to see if productivity could be increased, we investigated the effect of the plant hormones 3-indoleacetic acid, gibberellic acid, and kinetin on Chlorella pyrenoidosa in steady state continuous culture. The nutrient medium was the same as given in Table I, but with the addition of 5 mg/l of 3-indoleacetic acid, 0.5 mg/l of gibberellic acid, and 0.5 mg/l of kinetin. The experimental procedure was to achieve steady state at $\mu = 0.33$ day^{-1} without these hormones in the nutrient

medium, take pertinent data, then switch to a nutrient medium containing these hormones, wait 2 weeks, and again take pertinent data. The results are shown in Fig. 28 and Table III. The slight differences between the data with and without the hormones are well within the experimental error. We conclude that these plant hormones have no significant effect upon the physiology of Chlorella pyrenoidosa. Productivity was not improved, since there was no significant increase in the light saturated rate of photosynthesis.

Using Chlorella pyrenoidosa C. 1. 1. 10. 36, a Pale Green Mutant

Wild and Egle (1968) have investigated a pale green mutant of Chlorella pyrenoidosa, which they have described as having a low chlorophyll content and a high light saturated rate of photosynthesis. As discussed in Chapter IV, this is exactly the type of algae we would expect to give a high productivity at high light intensities. In a sequential comparison with the normal cells at 25° C, incident intensity of 8.6 mw/cm^2, and $\mu = 0.33$ day^{-1}, we obtained a productivity for the mutant cells of 2.41 mg dry wt./cm^2/day as compared to 2.48 mg dry wt./cm^2/day for the normal cells. These disappointing results for the mutant strain may have several possible explanation:

1. The maximum quantum efficiency of the mutant may be low.
2. The optimum growth conditions were not used.
3. Back-scattered (reflected) light is much greater for the mutant because of its lower chlorophyll content.

The above suggestions for the low mutant productivity are only speculations. No physiological parameters of the mutant were measured. The search should continue for algae with higher light saturated rates of photosynthesis.

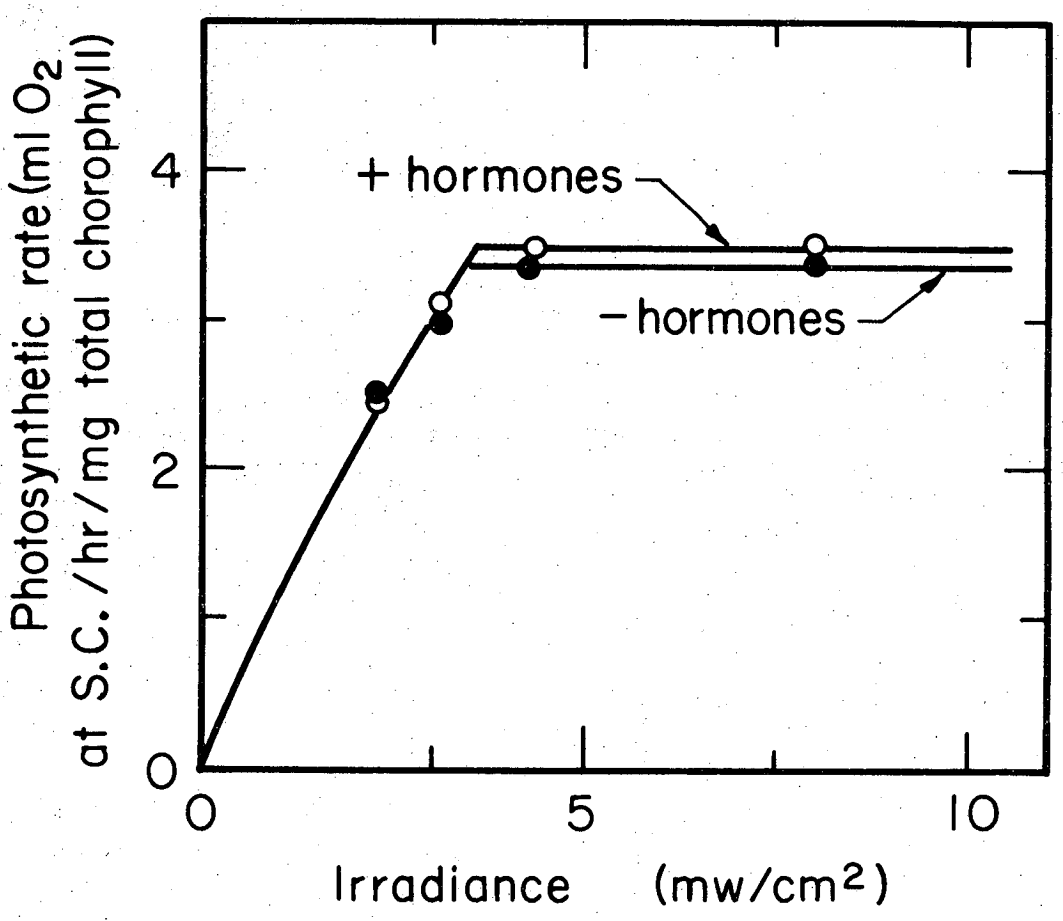

XBL 707-3292

Fig. 28. Light response curves with and without plant hormones added to the nutrient medium. Data were taken at 25° C. Algae were grown at $\mu = 0.33\ day^{-1}$ in both cases. Growth medium, but not respirometer buffer, for the + hormone case contained 5. mg/l 3-indoleacetic acid, 0.5 mg/l gibberellic acid (GA_3), and 0.5 mg/l kinetin.

Table III. Effect of Plant Hormones on the Physiology of Chlorella pyrenoidosa.

Temperature = 25° C, $\mu = 0.33\ day^{-1}$
Incident Light Intensity = 8.6 mw/cm^2.

	Without hormones	With hormones
Run number	D-38	D-46
Cell concentration, mg dry wt./ml	2.82	2.86
Productivity/area, mg dry wt./cm^2/day	2.48	2.51
Total chlorophyll, %	6.71	6.80
Chlorophyll a/chlorophyll b ratio	3.34	3.39

NOMENCLATURE

A = Illuminated surface area, cm^2

B = Conversion factor relating cell biomass weight produced to oxygen evolution, mg dry weight/mole O_2

F = Feed rate, ml/day

p = Productivity of cellular biomass, mg dry weight/cm^2/day

S_M = The light saturated rate of photosynthesis intrinsic to the photosynthetic electron transport system, moles O_2/hr/mg chlorophyll

X = Cellular biomass concentration, mg dry weight/ml

ϵ = Extinction coefficient of the pigments, cm^2/mg chlorophyll

μ = Specific growth rate, day^{-1}

Φ = Maximum quantum yield, moles O_2/einstein

IV. THE SIGNIFICANCE OF THE EXPERIMENTAL RESULTS

A. SELF-OPTIMIZING BIOLOGICAL SYSTEM

Species continuously self-optimize themselves for the particular environment they are in. Such is the conclusion to be drawn from the theory of natural selection, which Charles Darwin (1859) published in his well-known book, The Origin of Species. Let us review the basic tenets of the theory of natural selection to see what the data of the last chapter mean in terms of the ability of Chlorella to survive in nature as a species. We quote Darwin's three basic propositions. (a) "That gradations in the perfection of any organ or instinct, either do now exist or could have existed." (b) "That all organs and instincts are, in ever so slight a degree, variable." (c) "That there is a struggle for existence leading to the preservation of each profitable deviation of structure or instinct." The latter point makes two assumptions, that "profitable deviations" are inherited, and that more individuals of a species are born than can survive to reproduce themselves.

In summary, those best able to survive the competition with others, to the extent that they can reproduce themselves, are the fittest. Living to the point of being able to reproduce is the test of fitness. What characteristics would we expect to find in Chlorella pyrenoidosa so that it can survive in nature?

B. ADAPTATION TO THE ENVIRONMENT BY CHLORELLA PYRENOIDOSA

Algal cells growing faster than other algal cells have an advantage in the competition to survive, since they may produce offspring sooner or in larger quantity. But Chlorella pyrenoidosa cells are found in various environments. In nature light intensity, temperature, and nutrient concentration may vary with location and time. Certainly Chlorella pyrenoidosa would be better fit to survive in its competition with other algal species if it could

maintain a high growth rate by adapting to whatever environment it happens to find itself in. We will now limit our discussion to only one environmental variable, light intensity. How would we expect Chlorella pyrenoidosa to adapt to light intensity?

Chlorophyll Content

At low light intensities the growth rate (and photosynthetic rate) of a Chlorella cell is directly proportional to the percent chlorophyll content. This is because absorption of light is directly proportional to pigment (mainly chlorophyll) content, and at low light intensities the rate of photosynthesis is directly proportional to the rate of light absorption. Thus, we would expect Chlorella cells adapted to a low light intensity environment (e.g., a shaded pond) to have a high percent chlorophyll content.

But Chlorella cells growing in an environment of high light intensity (e.g., a sunny pond) are not limited in their growth by the amount of light they can harvest; in fact, they have an excess of light. So we might expect this type of "sun-adapted" cell to have a low chlorophyll content. A high chlorophyll content is not needed, since a low chlorophyll content will harvest sufficient light.

But how do the experimental data of Chapter III reconcile with the above suppositions? Figure 10 shows that the chlorophyll content in Chlorella pyrenoidosa does change in the manner predicted by the above arguments. Remember that cells growing at a low specific growth rate are in an environment of low average light intensity, while a high specific growth rate corresponds to a high average light intensity. Figure 10 shows that cells starved of light have higher chlorophyll contents than cells with an overabundance of light.

Light Saturated Rate of Photosynthesis

Cells in a low light intensity environment are growing and photosynthesizing at a low rate. Therefore we would not expect these cells to have a high concentration of the enzymes that allow a

high light saturated rate of photosynthesis. Instead, we would expect these cells to devote their energy to producing more chlorophyll so that more light might be harvested. For cells growing in an environment of high light intensity we would expect a situation converse to the above.

Figure 15 shows that the above arguments predict the actual experimental result; low μ cells have a low light saturated rate, and high μ cells have a high light saturated rate.

Figure 29 outlines how Chlorella pyrenoidosa adapts to the average light intensity in its environment. This adaptive response is beneficial to the survival of Chlorella pyrenoidosa as a species, and is consistent with Darwin's theory of natural selection.

Chlorophyll a/Chlorophyll b Ratio

Many researchers have shown that the concentrations of the various light harvesting pigments are strongly dependent upon the spectral distribution (or quality) of the illumination under which algal cells are grown (Brody and Emerson, 1959, Jones and Myers, 1964, Ghosh and Govindjee, 1966). Indeed, it was nearly a century ago when Englemann (1883, 1884) proposed that algal pigments adapt in the direction of maximum utilization of the light incident upon them. For example, algal cells growing in a particular wavelength would be expected to adapt in the direction of having more of the pigment (or pigments) that strongly absorb that wavelength. This theory does not appear to hold in all situations. Brody and Emerson (1959) found that with high intensities of blue and green light the changes in the red alga Porphyridium cruentum were contrary to Englemann's theory, but at low intensities of these colors the adaptations were as expected.

Our data, as shown in Figs. 11 and 12, seem to agree with Englemann's theory. Green and yellow wavelengths are most weakly absorbed by green plants, such as Chlorella. Thus, the concentrated suspension of cells growing at a low specific growth rate is, on the

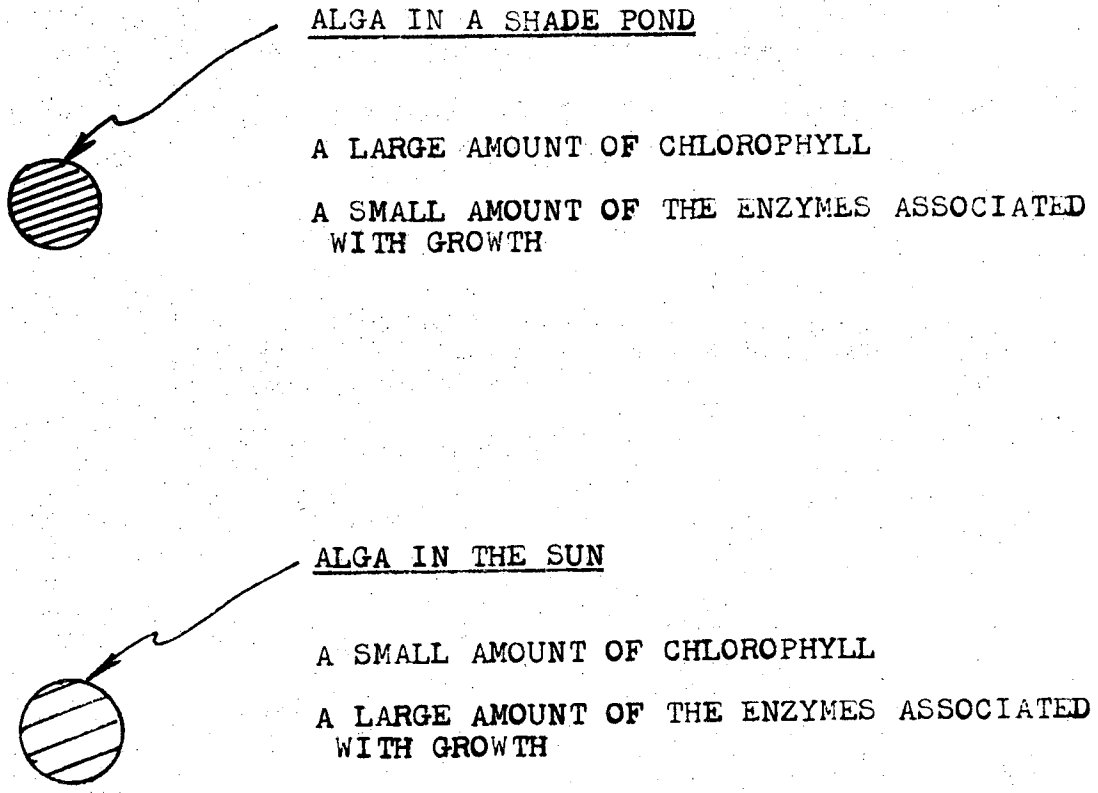

XBL 709-6502

Fig. 29. Physiological adaptation of Chlorella pyrenoidosa cells found in two environments differing in incident illumination.

average, in an environment richer in green and yellow wavelengths compared to the relatively thin suspension of cells obtained at high specific growth rates. For the low μ cells Fig. 12 shows greater absorption in the green and yellow regions, and Fig. 11 shows that the low μ cells have a greater chlorophyll b content. This increases absorption in regions where chlorophyll a does not have its peak absorbance. Thus, algae growing in an environment rich in green and yellow wavelengths seem to be more efficient in their absorption of those wavelengths.

C. OPTIMIZING AND INCREASING PRODUCTION OF CELLULAR MATERIAL IN ALGAL SYSTEMS

For the experimental conditions given in Chapter III, the optimum productivity of cellular material is obtained at a specific growth rate of about 1.6 day^{-1}. There is a high light saturated rate of photosynthesis at this specific growth rate, yet the specific growth rate is not so high that appreciable light is transmitted through the culture.

This optimum may shift slightly as a function of incident light intensity, but this was not investigated experimentally. At higher incident light intensities the optical thickness of the culture will increase at any given value of μ, tending to shift the optimum to a higher value of μ. But higher incident intensities may result in slightly lower chlorophyll contents (see Table II), tending to decrease optical thickness, and off-setting the increased cell concentration.

To increase productivity at a given incident light intensity we must increase the efficiency at either low light intensities, or high light intensities, or both. Increasing the efficiency of energy conversion at low light intensities means that the maximum quantum efficiency must be increased. This does not appear possible for Chlorella pyrenoidosa, since we found that Φ, the maximum quantum efficiency, was equivalent to one O_2 molecule evolved for each 8.8 quanta absorbed. This is close to the minimum of one O_2 per 8

quanta required for a photosynthetic system with two light reactions.

Thus, we must increase the efficiency at high light intensities, i.e., increase the light saturated rate of photosynthesis (on a per unit chlorophyll basis!). Species of algae should be screened to find those with high light saturated rates. Chlorella pyrenoidosa is notable for its low light saturated rate, even when grown at high specific growth rates. Algae with low pigment concentrations should particularly be examined, since these may have the quality for which we are looking, a high value for the ratio:

$$\frac{\text{concentration of the enzymes that determine light saturation}}{\text{concentration of the pigments that determine light absorption.}}$$

Schmid and Gaffron (1967) have investigated tobacco mutants that have much lower percentage chlorophyll content, but have a much higher light saturated rate of photosynthesis on a chlorophyll basis, and even on an area basis. This is exactly as expected from the above agruments.

Another way of achieving a high value for the above ratio is to illuminate with light sources having large amounts of their radiation in regions that are not strongly absorbed. For green algae this would be in the yellow and green wavelength regions. However, according to Emerson and Lewis (1943), one may have to sacrifice some in maximum quantum efficiency, Φ, particularly in the green region.

NOMENCLATURE

μ = Specific growth rate, day^{-1}

Φ = Maximum quantum yield, moles O_2/einstein

V. THE MAXIMUM RATE OF BIOLOGICAL PROCESSES

The rate of a biological process is limited by the enzymatic reaction having the smallest maximum forward rate. In other words, the rate of a series of linked enzymatic reactions cannot exceed the maximum rate of the slowest step.*

When virtually all molecules of an enzyme are saturated with its substrate, the enzyme has reached its maximum forward rate. Consider a process, such as photosynthesis, containing an enzymatic step that is proceeding at its maximum rate. Since this enzymatic reaction is one of a series of steps in the process, then the process must be at its maximum rate. The maximum rate of the process is independent of any other enzymatic steps, even if some of these other steps have maximum rates only slightly greater than the maximum rate of the slowest.

The process has reached its maximum rate when no external substrate, such as light intensity or CO_2 concentration, is limiting. Conversely, when an external substrate limits, neither the process nor any of the steps in it is operating at its maximum rate.

We will mathematically prove the above conceptual arguments for a simplified model consisting of N consecutive reversible Michaelis-Menten enzymatic reactions. The case of a <u>single</u> enzyme substrate complex undergoing successive transformations, as described by Hearon (1952), should not be confused with this case. Here, the product of each enzymatic reaction is the substrate for the next. There is one external limiting substrate, S.

---

*An exception exists. Consider two parallel reaction sequences producing the same product. Two enzymes, one in each of the parallel sequences, must reach their maximum rates before the process reaches its maximum rate. But if we treat these two limiting steps as a single enzyme, then the above arguments hold.

$$S + E_1 \underset{k_{-1}}{\overset{k_1}{\rightleftharpoons}} SE_1 \underset{k'_{-1}}{\overset{k'_1}{\rightleftharpoons}} P_1 + E_1$$

$$P_1 + E_2 \underset{k_{-2}}{\overset{k_2}{\rightleftharpoons}} P_1E_2 \underset{k'_{-2}}{\overset{k'_2}{\rightleftharpoons}} P_2 + E_2$$

$$\vdots$$

$$P_{n-1} + E_n \underset{k_{-n}}{\overset{k_n}{\rightleftharpoons}} P_{n-1}E_n \underset{k'_{-n}}{\overset{k'_n}{\rightleftharpoons}} P_n + E_n$$

$$\vdots$$

$$P_{N-1} + E_N \underset{k_{-N}}{\overset{k_N}{\rightleftharpoons}} P_{N-1}E_N \underset{k'_{-N}}{\overset{k'_N}{\rightleftharpoons}} P_N + E_N$$

E denotes the enzyme, P denotes the products of the enzymatic reactions, and k denotes the rate constants. Catalysis occurs in the substrate-enzyme complexes, such as $P_{n-1}E_n$. In this general case no reaction steps are considered to be irreversible; irreversibility is approached only by virtue of a large negative free energy change.

The velocity of the nth reaction, v_n, is found by assuming that steady state conditions are obtained. Steady state may be assumed even if we consider an autocatalytic process such as balanced cellular growth, if we express enzyme concentrations per unit of cellular mass. The solution (Haldane, 1930) is given here with v_n implicity expressed:

$$[P_{n-1}] = \frac{[P_n](V_{Bn} + v_n) + K'_n v_n}{K'_n/K_n(V_{Fn} - v_n)}, \qquad (5\text{-}1)$$

where $[P]$ and $[P_{n-1}]$ are concentrations of species P_n and P_{n-1}; v_n is the net rate of enzymatic reaction; $V_{Fn} = k'_n[E^0_n]$, the maximum forward rate; $V_{Bn} = k_{-n}[E^0_n]$, the maximum backward rate; $[E^0_n]$ is the total concentration of the nth enzyme; $K_n = (k_{-n} + k'_n)/k_n$; $K'_n = (k_{-n} + k'_n)/k'_{-n}$.

All of the individual reactions give equations of the form of Equation (5-1). We obtained the solution for the whole system of N equations by realizing that at steady state $v = v_1 = v_2 = \cdots = v_n \cdots = v_N$ and by making successive substitutions until the concentration of S, $[S]$, is related only to v and $[P_N]$, the concentration of final product. If P_N is a cellular constituent and cellular growth is balanced, then $[P_N]$ is constant with time (when expressed per unit of cellular mass). The solution is:

$$[S] = \sum_{n=1}^{N} \frac{K_n \prod_{i=1}^{n} (V_{B_{i-1}} + v)}{\prod_{i=1}^{n} \frac{K'_{i-1}}{K_{i-1}} (V_{Fi} - v)} + \frac{[P_N] \prod_{n=1}^{N} (V_{Bn} + v)}{\prod_{n=1}^{N} \frac{K'_n}{K_n} (V_{Fn} - v)}, \qquad (5\text{-}2)$$

where V_{Bo} is defined equal to zero, and K'_o/K_o is defined equal to one. If, for example, we have three enzymatic reactions, N = 3, and:

$$[S] = \frac{K_1 v}{(V_{F1} - v)} + \frac{K_2 v (V_{B1} + v)}{\frac{K'_1}{K_1}(V_{F1} - v)(V_{F2} - v)} + \frac{K_3 v (V_{B1} + v)(V_{B2} + v)}{\frac{K'_1}{K_1}\frac{K'_2}{K_2}(V_{F1} - v)(V_{F2} - v)(V_{F3} - v)}$$

$$+ \frac{[P_3](V_{B1} + v)(V_{B2} + v)(V_{B3} + v)}{\frac{K'_1}{K_1}\frac{K'_2}{K_2}\frac{K'_3}{K_3}(V_{F1} - v)(V_{F2} - v)(V_{F3} - v)}. \qquad (5\text{-}3)$$

In Equations (5-2) and (5-3), the steady state rate of the system, v is implicitly expressed, whereas the concentration of external substrate, $[S]$, is explicitly given.

In Equation (5-2) or (5-3), it should be readily observed that the maximum rate for the system is set by, and cannot exceed, the smallest V_{Fn}, since [S] approaches infinity as v approaches the smallest V_{Fn}. Thus, the enzymatic reaction having the smallest maximum forward rate sets the maximum rate for the whole system: a barrier that cannot be exceeded. An interesting corollary is that when [S] is large (i.e., not limiting), the system rate is operating near the maximum rate as set by the slowest V_{Fn}.

Such a limiting step cannot occur in chemical reactions of higher than zero-order (Denbigh et al., 1948), but does occur in enzymatic reactions, since an enzymatic reaction approaches zero-order as it nears its maximum rate.

Care must be used not to carry this concept of a limiting enzymatic reaction too far. Even though the slowest reaction sets the maximum rate for the system, it does not entirely determine the rate of the process as a function of limiting substrate concentration. At low external substrate concentrations, [S], all of the reactions in the series may influence the overall rate. For the system discussed above, the exact relationship is given by Equation (5-2).

NOMENCLATURE

E	= Enzyme
k	= Rate constant
K	= Equilibrium constant
N	= The total number of enzymatic steps in the sequence
P	= The product of an enzymatic reaction
S	= The substrate of the first enzymatic reaction in the sequence
v	= Net rate of an enzymatic reaction, moles/time/mass dry weight
V	= Maximum velocity, either forward or backward, of an enzymatic reaction, moles/time/mass dry weight
[ ]	= Concentration of the item enclosed, moles/mass dry weight

Superscripts

o	= Total amount of all states or forms of the species subscripted
'	= Denotes breakdown of substrate-enzyme complex to product or the reverse reaction

Subscripts

B	= Backward
F	= Forward
$1, 2, \cdot\cdot n, \cdot\cdot N$	= Number of the step in the sequence; if positive, the forward direction is implied; if negative, the backward direction is implied.

VI. PHOTOSYNTHESIS IN OPTICALLY THIN SUSPENSIONS

A. A MATHEMATICAL MODEL FOR THE LIGHT RESPONSE CURVE OF PHOTOSYNTHESIS

In Chapter II previous work on the mathematical modeling of the rate of photosynthesis as a function of light intensity was reviewed. These attempts in modeling the light response curve have largely been empirical. One exception is the model presented by Lumry et al. (1959) and Lumry and Rieske (1959). The Lumry model gives the rectangular hyperbola function expressed by Equation (2-16). The Lumry model was first proposed for the ferricyanide Hill reaction, but Lumry and co-workers (Muller et al., 1969) have recently suggested that this model may be valid also for overall photosynthesis. The Lumry model has been put to use by other workers, such as Fredrickson et al. (1961), attempting to model the performance of optically dense suspensions. But the Lumry model suffers when applied to overall photosynthesis, since it assumes only one light reaction and that the limiting step is the regeneration of an activated chlorophyll by a dark reaction. It now appears that there are at least two light reactions in photosynthesis, and that the rate limiting step is not the regeneration of any primary chemical trap. This latter point will be fully discussed in this chapter.

While the Lumry model appears to fit experimental ferricyanide Hill reaction data, it does not fit most data obtained for the overall rate of photosynthesis as a function of light intensity. Our data shown in Figs. 14 and 17, as well as the data of many other workers such as Kok (1956), Myers and Graham (1959)*, Steeman Nielsen and Jorgensen (1968), Pickett and Myers (1966), and Bonaventura and Myers (1969), give light response curves that "bend over" to the light saturated rate faster than predicted by the Lumry model.

*Some of the data of Myers and Graham is shown replotted in Fig. 4.

Some data taken on Chlorella do not show this fairly sharp bend over to the light saturated rate. Where the experimental conditions are given, such as by Shugarman and Appleman (1967), the missing bend can be explained on the basis that the data were taken on a suspension of algae that was not optically thin. Indeed, it is impossible to obtain a truly optically thin suspension of algae. A Chlorella cell can absorb as much as 40% of the light passing through it, causing an unequal illumination of the chlorophyll molecules within the cell. If this problem could be eliminated, the bend over to the saturated rate would be sharper than has been experimentally measured thus far.

A distinct characteristic of the Lumry model, or any rectangular hyperbola, is that the slope of the curve measured at one-half of the maximum rate should be one-quarter of the initial slope.* This rough check may be used at a glance, rather than going to the trouble of making a double reciprocal plot, such as Fig. 16, which also shows the strong deviations of overall photosynthesis from the Lumry model.

Further questions must also be raised, which no previous mathematical model of photosynthesis can answer. Why, as shown in Chapter III, can the light saturated rate for the quinone Hill reaction exceed the light saturated rate for overall photosynthesis? Why, as also shown in Chapter III, does the light saturated rate of photosynthesis change with growth conditions? Why, as shown in Figs. 4, 14, and 17, are the initial portions of the light response curves identical for algae grown in different conditions, but with light saturation being achieved by the various plateaus "peeing off" a curve that, initially at least, appears similar to the shape of a rectangular hyperbola? Why does the shape of our light response curves for the quinone Hill reaction, as given in Fig. 20, as well

*This is found by taking the derivative of the rectangular function with respect to the independent variable, which in this case is light intensity.

as the Hill reaction data of Lumry et al. (1959), Sauer and Biggens (1965), and others, conform closely to the shape of a rectangular hyperbola? In addition to answering the above four questions, can a mathematical model be devised based upon current knowledge of the chemical kinetics of the photosynthetic electron transport system and the carbon fixation cycle?

We believe a mathematical model can be devised that will provide satisfactory answers to all of the above questions. In devising the following model, heavy reliance is placed upon the kinetic data for the photo-electron transport system as obtained from the laboratories of Kok and Joliot. Before listing the bases and assumptions of our mathematical model for the light response curve, it should be mentioned that present day knowledge of the process of photosynthesis is far from complete, but we believe the following model to be consistent with the current picture. Figure 30, a diagrammatic scheme of our model, should be referred to at this point. Nomenclature given to chemical intermediates follows Kok et al. (1969).

Bases and Assumptions

1. Following Joliot et al. (1968), it is assumed that Photoact II is the reduction of Q by a quantum absorbed by System II pigment:

$$Q \xrightarrow{h\nu} Q^-$$

Q is assumed to be the primary chemical trap for System II. The fraction of open System II traps is $q = [Q]/[Q_0]$.

Similarly, Photoact I is the oxidation of P^- by a quantum absorbed by System I pigment:

$$P^- \xrightarrow{h\nu} P$$

P is assumed to be the primary chemical trap for System I, the chlorophyll a molecule P_{700}. The fraction of open System I traps is $p = [P^-]/[P_0]$.

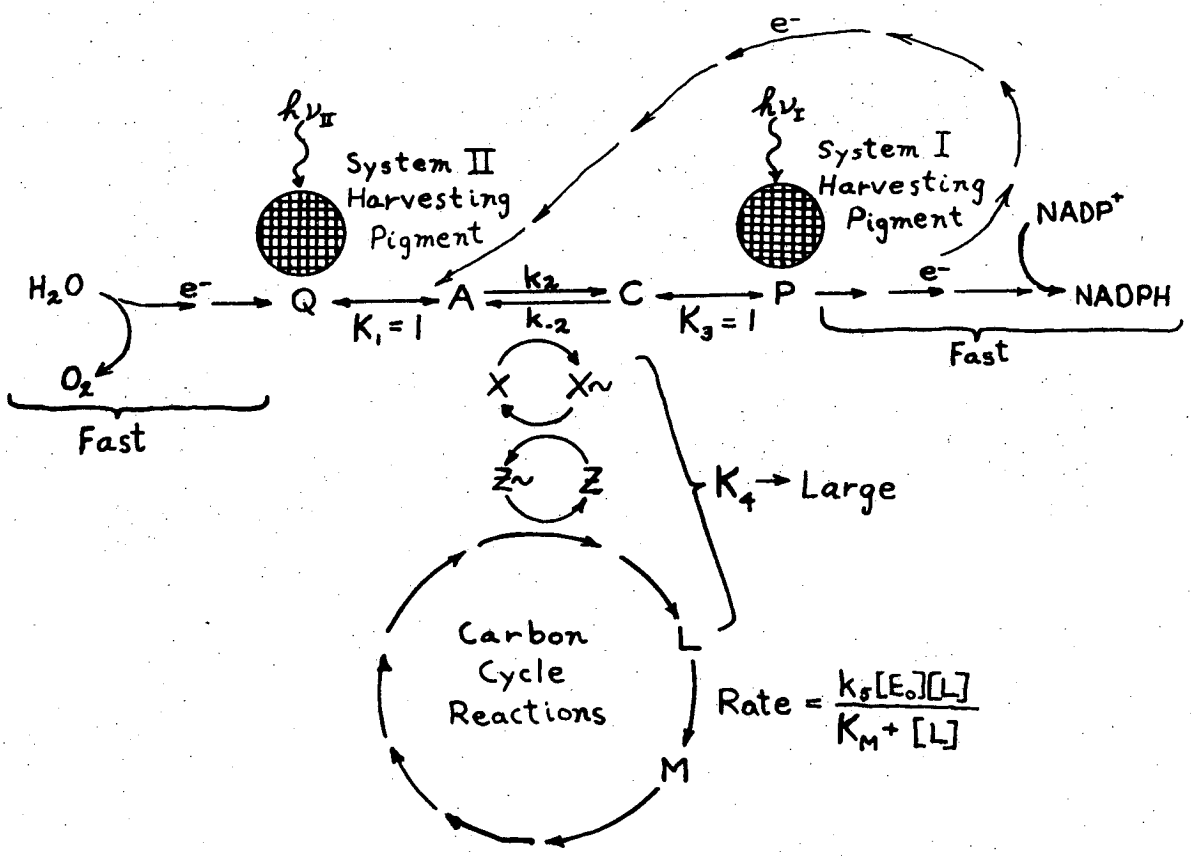

XBL 709-6501

Fig. 30. Our model for the light response curve of photosynthesis. This model assumes that a reaction in the carbon fixation cycle sets the light saturated rate of photosynthesis, and that its effect is manifested through the ATP generating system (Z ~ = ATP).

2. It is assumed that the trapping of absorbed light quanta by either photosystem can be described by the model of Joliot et al. (1966):

$$\text{Rate of trapping} = \psi \frac{f}{1-a(1-f)} \qquad (6-1)$$

where ψ is equal to the rate of absorpton of light by a particular photosystem times a maximum quantum efficiency, f is the fraction of open traps (equal to q in the case of System II and p in the case of System I), and a is a probability of quantum transfer between separate pigment units of a particular photosystem. Joliot's model assumes only one primary chemical trap per pigment aggregate and "perfect trapping". "Perfect trapping" results when the rate constant for photochemical trapping is much larger than the rate constants for dissipation of excitation energy into either heat or fluorescence. The reader should refer to Appendix III for the derivation of Equation (6-1) and a further discussion of Joliot's model.

3. Based on the modulated electrode results of Joliot et al. (1968), it is assumed that there is no possibility of photon excitation energy transfer between separate pigment aggregates of System I. Thus, for System I the term a in Equation (6-1) is equal to 0.0, and the rate of trapping is linearly related to the fraction of open System I traps, p.

As discussed in the above paper of Joliot et. al., their System I results can be physically interpreted in two ways: (1) Each P is associated with a certain number of harvesting chloro chlorophylls as a completely isolated unit. (2) An incoming quantum is always trapped by the trapping centers of System I, regardless of whether P is in the open or closed state. If P is in the closed state, the quantum is wasted. Regardless of which physical model is correct, the mathematics may be expressed by Equation (6-1) with a = 0.0.

4. The probability of photon excitation energy transfer between separate units of System II, a_2, is assumed to be equal to 0.5. Thus, the term a in Equation (6-1) is equal to 0.5, and Equation (6-1) becomes: rate of trapping $= \psi_2 \frac{2q}{1+q}$, for System II.

The probability of excitation energy transfer for System II has ranged between 0.5 and 0.6 based on the fluorescence work with Chlorella of Joliot and Joliot (1964), the fluorescence work with isolated chloroplasts of Forbush and Kok (1968), and the modulated electrode results of Joliot et al. (1968) with isolated chloroplasts. Joliot et al. comment that the System II value for a of 0.5 - 0.6 appears to be an invariant characteristic of photosynthetic material.

5. It is assumed that there is no transfer of excitation energy from System II to System I (spillover), or vice versa (Joliot et al., 1968, Kelly and Sauer, 1965, Eley and Myers, 1967).*

6. It is assumed that the reactions between oxygen evolution and System II are irreversible and infinitely fast; therefore these steps need not be considered in the mathematical model. These steps are fast, since the quinone Hill reaction may proceed faster than overall photosynthesis, as was shown in Chapter III. The data of Joliot (1966) and Sinclair (1969) also show these steps between oxygen evolution and System II to be quite fast compared to the overall rate of photosynthesis. Sinclair believes the rate constant for the transfer of electrons from water to System II to be about 5000 sec^{-1}, assuming first-order reaction kinetics. Assuming 500 chlorophyll molecules for each System II trap, Q (Joliot, 1965a, 1965b), this is equivalent to an oxygen evolution rate of 220 ml of oxygen/mg total chlorophyll/hr. This is much higher than the highest rate measured in Chapter II for overall photosynthesis, which was about 9 ml O_2/mg chlorophyll/hr.

*The recent results of Avron and Ben-Hayyim (1969) and Murata et al. (1970) suggest that this assumption may not be correct, at least not under all conditions.

7. Similarly, all electron transport steps beyond System I are assumed to be irreversible and infinitely fast. This assumption is based on the results of Izawa et al. (1966) that showed electron transport through System I (from ascorbate to methyl viologen) is fast. These workers measured, in DCMU* poisoned chloroplasts, a rate of electron transport as high as 6000 eq/chlorophyll/hr. This is equivalent to 32 ml O_2/mg chlorophyll/hr.

8. With the two above assumptions, the only kinetics of electron transport that are important are those located between the two photosystems. Yet as far as our steady state mathematical model is concerned, the relative pool sizes of the components shown on Fig. 30 are not important. With transient kinetics, however, the concentrations of these components would have to be considered. For information on the chemical identifies and relative pool sizes of the intermediates, Q, A, C, and P, the reader is referred to Chapter I.

9. It is assumed that Q and A are in equilibrium with regard to electron transfer and that the concentrations of the reduced and oxidized forms of Q and A are related by an equilibrium constant, K_1, that is equal to 1.0. Using spinach chloroplasts, Forbush and Kok (1968) followed the fluorescence decay curve after illumination with a brief intense flash of light and found the half time of reoxidation of reduced Q by the A pool was 0.6 msec. Assuming first-order kinetics and 500 chlorophyll molecules for each Q, a half time of 0.6 msec corresponds to an oxygen evolution rate of 50 ml O_2/mg chlorophyll/hr. This is more than 5 times the maximum rate of oxygen evolution measured in Chapter III. Forbush and Kok also found that the equilibrium constant for this reaction was in the order of unity.

10. Similarly to the above, it was assumed that the oxidized and reduced forms of C and P are in equilibrium and are related by an

*3-(3, 4-dichlorophenyl)-1, 1-dimethylurea.

equilibrium constant, K_3, that is equal to 1.0. This assumption is based upon the results of Kok et al. (1969). These workers viewed the photo-oxidation of P (P_{700}) with a 700 nm measuring beam. When a bright 10^{-5} sec flash was given, all P was instantly oxidized, but very quickly a signal was regenerated showing half of the original reduced P to be present. Kok et al. interpreted this to mean that another component, C, must be present, which is present in approximately the same concentration as P and related to P by an equilibrium constant of about unity.

11. The electron transport reactions within the photosynthetic electron transport chain will be assumed to be describable by bimolecular chemical kinetics. This assumption is made in spite of the fact that it now appears possible that the intermediates between the two photosystems may consist of independent reaction chains, containing one P and one Q, along with the other constituents. Direct experimental evidence for independent reaction chains has been given by Kok et al. (1969), and indirect mathermatical arguments have been presented by Malkin (1969).

Even if this independent reaction chain hypothesis is correct, it will not be used for the mathematical model developed here. To do so would make the mathematics much more complicated. Separate chain reaction kinetics are discussed in Appendix I. When the equilibrium are equal to 1.0, as K_1 and K_3 are assumed to be, there is no difference between separate chain kinetics and the bimolecular reaction kinetics assumed here. Only in the transfer of electrons from A to C will independent reaction kinetics make a difference. But even here, as Forbush and Kok have pointed out, bimolecular kinetics will not be far wrong, since the pool size of A is large. Appendix I should be referred to for further elaboration of these points.

It could also be assumed that the electron transport reactions follow Michaelis-Menten type enzyme kinetics, rather than bimolecular reactions. There are two reasons we do not use enzyme

kinetics to describe these reactions. First, most of the intermediates between the two photosystems appear to be membrane bound. If these intermediates do form completely independent reaction chains, then all must be tightly membrane bound.* Such a system could not follow Michaelis-Menten type kinetics, since no substrate-enzyme association-dissociation equilibria would be involved. Second, even if all electron transport reactions were describable by Michaelian enzyme kinetics, bimolecular kinetics would be appropriate if the enzymes involved are working in a region well below their saturated rates. It will be shown later that the saturated rate of electron transport appears to be somewhat larger than the light saturated rate of photosynthesis in Chlorella pyrenoidosa.

12. Fundamental to this model is the assumption that the rate limiting step in photosynthesis is located outside the photosynthetic electron transport system. Nevertheless, this slow step has an effect upon the photo-electron transport system, since this slow step is coupled, through a sequence of reactions, to electron transport at the phosphorylation site or sites. This rate limiting step may be located in the carbon fixation cycle, as shown in Fig. 30. Indirect evidence exists that the limiting step, at least in some plants, is the CO_2 fixing enzyme, carboxydismutase (Bjorkman, 1968a, 1968b). This enzyme must be the limiting step at low non-saturating concentrations of CO_2, unless there is some effect of CO_2 on another enzyme.

More direct evidence that the photosynthetic electron transport system does not itself contain the rate limiting step in photosynthesis was provided by Kok et al. (1969). Their experiments showed that a pool of intermediate, X, is coupled to the electron transport chain at a point between A and C. Movement of electrons

*The work of Katoh and Takamiya (1963), however, suggest that at least one component needed for electron transport, plastocyanin, is unbound or only loosely bound.

from A to C produces X~, a high energy intermediate that could either be or produce the proton gradient shown to exist across chloroplast membranes by Hind and Jagendorf (1963). This high energy intermediate, X~, is coupled to the manufacture of ATP from ADP.

In the scheme shown in Fig. 30, it is assumed that X~ is used to generate Z~(Z~ is ATP and Z is ADP), which is coupled to a carbon cycle intermediate. Kok et al. (1969), using spinach chloroplasts, obtained results that suggested that the flow of electrons from A to P is controlled by a slow step located in, or connected to the phosphorylation mechanism. Apparently, however, similar experiments have not been performed on whole algae.

ATP itself need not be involved in the bottleneck step. All that is necessary is that the bottleneck step approach its saturated rate. This causes the intermediates in front of L to accumulate; eventually ATP accumulates, and the increased ATP concentration slows down the rate of electron transport.

13. The assumption that only one enzymatic reaction in the carbon cycle sets the light saturated rate of photosynthesis is not unreasonable. In Chapter V it was shown that the rate of a biological process is limited by the enzymatic reaction having the smallest maximum forward rate. No other enzymatic reaction has any influence on the maximum rate.

14. It is assumed that all reactions between X and the rate-limiting step are fast and in equilibrium with each other. It is also assumed that the concentration of the carbon cycle intermediate that reacts with Z~ is constant.

It has been shown that all enzymatic reactions in a metabolic sequence do not proceed at more or less the same maximum forward rates. Racker (1965) points out that some of the enzymes of glycolysis exceed by hundreds of times the concentration one would think would be needed. The cell is not foolish, however, and the purpose of these seemingly high concentrations is to ensure that those enzymatic steps are both fast and reversible. Mahler and Cordes (1966) discuss this point in their chapter on the metabolism of carbohydrates:

> "The initial and final reactions in most metabolic sequences, be they anabolic or catabolic, are frequently rigged in such a fashion as to render them virtually irreversible thermodynamically; i.e. they possess $\Delta G^{0'}$ values (which we recall as the standard free energy change at pH 7) equal to $\leq$ -4 kcal/mole. Teleologically the reason for this is not hard to understand. It provides for easy flux through the pathway and minimizes the possibility of a logjam of intermediates somewhere along the line. The enzymes responsible for these essentially irreversible and unique steps have often been referred to as pacemaker enzymes."

Mahler and Cordes also discuss these pacemaker enzymes in regard to induction and repression, and activation and inhibition:

> "We shall see that frequently the most sensitive points for controls of this general nature are those that stand at the beginning or the end of specific metabolic sequences, i.e. the pacemaker enzymes mentioned earlier."

Bassham and Krause (1969) have recently presented evidence for two or three essentially irreversible pacemaker enzymes in the carbon fixation cycle. It would be logical to expect that the slowest of these steps is the rate-limiting step of our model, shown on Fig. 30 as being responsible for the conversion of L to M. We assume that this step can be described by the simple irreversible Michaelis-Menten equation.

15. The equilibrium constant, K_4, relating the concentration of X~, is assumed to be very large relative to K_M, the Michaelis constant for the conversion of L to M. This assumption is justified on three grounds: (1) Overall metabolic sequences in biochemical systems occur spontaneously; this means a large equilibrium constant must be associated with the sequence, i.e. a large negative standard free energy change. (2) The second justification for the large value of K_4/K_M is hindsight. This assumption must be made to obtain the relatively sharp bend in the light response curve as light saturation is approached, which has been experimentally

observed.** (3) The Michaelis constant of intracellular enzymes is usually small.

16. With all of the above assumptions, it will be found from the mathematical analysis that no significant amount of X~ exists below light saturation. X~ is quickly converted by the large equilibrium constant, K_4/K_M, to L-enzyme complex; hence the L to M step can have no effect on the kinetics of electron transport at low intensities. Only when light intensity is increased to the point where the enzyme converting L to M has reached its saturated rate does this step have any effect on electron transport. For at this point, a logjam of intermediates starts backing up behind L, causing the concentration of X~ to increase and diminishing the concentration of X*. This lower concentration of X, since X is a necessary reactant in electron transport, slows down the rate of electron transport such that it must keep pace with the conversion of L to M. Thus, the bottleneck at the L to M conversion manifests itself upon electron transport kinetics by causing a logjam of intermediates all the way from L to X~.

The above picture of a logjam responsible for slowing electron transport may not be entirely correct, since it is difficult to envision any organism allowing such a large logjam to develop. It is reasonable to expect a more sophisticated control system. For instance, as L builds up in concentration, it may inhibit the activity of some of the enzyme farther back up the chain toward X, hence diminishing the size of any logjam. L may also activate various enzymes that permit the leakage of electrons from the electron transport system to molecular O_2, and L might also stimulate the hydrolysis of Z~(ATP) by ATPase. Brown and Weis (1959)

---

*It is assumed that a material balance exists such that $[X] + [X\sim] = [X_0]$ = a constant.

**For the data shown in Figs. 14 and 17, K_4/K_M must be no less than 50.

and Weis and Brown (1959) found, by means of isotopic studies in a mass spectrometer, that "respiration" of photosynthetic reducing power to molecular O_2 increased after light saturation had been reached. Since our model is concerned only with net oxygen production, one need not be concerned with this type of respiration that takes electron from water and then gives the electrons to O_2 forming water once again. However, this type of cycle may have some use to the electron transport system, such as ridding it of excess electrons when light saturation has been reached.

17. A stoichiometric relationship between ATP production and electron transport is assumed. If cyclic photophoshorylation is not considered, it is easy to visualize such a stoichiometric relationship. But cyclic photophosphorylation introduces a complication, for ATP production is not stoichiometrically related to electron transport. In fact, electron transport for cyclic photophosphorylation competes with non-cyclic electron transport.

The answer is to assume that the ratio fo ATP production to the rate of electron transport is constant for any given spectral distribution of light. But we might expect different spectral distributions to result in different ratios of electron transport to ATP production. This ratio may also be dependent on growth conditions. If this ratio is not at its optimum a decrease in the quantum efficiency of CO_2 fixation and O_2 evolution will result. In other words, the variation in the rate of cyclic photophosphorylation will be built into the maximum quantum efficiency of O_2 evolution, Φ, which will be introduced later.

18. The model shown in Fig. 30 assumes that control of the photoelectron transport system is mediated through ATP rather than NADPH. Nevertheless, we have treated the case of NADPH control of the electron transport system. It may be found in Appendix II.

A problem arises if the ratio of NADPH production to ATP production is greater than the cell can utilize in balanced growth.

A hint of what may happen to this excess NADPH is given by the results of Brown and Weis (1959) and Weis and Brown (1959), which were discussed in the above Item 16. If the powerful reducing agents at the top of System I tend to accumulate in their reduced forms, then we might expect them to donate their electrons to molecular O_2, causing the increase in "respiration" that Brown and Weis found when light saturation was reached.

Derivation of the Mathematical Model

As shown in Fig. 30 and previously discussed, we have the following values for the equilibrium constants: $K_1 = 1$, $K_3 = 1$, and K_4/K_M is assumed to be very large. The rate constants, k_2, k_{-2}, and $k_5[E_0]$ will not be predetermined. Indeed, k_{-2} will be seen to drop out of the mathematics entirely. The total pool sizes of Q, A, C, P, and X are present in the concentrations $[Q_0]$, $[A_0]$, $[C_0]$, $[P_0]$, and $[X_0]$.* It will be shown that these pool sizes need not be explicitly determined for the steady state kinetics considered here.

As discussed above in Item 3, the rate of photochemical trapping by the trapping centers of System I is equal to $\psi_1 p$. This assumes the probability of excitation energy transferring between separate System I pigment aggregates, a_1, is equal to 0.0. Similarly, the rate of photochemical trapping by the trapping centers of System II is equal to $\psi_2 \frac{2q}{1+q}$. This assumes that $a_2 = 0.5$, as discussed in Item 4.

At steady state the rates of photochemical trapping by each photosystem must be equal:

$$\frac{d[Q^-]}{dt} = 0 = \psi_2 \frac{2q}{1+q} - \psi_1 p \qquad (6\text{-}2)$$

where $\psi_1 = I \epsilon \phi_1$ and $\psi_2 = I \epsilon \phi_2$. I is the incident light intensity (einstein/cm^2/hr), ϵ is the extinction coefficient of the pigments (cm^2/mg total chlorophyll), and ϕ_1 and ϕ_2 are the maximum quantum

*All concentrations are expressed equivalents per mg chlorophyll.

efficiencies (as I approaches zero) for Systems I and II in terms of electron transport (moles electrons/einstein). Therefore ψ_1 and ψ_2 are the rates of electron transport for the two photosystems when all traps are open, and are directly proportional to the quanta absorbed by each photosystem.

A similar steady state equation may be set up for the conservation of the species A^-:

$$\frac{d[A^-]}{dt} = 0 = \psi_2 \frac{2q}{1+q} - k_2([A_0]-[A])[C][X] + k_{-2}[A]([C_0]-[C])([X_0]-[X]). \tag{6-3}$$

In the above equation use is made of the material balances:

$$[A] + [A^-] = [A_0],\ [C] + [C^-] = [C_0],\ \text{and}\ [X] + [X\sim] = [X_0].$$

One more equation must be given, expressing the steady state rates of formation and disappearance of L:

$$\frac{d[L]}{dt} = 0 = \frac{1}{\beta}\ \psi_2\ \frac{2q}{1+q} - \frac{k_5[E_0][L]}{[L]+K_M} \tag{6-4}$$

where β is a stoichiometric factor equal to the number of electrons that must be transported through the photo-electron transport system so that one L will be converted to M. β is the total number of $Z\sim$ manufactured per electron transported. β is assumed invariant with respect to light intensity, but may be a function of other external variables such as growth conditions or CO_2 concentration. β also includes any contribution that cyclic photophosphorylation may make to ATP production.

Using the equilibrium relations for K_1, K_3, and K_4:

$$K_1 = 1 = \frac{q([A_0]-[A])}{(1-q)[A]} \tag{6-5}$$

$$K_3 = 1 = \frac{p[C]}{(1-p)([C_0]-[C])} \tag{6-6}$$

$$K_4 = \frac{[L][X]}{[X_0]-[X]}\ . \tag{6-7}$$

In these preceding six equations, (6-2) - (6-7), there are six unknowns, therefore all unknowns may be determined. First, [A] and [C] are eliminated from Equation (6-3) by using Equations (6-5) and (6-6). Solving for p:

$$p = \frac{k_2[A_0][C_0][X](1 - q) - \psi_2 \frac{2q}{1+q}}{k_2[A_0][C_0][X](1-q) + k_{-2}[A_0][C_0]([X_0]-[X])q} . \qquad (6\text{-}8)$$

Similarly, [L] can be eliminated from Equation (6-4) by using Equation (6-7). Solving for [X]:

$$[X] = [X_0] \frac{\frac{K_4}{K_M}(\beta k_5[E_0] - \psi_2 \frac{2q}{1+q})}{\frac{K_4}{K_M}(\beta k_5[E_0] - \psi_2 \frac{2q}{1+q}) + \psi_2 \frac{2q}{1+q}} . \qquad (6\text{-}9)$$

Examine the terms within the parentheses of Equation (6-9). The first term, $\beta k_5[E_0]$, is the light saturated rate of photosynthesis and is equal to the maximum rate of the slowest step in the carbon fixation cycle, the conversion of L to M (expressed in terms of electron transport). The second term, $2\psi_2 q/(1+q)$, is equal to the rate of electron transport. The important thing to recognize about Equation (6-9) is that since K_4/K_M is assumed very large, $[X] = [X_0]$ when the rate of electron transport, $2\psi_2 q/(1+q)$, is less than the saturated rate of photosynthesis, $\beta k_5[E_0]$. But when the rate of electron transport is equal to the light saturated rate of photosynthesis, then $[X] = 0$, since a positive term still remains in the denominator. Before proceeding, the reader should convince himself by examining Equation (6-9) that $[X] = [X_0]$, or that $[X] = 0$, and that the transition between these two values occurs sharply. Thus, two cases must be examined, the case where $[X] = [X_0]$, and the case where $[X] = 0$.

Below Light Saturation, $[X] = [X_0]$

Substituting $[X] = [X_0]$ into Equation (6-8) gives:

$$p = \frac{k_2[A_0][C_0][X_0](1-q) - \psi_2 \frac{2q}{1+q}}{k_2[A_0][C_0][X_0](1-q)} . \qquad (6\text{-}10)$$

Note that the back reaction term, containing the rate constant k_{-2}, disappears in this case; the physical significance being that there can be no backward reaction if no $[X^-]$ is present. No $[X^-]$ is present until light saturation is reached, since K_4/K_M is assumed to approach infinity. Substituting Equation (6-10) into Equation (6-2), and clearing of fractions:

$$q^2(\psi_1 - 2\psi_2) + q(2\psi_2 + \frac{2\psi_1\psi_2}{S'_M}) - \psi_1 = 0 \qquad (6\text{-}11)$$

where $S'_M = k_2[A_0][C_0][X_0]$ and is the saturated rate of electron transport intrinsic to the photo-electron transport system (when not coupled to the slower steps in the carbon fixation cycle).

Here we are interested in the case of green plants illuminated by polychromatic white light. It is therefore logical to assume that $\phi_1 \tilde{=} \phi_2$. Even though ϕ_1 may be different from ϕ_2 at any particular wavelength, it will be assumed that over the whole spectrum $\phi_1 = \phi_2$; hence ψ_1 will be equal to ψ_2. Henceforth only the symbol ψ will be used. Equation (6-11) becomes:

$$q^2 - (2 + \frac{2\psi}{S'_M})\, q + 1 = 0. \qquad (6\text{-}12)$$

Using the quadratic formula to solve the above equation for q:

$$q = 1 + \frac{\psi}{S'_M} - \sqrt{\frac{2\psi}{S'_M} + (\frac{\psi}{S'_M})^2} . \qquad (6\text{-}13)$$

The negative square root is chosen as the only physically realistic one. The rate of electron transport, R_{ET}, is equal to $2\psi q/(1+q)$.

Since q is given by Equation (6-13):

$$R_{ET} = \frac{2\psi\,(S'_M + \psi - \sqrt{2S'_M\psi + \psi^2})}{2\,S'_M + \psi - \sqrt{2S_M\psi + \psi^2}} \,. \qquad (6\text{-}14)$$

Equation (6-14) may be rearranged to give a more convenient form:

$$R_{ET} = \frac{2\psi\,S'_M}{2S'_M + \psi + \sqrt{2S'_M\psi + \psi^2}} \,. \qquad (6\text{-}15)$$

Equation (6-15) is similar in form to a rectangular hyperbola, except for the added square root term in the denominator. In fact, this equation would have been a rectangular hyperbola if K_1 and/or K_3 had been assumed to have certain slightly different values. Equation (6-15) gives a nearly straight line on a double reciprocal plot, and since K_1 and K_3 are not known with great certainly, we have no strong preference for Equation (6-15) over the rectangular hyperbola function or any other form resulting from a slight variation in the equilibrium constants.

Above Light Saturation, $[X] = 0$

When the step that converts L to M has reached its saturated rate and can no longer accommodate all of the X~ that the photoelectron transport system is capable of generating, $[X] = 0$. At this point the model predicts that intermediates back up behind L, causing a logjam that converts all X to X~. As discussed in the above Item 16, feed-back inhibition, rather than the logjam of intermediates predicted by our mathematical model, may be the main control mechanism. The effect is the same in either case: control such that the net rate of electron transport is no greater than the saturated rate of photosynthesis, $\beta k_5[E_0]$.

The mathematics of this situation are expressed in Equation (6-9). When the rate of electron transport, $2\psi\,q/(1+q)$, equals

the saturated rate of photosynthesis, $\beta k_5 [E_0]$, the numerator quickly goes to zero while the denominator is still positive. The rate of electron transport can never exceed the saturated rate of the limiting step, or the numerator and [X] would become negative, which is physically impossible. Thus, above light saturation:

$$R_{ET} = S'_A, \text{ when } \psi \geq \frac{S'_A (4 S'_M - S'_A + \sqrt{(S'_A)^2 + 8 S'_M S'_A})}{4 S'_M - 4 S'_A} \qquad (6\text{-}16)$$

where $S'_A = \beta k_5 [E_0]$ and is the actual light saturated rate of electron transport.

All previous equations in this chapter have been in terms of electron transport. They will now be put in terms of oxygen evolution, since this is the quantity most often experimentally measured.

The Light Response Curve in Terms of Oxygen Evolution

In terms of oxygen evolution Equations (6-15) and (6-16) become:

$$R_{O_2} = \frac{2 \Phi \epsilon I S_M}{2 S_M + \Phi \epsilon I + \sqrt{2 \Phi \epsilon I S_M + \Phi^2 \epsilon^2 I^2}},$$

$$\text{when } I \leq \frac{S_A (4 S_M - S_A + \sqrt{S_A^2 + 8 S_M S_A})}{4 S_M - 4 S_A} \qquad (6\text{-}17)$$

$$R_{O_2} = S_A, \text{ when } I \geq \frac{S_A (4 S_M - S_A + \sqrt{S_A^2 + 8 S_M S_A})}{4 S_M - 4 S_A} \qquad (6\text{-}18)$$

where:

R_{O_2} = rate of O_2 evolution (moles O_2/hr/mg chlorophyll)

Φ = maximum quantum yield, as I approaches zero (moles O_2/einstein)

ϵ = extinction coefficient of the pigments, expressed as a function of wavelength (cm^2/mg chlorophyll)

I = light intensity, expressed as a function of wavelength (einsteins/cm^2/hr)

S_M = the saturated rate of O_2 evolution intrinsic to the photo-electron transport system (when no steps in the carbon fixation cycle limit) (moles O_2/hr/mg chlorophyll)

S_A = the actual saturated rate of O_2 evolution, caused by a bottleneck in the carbon fixation cycle (moles O_2/hr/mg chlorophyll)

Figure 31 shows a representative plot for Equations (6-17) and (6-18).

S_M is the maximum possible rate of photosynthesis. But S_M will be realized only when the photo-electron transport system is not coupled to the carbon fixation cycle or when the maximum forward rates of all enzymatic reactions in the carbon fixation cycle are larger than S_M. Note that there are three constants to be determined in Equation (6-17) and (6-18), Φ, S_M, and S_A. Φ is the maximum quantum yield, which must be measured at low light intensities. In Chapter III, by fitting our respirometer data on Chlorella pyrenoidosa to Equation (6-17), we found a value for Φ of 0.114. The other two experimental constants, S_M and S_A, may be estimated from a double reciprocal plot, such as Fig. 32, or may be more accurately determined by a non-linear least squares fitting procedure. In Chapter III, S_A was found to change with growth conditions, but Φ and S_M did not appear to vary with the growth conditions that we investigated.

The questions raised at the beginning of this chapter may now be answered. The light saturated rate for the quinone Hill reaction may exceed the light saturated rate for overall photosynthesis, since the quinone Hill reaction is uncoupled from the carbon fixation cycle, in which the rate limiting step in photosynthesis appears to be located.

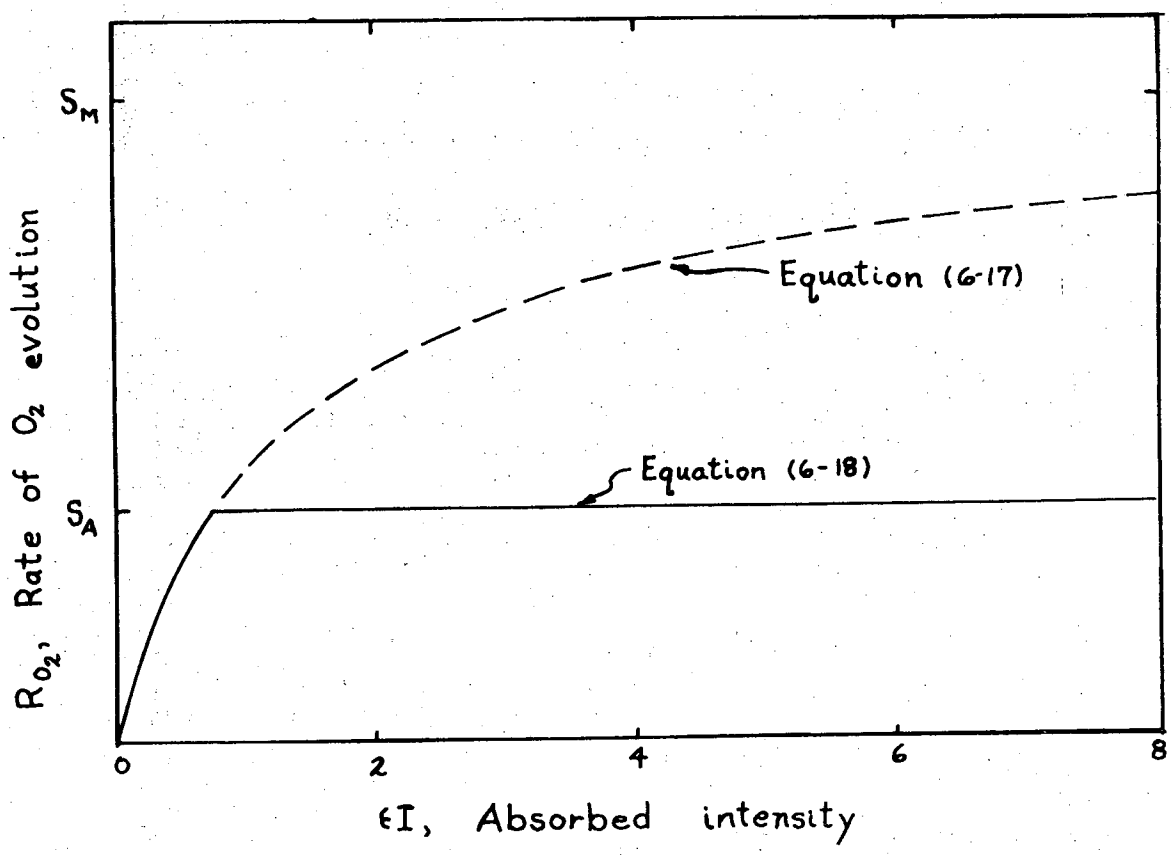

XBL 709-6500

Fig. 31. A typical light response curve generated by Equations (6-17) and (6-18), which express our mathematical model for the light response curve of photosynthesis.

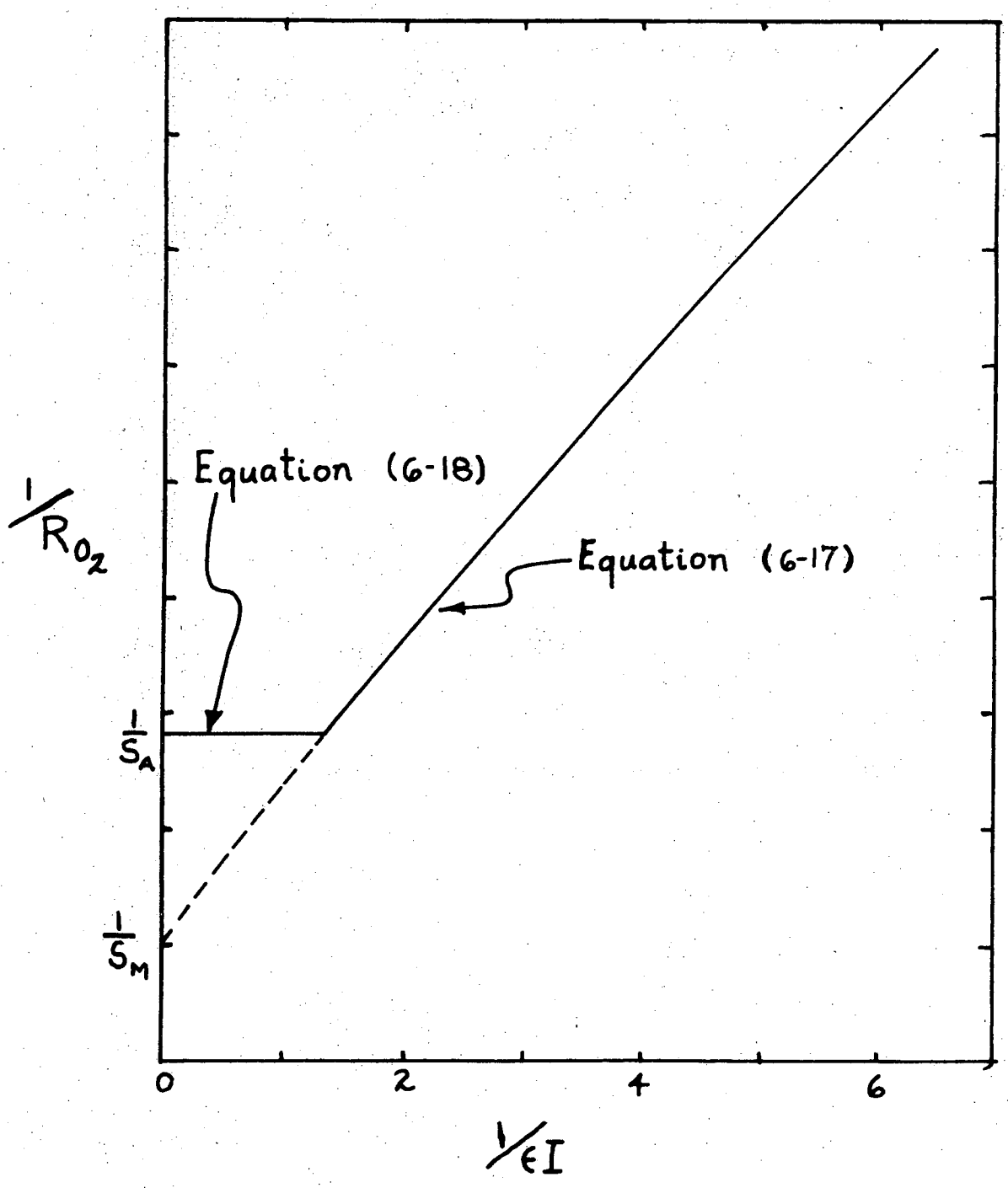

XBL 709-6499

Fig. 32. A double reciprocal plot of the curves shown in Fig. 31.

The next question asked why the light saturated rate of photosynthesis, S_A, changes with growth conditions. The explanation is that the concentration of the limiting enzyme per mg chlorophyll changes with growth conditions. In Chapter IV, we proposed that this adaptive response may be of value to the Chlorella cell in its competition for survival.

A further question asked why the initial portions of the light response curve were the same, regardless of growth conditions. The photosynthetic electron transport system governs the quantum efficiency, Φ, and the saturated rate intrinsic to the electron transport system, S_M. Apparently these quantities, which determine the initial portion of the light response curve, do not change with the growth conditions investigated. This suggests that although chlorophyll content may change, the ratio of components along the photoelectron transport chain may not change with respect to each other.

The Sharp Bend in the Light Response Curve

The mathematical model just developed, expressed by Equations (6-17) and (6-18), predicts a sharp bend in the light response curve when light saturation is reached. Experimental data do not show such a perfectly sharp bend. There are four reasons why experimental data show light response curves that are rounded in the region where light saturation is approached.

1. The equilibrium constant K_4/K_M, which relates the concentration of X to the concentration of L, in reality cannot be equal to infinity, as was assumed in the derivation. The smaller the value of K_4/K_M, the more pronounced will be the rounding at the transition to light saturation.
2. Even if K_4/K_M does approach infinity, the assumption that the reactions involved in this equilibrium are so fast that their kinetics need not be considered is an oversimplification. No reactions proceed at an infinitely fast rate. The farther this assumption is from the truth, the more rounded will be the break point.

3. A rounding at the transition will be present in experimental data simply because it is impossible to illuminate equally all chlorophyll molecules in an algal suspension. Because light is absorbed as it passes through an algal cell, the chlorophyll molecules on the far side of the cell receive less illumination than those nearer the light source.

4. All cells within a suspension are not identical. The light saturated rate of photosynthesis, S_A, may change with life cycle stage. This problem might be reduced by the use of synchronous cultures.

We can expect all four of these phenomena to cause experimental data to deviate from the mathermatical model. Therefore it is surprising that the experimental light response curves of Chapter III bend as sharply as they do as light saturation is approached.

But what if several slow reactions in the carbon fixation have similar maximum forward rates? Only one such slow reaction was considered in the mathematical model. If K_4/K_M is reversible and very large, as assumed in our mathematics, only the slowest of these several slow reactions have any effect on the light response curve. In Chapter V it was shown that the maximum rate of a sequence of reactions is set by the reaction with the smallest maximum forward rate. Only when light intensity is raised to the point where the maximum rate of the slowest step is reached will there be a back-up of intermediates, causing an accumulation of $X^{\sim}$, and resulting in a limitation in the rate of electron transport. Because K_4/K_M is very large, none of the slow steps exert any effect until the slowest has reached its maximum rate; at this point the light response curve bends over sharply to a flat plateau. The magnitude of this plateau is set by the slowest, and only the slowest of the slow steps in the carbon fixation cycle. If K_4/K_M does not approach infinity, other slow steps will influence the shape of the light response curve at intermediate light intensities, but not at very low or very high intensities.

B. THE SIGNIFICANCE OF THE SHAPE OF THE LIGHT RESPONSE CURVE OF THE SYSTEM II HILL REACTION

There are at least two types of Hill reactions (partial reactions of photosynthesis involving artificial electron acceptors and donors) investigated by workers in recent years. Hill oxidants such as ferricyanide, DCPIP,* and quinone probably involve only System II, while low redox potential oxidants such as NADP and methylviologen almost certainly involve System I as well. Here we will discuss only the former type, which we will call the System II Hill reaction.

How does one explain the experimental data of Lumry et al. (1959), Sauer and Biggens (1965), and our own, showing the rate of the System II Hill reaction as a function of light intensity to be approximately a rectangular hyperbola? Two possibilities will be considered. In the first case it is assumed that the regeneration of the primary System II chemical trap, Q, is the rate limiting step. In the second case, which will be shown to be more realistic, it is assumed that the regeneration of a secondary chemical trap, A, is the rate limiting step.

Case 1: The Regeneration of the Primary Chemical Trap, Q, as the Rate Limiting Step

This first case is similar to the Lumry model as derived by Lumry et al. (1959). As in the Lumry model, we assume the rate limiting step is the regeneration of the primary chemical trap, Q. But unlike the Lumry model, we assume there is a 50 per cent probability of excitation energy transfer between the separate System II units, based on the results of Joliot and Joliot (1964), Joliot et al. (1968), and Forbush and Kok (1968).

A steady state equation, similar to Equation (6-2) may be set up for the rate of formation and disappearance of Q^-.

---

*2, 6-dichlorophenolindophenol.

$$\frac{d[Q^-]}{dt} = 0 = \psi_2 \frac{2q}{1+q} - k_1[Q^-] \qquad (6\text{-}19)$$

where the terms are defined as they were for Equation (6-2), but with the addition of the term $k_1[Q^-]$. k_1 is a pseudo first-order rate constant, which will be constant only during the initial stages of the reaction before the concentration of the Hill oxidant has decreased appreciably.

Making use of the material balance, $[Q] + [Q^-] = [Q_0]$, and the definition of q, $q = [Q]/[Q_0]$, $[Q^-]$ is obtained:

$$[Q^-] = [Q_0] + \frac{\psi_2}{k_1} - \sqrt{[Q_0]^2 + \frac{\psi_2^2}{k_1^2}} \,. \qquad (6\text{-}20)$$

The rate of product formation (or rate of electron transport) is:

$$R_{ET} = k_1[Q^-] \qquad (6\text{-}21)$$

$$= \psi_2 + k_1[Q_0] - \sqrt{\psi_2^2 + k_1^2[Q_0]^2} \qquad (6\text{-}22)$$

$$= I\phi_2\epsilon + k_1[Q_0] - \sqrt{(I\phi_2\epsilon)^2 + k_1^2[Q_0]^2} \,. \qquad (6\text{-}23)$$

The above equation is labeled as Case 1 in Fig. 33. Equation (6-23) deviates from the rectangular hyperbola function, which is shown in Fig. 33 labeled Case 2: $K_1 = 0.5$.

But there is another serious problem with the above model. The regeneration of the primary chemical trap, Q, does not seem to be the rate limiting step in the Hill reaction, and Lumry and Rieske (1959) realized that this assumption was fundamental to their derivation. Kelly and Sauer (1968) investigated the DCPIP Hill reaction and found, by using relatively long flashes of light (6-100 msec), a large pool of System II intermediates (1 equiv/55 chlorophylls).* This pool size is 6-10 times higher than the

*This pool is very likely identical to A, as designated in this chapter.

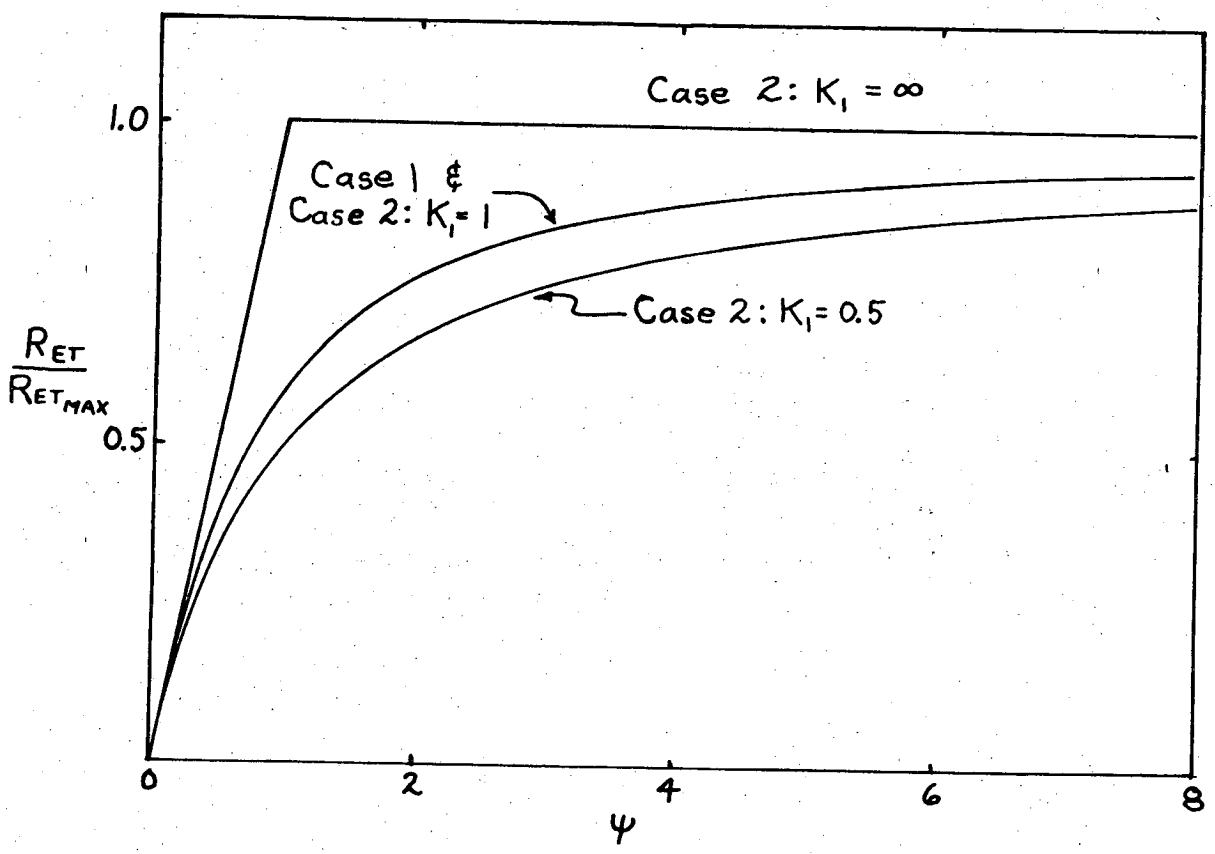

XBL 709-6498

Fig. 33. Light response curves for the System II Hill reaction resulting from the various situations discussed in this chapter. Case 1, Equation (6-23), results when the regeneration of the primary chemical trap, Q, is the rate limiting step. Case 2 assumes that the regeneration of a secondary chemical trap, A, is the rate limiting step. K_1 is the equilibrium constant for electron transfer between Q and A, here assumed to be completely reversible.

concentration of primary System II traps, Q, which are present in a concentration of approximately 1 equiv/500 chlorophyll, according to the oxygen gush studies of Joliot (1965a, 1965b). The main point to be made here is that Kelly and Sauer were able to measure a pool of intermediate much larger than the pool size of Q. This means the regeneration of the primary chemical trap, Q, cannot possibly be the rate limiting step in the steady state System II Hill reaction, otherwise Kelly and Sauer could not have measured the size of a larger secondary pool with their flashing light experiments.

As earlier discussed in this chapter, Kok et al. (1969) found the rate of electron transport from A to P was slower than the rate of electron transport from Q to A.

All the above experimental results suggest that equilibrium can be assumed between the primary chemical traps, Q, and the secondary chemical traps, A. This was, in fact, previously assumed in the derivation of our mathematical model for photosynthesis. But if the equilibrium between Q and A is fast, how can a rectangular hyperbola be obtained for the light response curve of the System II Hill reaction? As shown in Case 2, which follows, there is only one possible way: the equilibrium constant for electron transfer between Q and A, K_1, must equal 0.5, a value consistent with the experimental measurements of Forbush and Kok (1968).

Case 2: The Regeneration of a Secondary Chemical Trap, A, as the Rate Limiting Step

As mentioned above, Q and A are assumed to be in equilibrium:

$$K_1 = \frac{[A^-][Q]}{[Q^-][A]} \quad . \tag{6-24}$$

In the following derivation K_1 will be kept as a variable, enabling us to see the effect of the value of K_1 on the System II Hill reaction light response curve.

Equation (6-19) of the previous case is replaced by:

$$\frac{d[Q^-]}{dt} = \psi_2 \frac{2q}{1+q} - k_2[A^-]. \tag{6-25}$$

Using the above two equations along with the material balances, $[Q] + [Q^-] = [Q_0]$ and $[A] + [A^-] = [A_0]$, we find after considerable algebraic manipulation:

$$[A^-] = \frac{2\psi_2[A_0]}{\psi_2 + k_2[A_0] + \sqrt{k_2^2[A_0]^2 + \psi_2^2 - 2\psi_2 k_2[A_0] + \frac{2\psi_2 k_2[A_0]}{K_1}}}. \tag{6-26}$$

The rate of product formation (or rate of electron transport) is:

$$R_{ET} = k_2[A^-] \tag{6-27}$$

$$= \frac{2\psi_2 k_2[A_0]}{\psi_2 + k_2[A_0] + \sqrt{k_2^2[A_0]^2 + \psi_2^2 - 2\psi_2 k_2[A_0] + \frac{2\psi_2 k_2[A_0]}{K_1}}} \tag{6-28}$$

where $\psi_2 = I\phi_0\epsilon$.

Equation (6-28) is the general solution where K_1 is not specified. We now examine the effect of the value of K_1 on the light response curve of the System II Hill reaction. Four values for K_1 will be examined.

a) $K_1 = 0$

This is a trivial case since if $K_1 = 0$, then no electrons ever move from Q^- to A, and the rate of electron transport, R_{ET}, is zero. This is also seen from Equation (6-28), since the denominator becomes infinite.

b) $K_1 = \infty$

When K_1 approaches infinity the last term in the square root of Equation (6-28) becomes insignificant, and the equation becomes:

$$R_{ET} = \frac{2\psi_2 k_2 [A_0]}{\psi_2 + k_2[A_0] + \sqrt{k_2^2[A_0]^2 + \psi_2^2 - 2\psi_2 k_2[A_0]}} . \quad (6\text{-}29)$$

The terms within the square root are a perfect square with two equally valid roots, $\pm(\psi_2 - k_2[A_0])$. If the positive root is used, the $k_2[A_0]$ terms cancel each other in the denominator yielding:

$$R_{ET} = \psi_2 . \quad (6\text{-}30)$$

This solution is valid at all light intensities below light saturation. Using the negative root, the two ψ_2 terms in the denominator cancel, leaving:

$$R_{ET} = k_2[A_0] . \quad (6\text{-}31)$$

This is simply the light saturated rate. Equations (6-30) and (6-31) describe a Blackman-type curve: first-order behavior below light saturation and zero-order behavior above light saturation. Figure 33 shows this case.

On physical grounds this behavior may be explained as follows. Since K_1 is large and the equilibrium is fast, Q^-, as it forms, is immediately converted to A^-. Thus, there is absolutely no build-up of the closed primary traps, Q^-, and hence no lessening of photochemical trapping efficiency until <u>all</u> A have been converted to the A^- state.

But if light intensity is increased, a point is reached where $[A^-] = [A_0]$, and the reaction is proceeding at its saturated rate. Now there is a build-up of the closed primary traps, Q^-, and a resultant decrease in the efficiency of photochemical trapping. The rate of photochemical trapping can never exceed $k_2[A_0]$.

This case of $K_1 = \infty$ cannot be correct, since it is not consistent with experimental data: Blackman behavior is not observed experimentally for the System II Hill reaction.

c) $K_1 = 1$

If $K_1 = 1$, Equation (6-28) b ecomes:

$$R_{ET} = \frac{2\psi_2 k_2[A_0]}{\psi_2 + k_2[A_0] + \sqrt{k_2^2[A_0]^2 + \psi_2^2}} . \qquad (6\text{-}32)$$

This may be given equivalently as:

$$R_{ET} = \psi_2 + k_2[A_0] - \sqrt{k_2^2[A_0]^2 + \psi_2^2} . \qquad (6\text{-}33)$$

This equation is the same form as Equation (6-22), which describes Case 1. In this case $k_2[A_0]$ is found in place of $k_1[Q_0]$. Figure 33 shows coincident curves for these two cases.

This case of $K_1 = 1$ is of interest, since this was the value of K_1 assumed in the derivation of the light response curve for overall photosynthesis treated earlier in this chapter.

d) $K_1 = 0.5$

If $K_1 = 0.5$, the result is an exact rectangular hyperbola, the function that best seems to fit the System II Hill reaction data of Lumry et al. (1959), Sauer and Biggins (1965), and many other workers. Also, this value of K_1 was exactly the value suggested by Forbush and Kok (1968) for the equilibrium between Q and A_1*, based on fluorescence rise data.

For a K_1 of 0.5, Equation (6-28) becomes:

$$R_{ET} = \frac{\psi_2 k_2[A_0]}{\psi_2 + k_2[A_0]} . \qquad (6\text{-}34)$$

*Forbush and Kok's data indicated that the A pool is biphasic, consisting of two components, A_1 and A_2. The equilibrium constant between Q and A_1 was found to be rapid and best described by an equilibrium constant of 0.5. The equilibrium between Q and A_2 was slower and was best fit by a K-value of 6. Kok et al. (1969) found that System I reacts only or mainly with A_1.

$$R_{ET} = \frac{I\phi_2 \epsilon k_2[A_0]}{I\phi_2 \epsilon + k_2[A_0]} . \qquad (6\text{-}35)$$

The above Equation (6-35) is shown in Fig. 33 labeled as Case 2: $K_1 = 0.5$.

Both the Lumry model and Equation (6-35) give a rectangular hyperbola function. We prefer the model that gave Equation (6-35), since it, unlike the Lumry model, is consistent with the previously discussed results of Kelly and Sauer (1968), which showed the rate limiting step for the System II Hill reaction to be the regeneration of a secondary chemical trap, rather than a primary chemical trap.

Even though the probability of excitation energy transfer, which here was assumed equal to 0.5, may vary with organism or growth conditions, some value of K_1 can be found that will give a rectangular hyperbola regardless of the probability of energy transfer.

NOMENCLATURE

a = Probability of transfer between separate pigment units

A = A pool of intermediate that communicates with Q

C = A pool of intermediate that communicates with P

E = The rate-limiting enzyme that catalyzes the conversion of L to M

f = The fraction of open primary chemical traps, equal to q for System II and p for System I

$h\nu$ = A quantum of light

I = Light intensity, einsteins/cm^2/hr

k = Various rate constants

K = Various equilibrium constants

L = The immediate substrate of the rate-limiting step

M = The immediate product of the rate-limiting step

p = The fraction of open System I primary chemical traps

P = The primary chemical trap of System I

q = The fraction of open System II primary chemical traps

Q = The primary chemical trap of System II

R = Rate of a process, moles/hr/mg chlorophyll

S = The light saturated rate of a process, moles/hr/mg chlorophyll

X = A pool intermediate that couples to electron transport between A and C

X ~ = The high energy state of X, which can produce ATP (Z ~) from ADP (Z)

Z = ADP

Z~ = ATP

[ ] = Concentration of the species enclosed, moles/mg chlorophyll

β = A stoichiometric factor equal to the number of electrons that must be transported through the photo-electron transport system so that one L will be converted to M

ϵ = Extinction coefficient of the pigments, cm^2/mg chlorophyll

ϕ = Maximum quantum yield for electron transport, moles electrons/einstein

Φ = Maximum quantum yield for oxygen evolution, moles O_2/einstein

ψ = $I\epsilon\phi$, light absorbed times the quantum yield

Superscripts

' = pertaining to electron transport

Subscripts

A = The actual light saturated rate of photosynthesis

ET = Electron transport

M = The light saturated rate of photosynthesis intrinsic to the photo-electron transport chain

$_0$ = Total amount of all states or forms of the species subscripted

1 = System I

2 = System II

1, 2, 3, 4, 5 = Designate various rate or equilibrium constants

VII. THE PERFORMANCE OF OPTICALLY DENSE CULTURES OF ALGAE

Optically dense cultures are of practical interest in the mass culture of algae, since if light is not absorbed by the culture, it is wasted. But because light is absorbed by the algal cells as it travels into a dense culture, light intensity decreases as a function of distance into the culture.

To model such a system mathematically, the manner in which light intensity changes as a function of distance into the culture must be known. If the rate of photosynthesis as a function of light intensity is also known, the local rate of photosynthesis at any point in the system may be calculated. By integrating the local rate of photosynthesis over the distance into the culture, the total rate of photosynthesis in the system may be found. Since photosynthesis results in growth, the productivity of algal biomass can be predicted.

The above procedure for mathematically predicting the performance of dense algal systems was first suggested by Tamiya et al. (1953a). Recently Shelef et al. (1968) used a more sophisticated approach, which used Beer's law to describe the attenuation of light intensity as a function of distance into the culture, but took into account that the extinction coefficient is a function of wavelength. The approaches of these and other workers was discussed in Chapter II.

Our model, presented below, is an extension of the approaches of previous workers, but differs from previous models in two respects. First, the local rate of photosynthesis will be expressed by Equation (6-17) and (6-18), which describe the photosynthetic light response curve formulated in the last chapter. Second, the effects of the specific rate of growth, μ, on the light saturated rate of photosynthesis, chlorophyll content, dark respiration rate, and cellular composition will be accounted for.

Consider a system of algae in steady state continuous culture in the element of volume shown below.

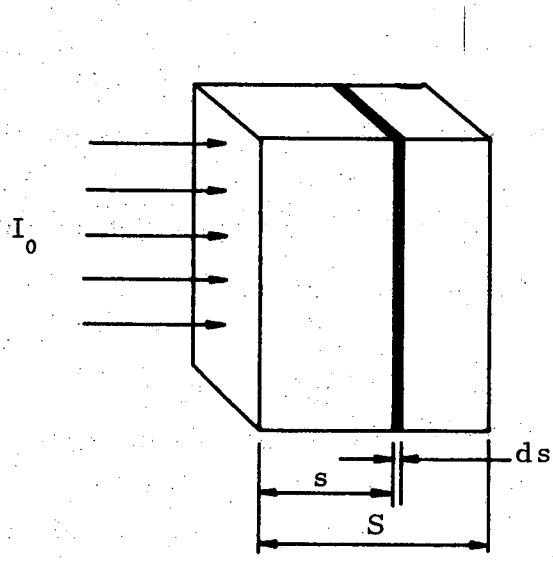

The system is operating at an average specific growth rate, μ, and light is impinging perpendicularly onto the left-hand vertical surface. Symbols on the diagram are defined as follows:

$I_0(\lambda)^*$ = incident light intensity expressed as a function of λ (einsteins/cm^2/hr)

λ = wavelength of light (nm)

s = distance from illuminated surface (cm)

ds = differential distance at any point s (cm)

S = total algal suspension thickness (cm)

To find the total rate of photosynthesis, the local rate of photosynthesis at any point s, $R_{O_2}(\mu, I)\big|_s$, must be integrated over the entire algal culture thickness, S. From this integrated gross rate must be subtracted the loss due to respiration. Solving for μ:

*Parentheses denote that a variable is a function of the quantities within the parentheses.

$$\mu = \mu_{ave} = \frac{1}{S}\int_0^S R_{O_2}(\mu, I)\big|_s C(\mu)B(\mu)ds - U(\mu)B(\mu) \qquad (7\text{-}1)$$

where

μ = specific growth rate (hr^{-1})

$R_{O_2}(\mu, I)\big|_s$ = local rate of photosynthesis in terms of O_2 evolution at any point s (moles O_2/hr/mg chlorophyll)

$C(\mu)$ = weight fraction of chlorophyll in the cells (mg chlorophyll/mg dry wt.)

$B(\mu)$ = factor for converting O_2 evolved to cell dry weight (mg dry weight/mole O_2)

$U(\mu)$ = uptake of O_2 due to respiration (moles O_2/hr/mg dry wt.)

The local rate of photosynthesis will be expressed by Equations (6-17) and (6-18), which were formulated in the last chapter. These equations are consistent with both experimental data and current knowledge of the chemical kinetics of photosynthesis.

$$R_{O_2}(\mu, I)\big|_s = \int_{380}^{720} \frac{2\Phi\epsilon(\lambda)I(\lambda)\big|_s S_M\, d\lambda}{2S_M + \Phi\epsilon(\lambda)I(\lambda)\big|_s + \sqrt{2\Phi\epsilon(\lambda)I(\lambda)\big|_s S_M + \{\Phi\epsilon(\lambda)I(\lambda)\big|_s\}^2}} \qquad (6\text{-}17)$$

or, if it gives a smaller value:

$$R_{O_2}(\mu, I)\big|_s = S_A(\mu) \qquad (6\text{-}18)$$

where

Φ = maximum quantum yield, as I approaches zero (moles O_2/einstein)

$\epsilon(\lambda)$ = extinction coefficient of the pigments expressed as a function of λ (cm^2/mg chlorophyll)

$I(\lambda)\big|_s$ = light intensity at any point s expressed as a function of λ (einsteins/cm^2/hr)

S_M = the saturated rate of O_2 evolution intrinsic to the photo-electron transport system (when no steps in the carbon fixation cycle limit) (moles O_2/hr/mg chlorophyll)

$S_A(\mu)$ = the actual rate of O_2 evolution, caused by a bottleneck in the carbon fixation cycle (moles O_2/hr/mg chlorophyll)

In equation (6-17), $I(\lambda)\big|_s$ varies with distance into the culture. Values of λ are limited to the region 380 to 720 nm, which is the region of importance in photosynthesis. Beer's law will be used to describe this variation, taking into account the change of extinction coefficient, $\epsilon(\lambda)$, with λ.

$$I(\lambda)\big|_s = I_0(\lambda) \exp\{-X\, s\, \epsilon(\lambda)\, C(\mu)\} \qquad (7\text{-}2)$$

where

X = concentration of algal biomass (mg dry wt./ml).

The above four equations may be solved by substituting Equation (7-2) into Equation (6-17) and using Equation (6-17) or Equation (6-18), whichever is appropriate, in Equation (7-1).
Equation (7-1) cannot be integrated analytically, except for monochromatic light or the use of an average extinction coefficient. In general, the way to solve Equation (7-1) is to pick μ, and by trial and error assume values for X until the right hand side of Equation (7-1) becomes equal to the value of μ originally picked.

Checking the Dense Culture Model Against Experimental Data

Our model for optically dense cultures will be checked against the productivity data given in Fig. 7, which were obtained in our continuous culture unit.

The computer program given in Appendix IV, Program Algae, will be used to solve the above equations. But first, many of the constants and variables in the above equations will be empirically expressed based upon the data of Chapter III. From Figs. 10, 15, and 19:

$$C(\mu) = -2.61\times 10^{-2}\,\mu + 7.43\times 10^{-2} \qquad (7\text{-}3)$$

$$S_A(\mu) = 1.334\times 10^{-4}\,\mu + 1.174\times 10^{-4} \qquad (7\text{-}4)$$

$$U(\mu) = 2.18\times 10^{-7}\,\mu + 7.81\times 10^{-8} \qquad (7\text{-}5)$$

$B(\mu)$ is given by Equation (3-2), which was derived from Figs. 21, 22, and 23:

$$B(\mu) = 0.065\times 10^{4}\,\mu + 1.64\times 10^{4}. \qquad (3\text{-}2)$$

From the data of Fig. 18, which was fit to Equation (6-17) by a non-linear least squares technique, $\Phi = 0.1138$ and $S_M = 0.00221$. The thickness of the culture, S, equals 2.8 cm.

$I_0(\lambda)$ for the computer program is shown in Fig. 34. This figure is based upon the data of Fig. 6, but has been broken into 10 nm bands, each with its own characteristic light intensity.

$\epsilon(\lambda)$ is given by Fig. 35, which is based upon the average of the two curves shown in Fig. 12. $\epsilon(\lambda)$ is also broken up into 10 nm bands. Figure 35 does not include light scattering, which was assumed to equal the absorbance measured at 750 nm, where there is no pigment absorption.

But light scattering increases light absorption, since light scattered sideways travel a path of increased length before reaching the back side of the culture vessel. The culture is very opaque, resulting in multiple scattering. Therefore the light scattering extinction coefficient, ϵ_{scat}, is added back into the Beer's law expression for light absorption. $\epsilon_{scat} = 10.$ cm^2/mg chlorophyll, based upon the average scattering measured at 750 nm.

The reader should consult Program Algae, the computer program given in Appendix IV, for the exact procedures used to calculate the performance of dense algal systems. A brief summary of the procedure used by the computer program is given in Fig. 36. Once the algal biomass concentration, X, is known, productivity, p, may be found from Equation (2-13):

$$p = X\mu S. \qquad (2\text{-}13)$$

The results of the computer program are compared with the experimental data in Figs. 37 and 38. The experimental productivity data are approximately 16% lower than the curve calculated by the computer. If the computer curve is arbitrarily lowered by 16%, it fits the data quite well. The transmittance of light through the culture is shown in Fig. 38, where the computer curve and the experimental data match quite well.

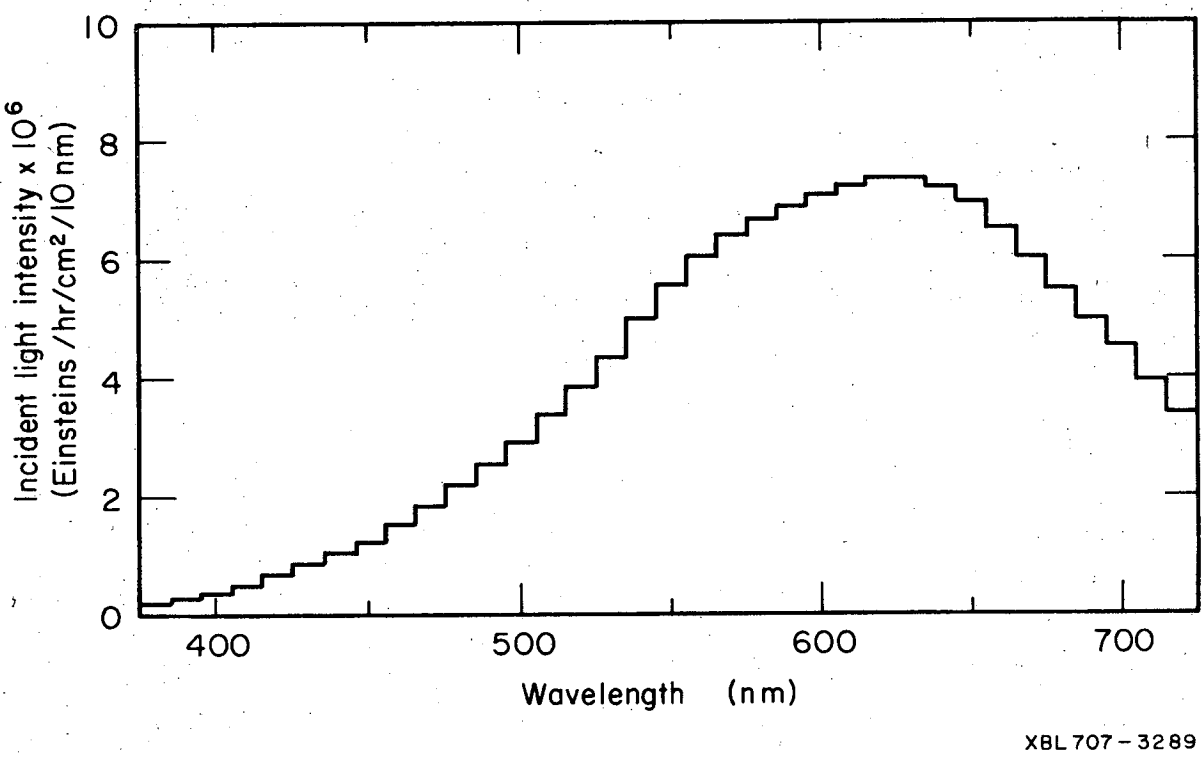

Fig. 34. Incident light intensity function used in Program Algae, the computer program used to predict the performance of optically dense algal suspensions. This figure is based upon the experimental data shown in Fig. 6.

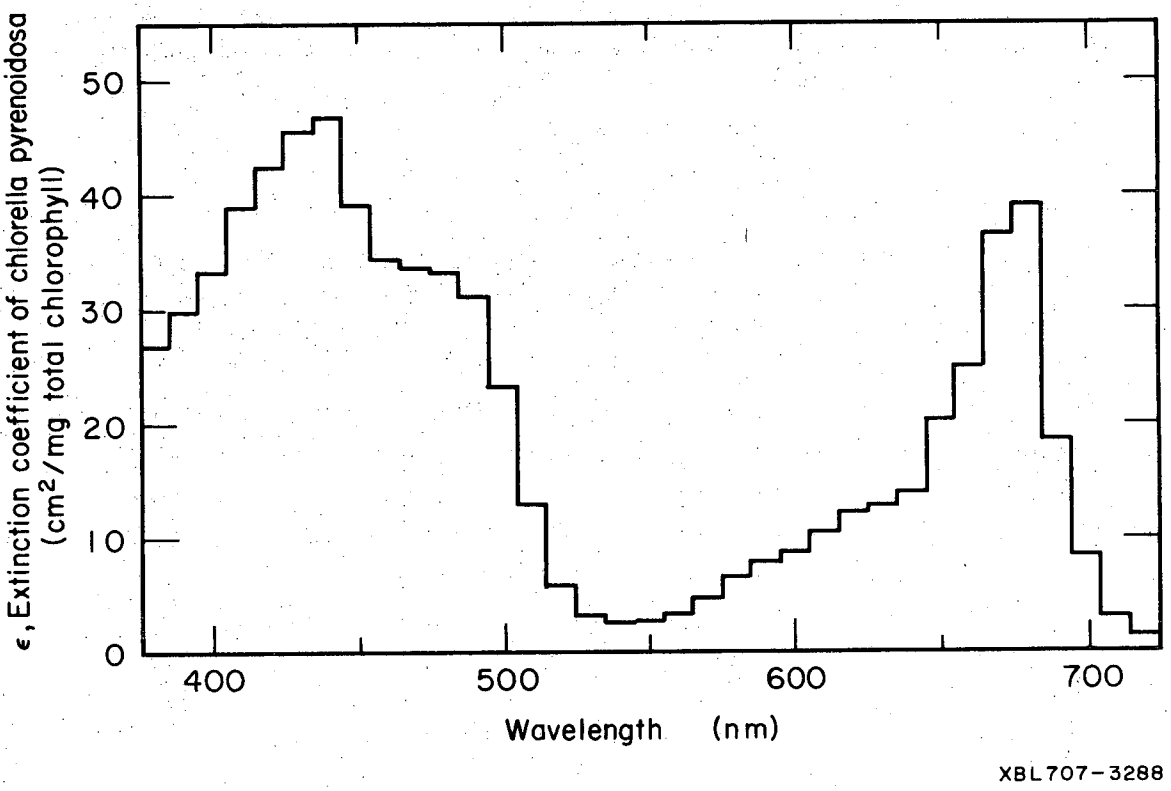

Fig. 35. Extinction coefficients used in Program Algae. These values were calculated from the average of the curves shown in Fig. 12. These extinction coefficients do not include light scattering.

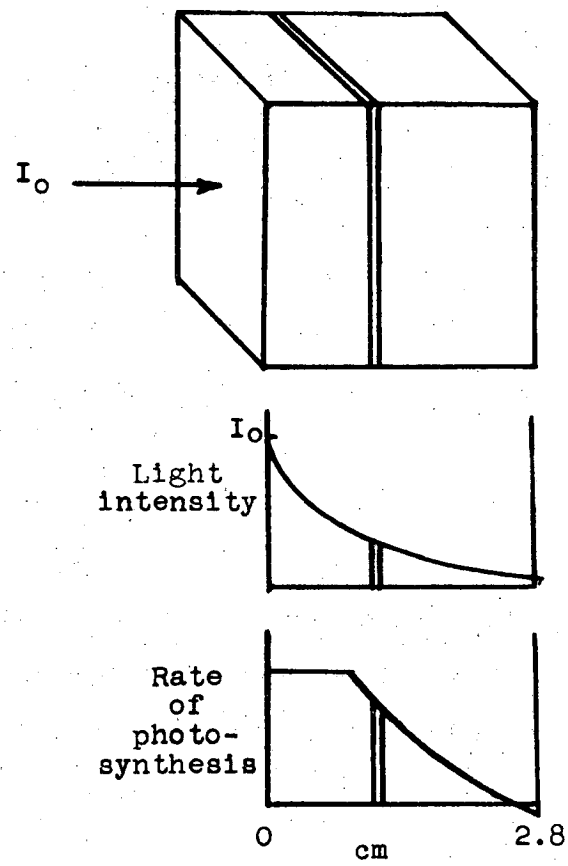

For one given specific growth rate, μ:

1. Calculate chlorophyll content, respiration rate, saturated rate of photosynthesis, cell dry weight produced per mole of oxygen evolved.
2. Pick a trial value for the cell concentration.
3. Calculate light intensity at each thin layer.
4. Calculate the rate of photosynthesis in these layers.
5. Add up the photosynthetic rates in all these layers.
6. Calculate the specific growth rate, μ, and check to see if it matches the value we started with. If not, take a new cell concentration and go back to step 3.

XBL 703-546

Fig. 36. A summary of Program Algae, the computer program used to predict the performance of optically dense algal suspensions. The complete computer program is given in Appendix VI.

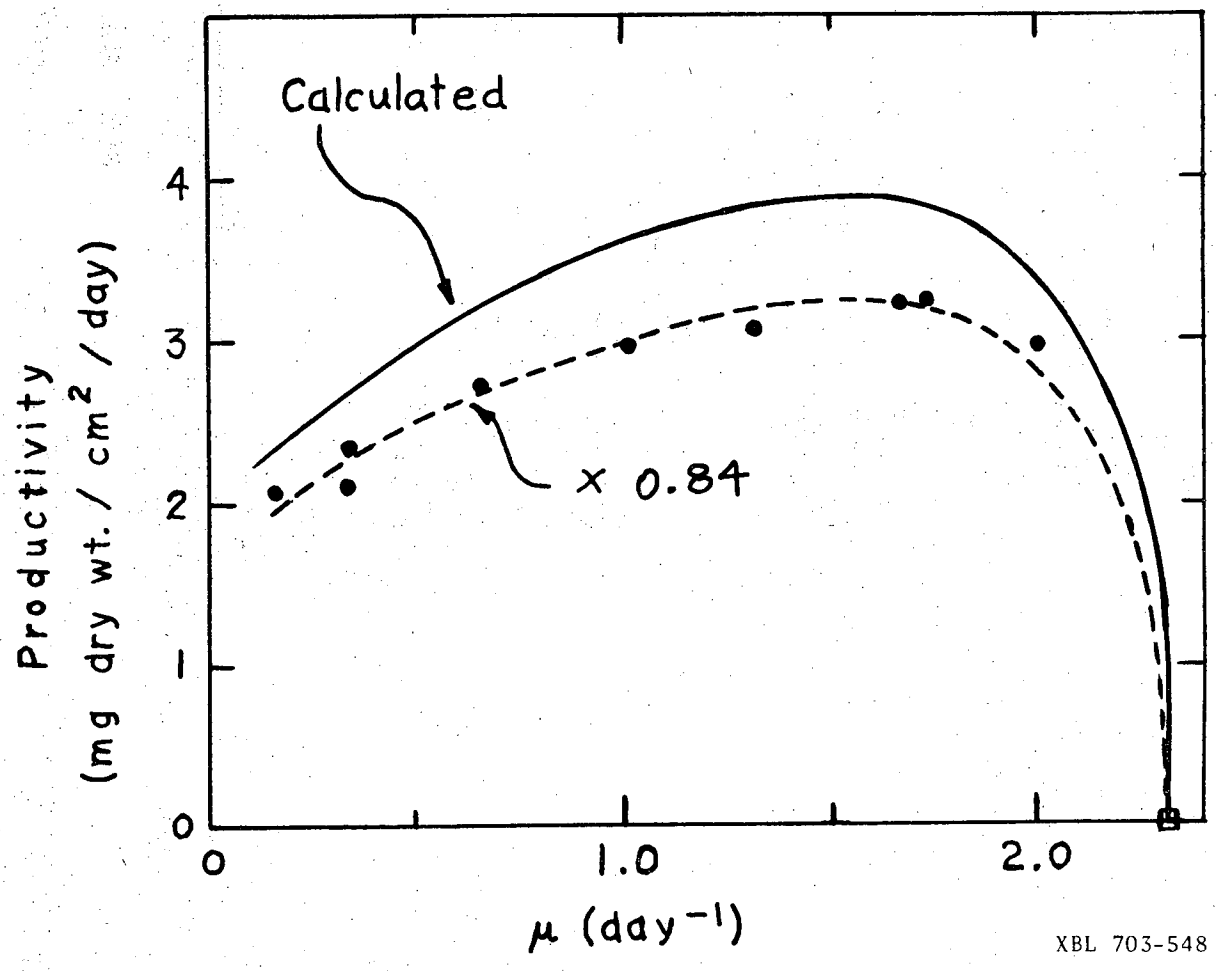

Fig. 37. Productivity of Chlorella pyrenoidosa in continuous culture as a function of the steady state specific growth rate, μ. The data shown are from Fig. 7. The top line was predicted by Program Algae. Washout occurs when $\mu = 2.3$ day^{-1}.

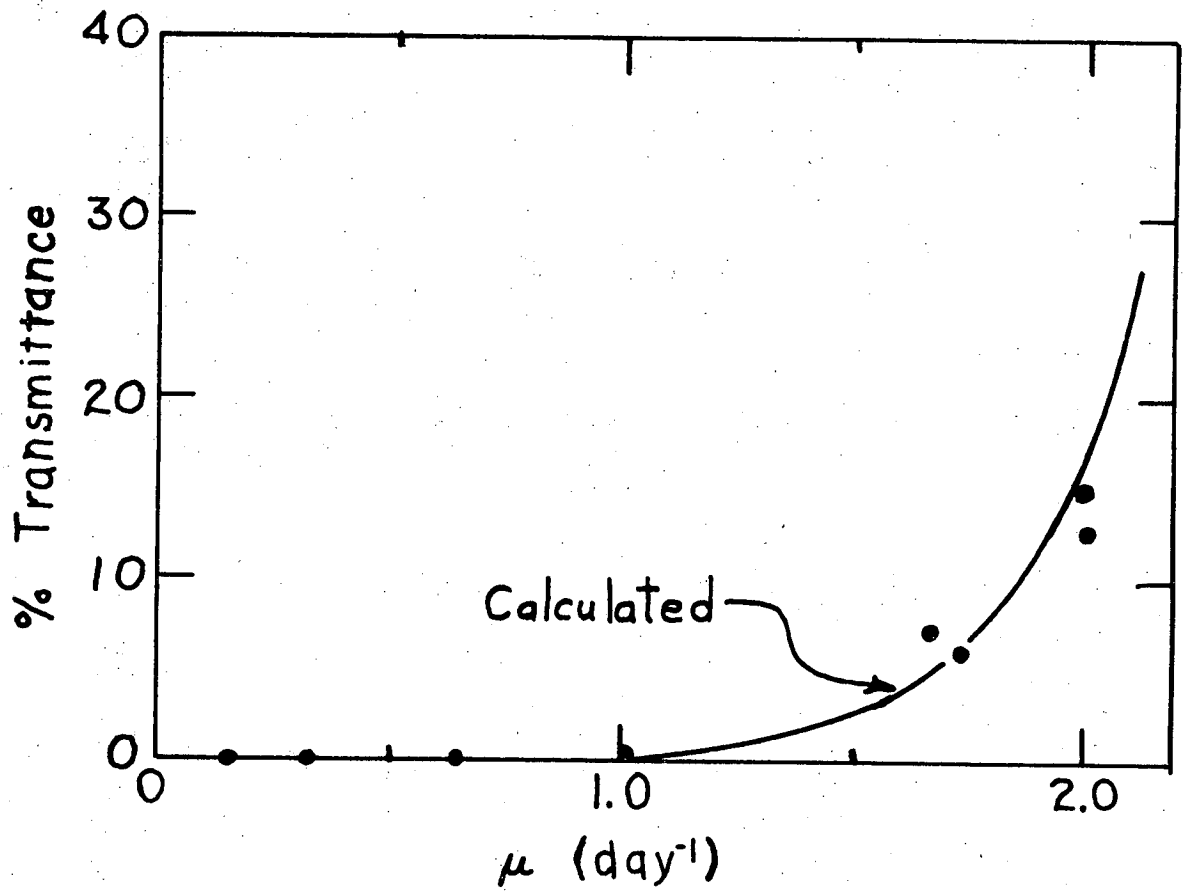

XBL 709-6497

Fig. 38. % transmittance of light through the culture versus specific growth rate. The data are from Fig. 9, while the line was calculated by Program Algae.

The following reasons may have caused the computer productivity curve to be higher than the actual data:

1. A value of 0.1138 moles O_2/einstein was used for the maximum efficiency, Φ. This may be too high, as discussed in Chapter III.

2. Back-scattering, or reflection of incident light, was not accounted for in the computer program.

3. The "sieve effect", considered by Monteith (1965) for crops, is a factor (but a smaller factor in tiny Chlorella cells) causing deviations from Beer's law.

4. A certain amount of experimental error in the values obtained for S_M, $S_A(\mu)$, $B(\mu)$, etc. can be expected.

5. Even though the edges of the culture vessel were coated with platinum to reduce edge effects, platinum is not perfectly reflecting.

6. Respiration losses are undoubtedly larger than predicted by the relation for $U(\mu)$ used in our model. Equation (7-5) gives this relation, which is based on the measured respiration rates of cells adapted to darkness for about an hour. However, cells in the culture vessel do not have such low respiration rates, since when they float into a dimly illuminated region they will have recently come from a region of high illumination. Such recently illuminated cells are known to have higher dark respiration rates (Cramer and Myers, 1949), We also noticed this phenomenon in our respirometer work.

Notice that Fig. 37 shows an optimum for the production of cell material at $\mu = 1.6\ day^{-1}$. Previous workers (such as Shelef et al., 1968) have ascribed low productivities at low values of μ as resulting from increased respiration losses of the larger cell populations. This would be true if dark respiration rate were independent of μ. But both the data of Myers and Graham (1959) and Fig. 19 show this is not true; dark respiration rate decreases nearly with decreasing μ. We believe the optimum in the productivity curve to result primarily from changes in the light saturated rate of photosynthesis, $S_A(\mu)$.

Use of the Dense Culture Model in Screening Other Species of Algae

For the preliminary screening of algae with respect to their productivity in dense cultures, the above model can be of use. Our objective is to eliminate the need for the tedious collection of continuous culture data. The following is a suggested procedure:

1. Grow the algae in batch culture.

2. Take a sample of young cells while the culture is in exponential growth; the specific growth rate of these cells is μ_{max}. Let the culture keep growing. Take another sample when the culture has become very dense, but before any nutrients become limiting. Calculate a rough specific growth rate for these "old cells" from Equations (2-8) and (2-10).

3. For these two types of cells, determine chlorophyll content and elemental composition. All other parameters needed for the computer program may be estimated from respirometer data.

4. For those parameters that are functions of μ, assume a linear relation between the two values of μ.

5. Use the computer program to predict productivity as a function of μ. A maximum quantum efficiency, Φ, of approximately 0.10 may be assumed, if this quantity is not known.

NOMENCLATURE

$B(\mu)$	=	Factor for converting O_2 evolved to cell dry weight, mg dry weight/mole O_2
$C(\mu)$	=	Weight fraction of chlorophyll in the cells, mg chlorophyll/mg dry wt.
ds	=	Differential distance at any point s, cm
$I(\lambda)\|_s$	=	Light intensity at any point s expressed as a function of λ, einsteins/cm^2/hr
$I_0(\lambda)$	=	Incident light intensity expressed as a function of λ, einsteins/cm^2/hr
p	=	Productivity of algal biomass, mg dry weight/cm^2/hr
$R_{O_2}(\mu, I)\|_s$	=	Local rate of photosynthesis in terms of O_2 evolution at any point s, moles O_2/hr/mg chlorophyll
s	=	Distance from illuminated surface, cm
S	=	Total algal suspension thickness, cm
$S_A(\mu)$	=	The actual rate of O_2 evolution, caused by a bottle-neck in the carbon fixation cycle, moles O_2/hr/mg chlorophyll
S_M	=	The saturated rate of O_2 evolution intrinsic to the photo-electron transport system (when no steps in the carbon fixation cycle limit), moles O_2/hr/mg chlorophyll
$U(\mu)$	=	Uptake of O_2 due to respiration, moles O_2/hr/mg dry weight
X	=	Concentration of algal biomass, mg dry weight/ml
$\epsilon(\lambda)$	=	Extinction coefficient of the pigments expressed as a function of λ, cm^2/mg chlorophyll
λ	=	Wavelength of light, nm
μ	=	Specific growth rate, hr^{-1}
Φ	=	Maximum quantum yield, as I approaches zero, moles O_2/einstein

VIII. SOME ECONOMIC CONSIDERATIONS IN THE MASS CULTURE OF ALGAE

Of prime concern to the economics of any process is the efficiency of converting substrate into product. The most expensive substrate required for growing algae in artifically illuminated systems is light, which is generally created from electricity. Even when solar illumination is used, there is a high investment cost in providing the large required surface areas.

To gain insight into this problem of light energy conversion, the data of Chapter III will be examined. Figure 7 shows productivity plotted against specific growth rate. The optimum productivity is 3.25 mg/cm^2/day at a specific growth rate of 1.6 day^{-1}; the incident illumination energy between 380 to 720 nm was 8.05 mw/cm^2.

Calculation of the efficiency of light conversion requires knowledge of the heat of combustion of the algae, but this was not measured by us. An estimate of the heat of combustion could be obtained from the chemical composition of the algae, which is given as a function of specific growth rate in Figs. 21, 22, and 23. But instead, we will use the value of 5.5 cal/mg, which was recommended by Myers (1964) for Chlorella. Using these numbers the efficiency is readily calculated to be 10.7% at the optimum specific growth rate. This efficiency and the efficiencies at other incident light intensities, which were given in Table III in Chapter III, are consistent with the results of other workers (Kok, 1952, van Oorschot, 1955, Myers and Graham, 1959). The efficiency of light conversion decreases with increasing incident intensity because of light saturation effects.

The quantum requirement at the optimum specific growth rate may also be calculated. Using Planck's law and the spectral distribution of the incident light source as shown in Fig. 6, an incident intensity of 1.42×10^{-4} einsteins/hr/cm^2 is calculated. Equation

(3-2) gives the relation between cellular biomass production and O_2 evolution: $B = 1.744 \times 10^4$ mg/mole O_2 at a specific growth rate of 1.6 day^{-1}. With these numbers the quantum requirement is found to be 18.3 quanta absorbed/O_2 evolved.

There are two possible ways to reduce the light saturation effects that cause lower light conversion efficiencies. One way, which was discussed earlier in Chapter IV, is to find algae with higher light saturated rates of photosynthesis when expressed on a per mg chlorophyll basis. The second method is to reduce the incident light intensity by increasing the effective surface area. This can be done simply by illuminating the culture surface at an angle that deviates greatly from the perpendicular, but this is not possible for ponds using solar illumination. Another way to increase the effective surface area is the use of diffusing cones, which are immersed into the culture. Myers and Graham (1961) employed these cones and found they gave a twofold increase in efficiency for Chlorella ellipsoidea illuminated at an incident intensity of approximately 35 mw/cm^2 (reasonably close to overhead solar illumination).

A. ARTIFICIAL ILLUMINATION

Only the electrical cost of providing the artificial illumination will be considered here, since it would probably be the largest single expense in artificially illuminated systems. Assuming that a 20% energy conversion efficiency could be attained, the cost of a poind of dried algae will be calculated. The 20% figure is a maximum; it would require a very weak illuminating intensity and would result in a low production rate per unit area. For the cost of electricity we will assume $0.01/kw-hr, a figure generally obtainable for industrial processes. For the light source we will assume that the conversion of electrical energy to light is 25%, a figure attainable for high temperature sodium vapor arc lamps (Shelef et al., 1968). The heat of combustion of the algae, as before, is assumed to be 5.5 kcal/g. Thus, the lowest attainable electrical cost may

be calculated:

$$\frac{\$0.01}{\text{kw-hr}} \left| \begin{array}{c} \\ 0.20 \end{array} \right| \left| \begin{array}{c} \\ 0.25 \end{array} \right| \frac{5.5\,\text{kcal}}{\text{g}} \left| \begin{array}{c} 454\ \text{g} \\ \text{lb} \end{array} \right| \frac{\text{kw-min}}{14.34\ \text{kcal}} \left| \begin{array}{c} \text{hr} \\ 60\ \text{min} \end{array} \right| = \$0.58/\text{lb algae.}$$

A 10% efficiency for converting light energy into photosynthetic product would be more reasonable for any practical system; this would double the above cost for electricity.

The above cost does not include any other utility or operating costs and does not include any investment costs. We conclude on the basis of the above number that the mass culture of algae using artificial illumination cannot compete with other food sources such as soybeans, which are currently marketed for approximately $0.10/lb.

B. ILLUMINATION BY SUNLIGHT

An economic study of all the costs that go into the mass culture of algae using solar illumination is beyond the scope of this work. Several possible ways of cutting the costs of such a system, however, will be considered.

Vincent (1969) argues against CO_2 enrichment, recirculation pumps for keeping algae in suspension, temperature control, and expensive harvesting processes such as centrifugation. Certainly his arguments must be considered, since the present agriculturally important crops use none of these above expensive practices. To reduce costs, Vincent says that filamentous floating algae, such as Spirulina or Spirogyra, should be used. For this type of algae no special effort is needed to keep the cells in suspension. Harvesting is easy because of the mats that are formed on the water's surface.

Another method of reducing expensive harvesting costs is by using phototactic separation. We, along with another member of our laboratory (Mr. S. F. Miller), have studied the design of such a process for the volvocalian Pandorina morum. Pandorina morum has 16 cells in each fused colony, has 2 flagella per cell, is spherical in shape, and has a diameter ranging from 15-50 microns. In

its motile phase (it loses its flagella when undergoing asexual reproduction) it has a swimming velocity ranging from 0.4 to 1.6 cm/min with a mean at about 1.0 cm/min. Pandorina will orient itself to swim towards a light source.

We performed experiments in a rectangular lucite flow chamber 3 ft long × $5\frac{1}{2}$ in.wide × $\frac{1}{2}$ in.thick. It was inclined at an angle of about 30 degrees from the vertical and illuminated beneath. The algae would swim towards the light until reaching the illuminated face, where they would congregate. They would then move downwards by means of aided settling towards the product take-off. A typical run with a feed rate of 135 ml per min resulted in 99.9% of the motile cells and 91.4% of the total cells in the product. By comparison a darkened control run gave only 38.3% of the motile and total cells in the product, which resulted from gravitational settling. The product stream was estimated to be approximately 80 times more concentrated in algae than the feed. This process and additional results will be discussed in greater detail elsewhere (Miller, 1971).

On the basis of the above experiments we have estimated the size of a phototactic separator that would be required by a 15,000 gal/day (5.5 billion gal/yr) processing rate. Such a rate would require a phototactic separator of the following dimensions: 6 ft long × 24 ft wide × 1 in. thick. Such a separation device would be much cheaper than continuous centrifugation. A phototactic separator would require virtually no operating costs and little investment cost. In summary, further research on phototactic separation appears justified, in view of these favorable results.

Criteria for the Design of Algal Systems

Consider the design of an algal production system where the objective is to produce algal biomass equal to P, mass/time. There are certain limits that restrict the design and operation of such algal systems. The criteria for design and operation that must be kept in

mind are discussed in the following items.

1. In order to determine the illuminated area necessary to achieve the production rate P, an estimate of the productivity, p, must be obtained. p is equal to P/A and has the units mass/time area. A is the illuminated surface area. For Chlorella pyrenoidosa growing under the conditions investigated in Chapter III, an optimum productivity of 3.25 $mg/cm^2/day$ was obtained at a specific growth rate, μ, of 1.6 day^{-1}. For other systems the mathematical model for optically dense cultures, which is given in Chapter VII and the computer program in Appendix VI, should be used to estimate the optimum productivity and specific growth rate. A suggested outline, which uses the computer program given in Appendix VI, is given at the end of Chapter VII. This estimate for the optimum p and μ, once obtained, assumes that no nutrients, other than light, are limiting. This estimate does not depend upon the culture volume or depth, which still remain to be determined.

The estimate of p gives us the required illuminated surface area, since $A = P/p$.

The estimate of μ that goes with the above p determines the dilution rate to the system, F/V, since at steady state $\mu = F/V$. μ is the specific growth rate, $time^{-1}$; F is the feed rate to the system, volume/time; and V is the volume of the system.

2. A and F/V for the system have been determined above. Two more items need to be specified, the depth of the algal suspension and the concentration of minerals in the feed. As will be seen in the equations below, these two items are intimately related. As a design criterion it will be assumed that essentially none of the minerals in which we are interested will be allowed to be wasted by leaving in the effluent stream. In other words, the design will be based upon essentially all of such minerals ending up in the algal biomass. With this assumption the following material balance may be written, where the quantity of any nutrient mineral entering in the feed stream is equal to the amount of that mineral converted

into algal biomass, when the system is at steady state:

$$pAW_N = FC_N \tag{8-1}$$

where W_N is the fraction of the mineral in the algae as determined by chemical analysis, mass/mass; and C_N is the concentration of the limiting nutrient in the feed stream, mass/volume. Rearranging and making use of $V = AS$, where S is the thickness of the system:

$$C_N S = \frac{pW_N}{\frac{F}{V}}. \tag{8-2}$$

All terms on the left-hand side of Equation (8-2) have been previously determined or are a property of the algae; C_N and S are the only remaining independent variables.

A decision must now be made concerning either C_N or S. If the feed stream is fixed in composition and cannot be changed, then the decision has already been made for us. This might be the case if algae production is to be tied in with sewage treatment facilities. Nevertheless, even in this case the feed stream can be supplemented with minerals.

In the interest of having as concentrated a suspension of algae as possible to harvest, one should minimize S, since algal concentration is inversely proportional to S when all else is held constant. But there are physical limitations on how thin a pond can be built. It is inconceivable from a civil engineering standpoint to build large ponds that are 1 mm or even 1 cm in depth. Other considerations are also important. If algae such as Chlorella or Scenedesmus are being grown, the pond should be periodically agitated because these algae settle to the bottom. Increasing the depth of the pond allows the algae to stay in suspension longer. This settling problem has led to the 8 inch depth that was suggested by Oswald and Golueke (1968) as being optimum for Chlorella systems. But in systems

where settling is not a problem, thinner depths would probably be desirable.

Several equations that set the boundaries of operation are listed below. Operation outside of these limits is impossible. Equations (8-3) and (8-5) have as their basis Equation (8-2).

$$S \geq \frac{pW_N}{C_N \mu_{max}} . \tag{8-3}$$

μ_{max} is the maximum specific growth rate of the algae, day^{-1}. If the above criterion is not met, the nutrient limits, and p cannot be attained.

$$\frac{F}{V} \leq \mu_{max} . \tag{8-4}$$

The above simply says that all algae are washed out if F/V exceeds the maximum specific growth rate of the algae.

$$\frac{F}{V} \geq \frac{pW_N}{C_N S} . \tag{8-5}$$

If Equation (8-5) is not met, p cannot be attained.

NOMENCLATURE

A	=	Illuminated surface area
C_N	=	Concentration of the limiting nutrient in the feed stream, mass/volume
F	=	Feed rate, volume/time
p	=	Productivity, mass of algal biomass/area/time
P	=	Production of algal biomass, mass/day
S	=	Total depth of the illuminated algal system
V	=	Volume of the algal system
W_N	=	Weight fraction of a mineral in the algal biomass, mass/mass
μ	=	Specific growth rate, $time^{-1}$
μ_{max}	=	Maximum specific growth rate, $time^{-1}$

Appendix I

ON SEPARATE REACTION CHAIN KINETICS: THE EQUILIBRIUM BETWEEN TWO ADJACENT SPECIES WITHIN A SINGLE CHAIN

Separate chain kinetics differs from the kinetics of homogeneous chemical reactions in solution. In separate chain kinetics, species are restricted to reacting with species adjacent in the chain. The discussion here will be restricted to two topics that are important to the models proposed in Chapter VI. For a more complete discussion the reader is referred to Malkin (1969).

Case 1: Two Adjacent Reacting Species, Each With a Pool Size of 1

Consider the 2 species, U and V, adjacent to each other in a chain. It is assumed that there is only one of each of these species within the chain. Consider the case of electron transfer; there are 2 possible states for each of the species, U or U^- and V or V^-.

But since a single U is bound to a single V as a system, there are 4 possible states for the UV system:

1) UV
2) $U^- V^-$
3) $U^- V$
4) UV^-

The first 2 system states, UV and $U^- V^-$, cannot result in electron transfer between U and V. But the last 2 system states, $U^- V$ and UV^-, can result in electron transfer between U and V. The relationship between the concentrations of $U^- V$ and UV^- ($[U^- V]$ and $[UV^-]$, respectively) is given by the equilibrium constant K:

$$K = \frac{[UV^-]}{[U^- V]} . \qquad (A-1)$$

But the apparent equilibrium constant, K_{app}, is based upon homogeneous chemical kinetics, and considers not only the system states

$U^- V$ and $U V^-$, where electron transport is possible, but also the system states UV and $U^- V^-$, where electron transport is not possible:

$$K_{app} = \frac{[U][V^-]}{[U^-][V]} . \qquad (A-2)$$

First we will consider the case where the true equilibrium constant, K, has a value of 1, and prove that in this case $K = K_{app} = 1$. This is an important case, since the equilibria between q and A and between C and P were assumed describable by K-values of 1.

Considering the 2 non-reacting system states, UV and $U^- V^-$, $[U] = [V]$ and $[U^-] = [V^-]$. For the 2 reacting system states, since $K = 1$, $[U^- V] = [U V^-]$; therefore $[U] = [V]$ and $[U^-] = [V^-]$. Using these relationships in Equation (A-2):

$$K_{app} = \frac{[V][V^-]}{[V^-][V]} = 1.$$

Hence, if $K = 1$, then also $K_{app} = 1$.

If $K = \infty$ and there is an equal probability of an electron being donated to U as there is for an electron leaving V, then $K_{app} = 4$, as was demonstrated by Malkin (1969).

Case 2: Pool Size of One of the Reacting Species on the Chain is Large

In this case there is only one U per chain, but the number of V is equal to n. The single U may engage in electron transfer with any of the V. Again we wish to examine the relationship between the true equilibrium constant, K, and the apparent equilibrium constant, K_{app}. The possible states of the system are:

$\{U^-\}\ \{nV\}$	$\{U\}\ \{nV\}$
$\{U^-\}\ \{(n-1)V, V^-\}$	$\{U\}\ \{(n-1)V,\ V^-\}$
$\{U^-\}\ \{(n-2)V,\ 2V^-\}$	$\{U\}\ \{(n-2)V,\ 2V^-\}$
.	.
.	.
.	.
.	.
.	.
$\{U^-\}\ \{(n-j)V,\ jV^-\}$	$\{U\}\ \{(n-j)V,\ jV^-\}$
.	.
.	.
.	.
.	.
.	.
$\{U^-\}\ \{nV^-\}$	$\{U\}\ \{nV^-\}$

If n is large, this system approaches bimolecular kinetics in solution, as was noted by Forbush and Kok (1968). The reason is that electron transport is possible for all possible states except for $\{U\}\ \{nV\}$ and $\{U^-\}\ \{nV^-\}$, and if n is large these 2 species are only a tiny fraction of the total possible reacting species. In Case 1 the reason K_{app} varied from K was that fully 1/2 of the species (UV and U^-V^-) could not have electron transfer between U and V. Such is not the case here. In fact, as n approaches infinity, bimolecular kinetics are obeyed exactly.

Appendix II

NADPH CONTROL OF THE PHOTO-ELECTRON TRANSPORT SYSTEM

This model assumes that NADPH build-up, when an enzyme in the carbon fixation cycle has readhed its maximum rate, limits the rate of the photo-electron transport system. In Chapter VI it was assumed that ATP, rather than NADPH, exerted such an effect on the rate of electron transport.

The model under consideration is shown in Fig. 39. This case has the following differences from the case of ATP control treated in Chapter VI:

1. The transfer of electrons between Q and P is fast, reversible, and at any given light distribution is describable by the equilibrium constant, K_1.
2. Species F immediately accepts an electron from P^-, when a quantum of light has been photochemically trapped by P^-.
3. The steps between F and L are assumed to be fast. The equilibrium between F and L is described by the equilibrium constant K_4, which is assumed to be very large relative to K_M, the Michaelis constant for the conversion of L to M.*

The following four equations describe the system:

$$\frac{d[Q^-]}{dt} = 0 = \psi_2 \frac{2q}{1+q} - \psi_1 p. \qquad \text{(A-3)}$$

$$\frac{d[L]}{dt} = 0 = \frac{1}{\beta}\psi_2 \frac{2q}{1+q} - \frac{k_5[E_0][L]}{[L] + K_M}. \qquad \text{(A-4)}$$

*For the data shown in Figs. 14 and 17, the rounding in the light response curves as light saturation is approached requires that K_4/K_M be no less than 50.

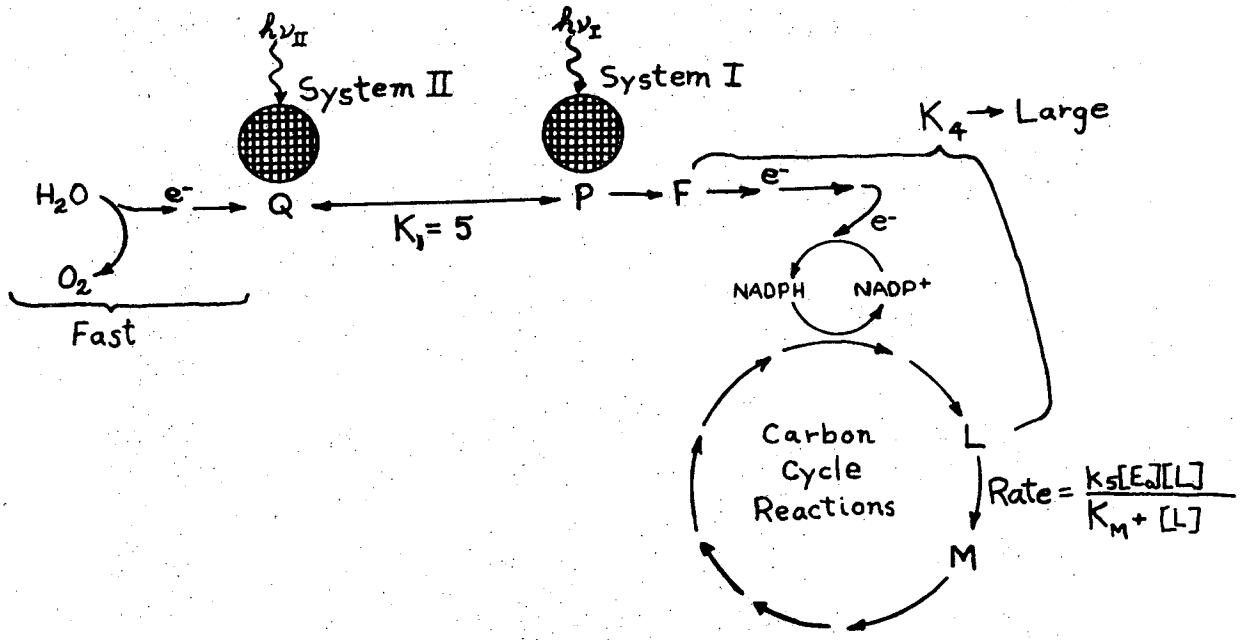

XBL 709-6496

Fig. 39. A model for the light response curve of photosynthesis that assumes NADPH control of the photoelectron transport system. This case is discussed in Appendix II.

$$K_1 = \frac{[Q][P^-]}{[Q^-][P]} = \frac{qp}{(1-q)(1-p)} . \qquad (A-5)$$

$$K_4 = \frac{[F][L]}{[F^-]} . \qquad (A-6)$$

The variables are defined as they were in Chapter VI. Use will also be made of the material balance, $[F] + [F^-] = [F_0]$. Substituting Equation (A-6) into Equation (A-4) and solving for $[F]$:

$$[F] = [F_0] \frac{\frac{K_4}{K_M}\left(\beta k_5 [E_0] - \psi_2 \frac{2q}{1+q}\right)}{\frac{K_4}{K_M}\left(\beta k_5 [E_0] - \psi_2 \frac{2q}{1+q}\right) + \psi_2 \frac{2q}{1+q}} . \qquad (A-7)$$

Since the value of K_4/K_M approaches infinity, $[F] = 0$ when $\beta k_5 [E_0] = \frac{2q}{1+q}$ (above light saturation), and $[F] = [F_0]$ when $\beta k_5 [E_0] > \frac{2q}{1+q}$ (below light saturation).

Below Light Saturation, $[F] = [F_0]$

Because K_4/K_M is assumed to be very large, $[F] = [F_0]$. F can always accept electrons from P^- that trap quanta of light. Hence there are no inefficiencies in electron transfer from P^- to F. As in Chapter VI, we will assume $\psi_1 = \psi_2 = \psi$. Substituting Equation (A-5) into Equation (A-3) and solving for q:

$$q = \frac{1 - \sqrt{2/K_1}}{1 - 2/K_1} . \qquad (A-8)$$

The rate of electron transport, R_{ET}, is:

$$R_{ET} = \psi \frac{2q}{1+q} . \qquad (A-9)$$

$$R_{ET} = \psi \frac{2 - 2\sqrt{2/K_1}}{2 - 2/K_1 - \sqrt{2/K_1}} . \qquad (A-10)$$

Before discussing these results, the case of light saturation will be treated mathematically.

Above Light Saturation, [F] = 0

When the rate of electron transport, $\psi \frac{2q}{1+q}$, becomes equal to the maximum rate of the bottleneck step, $\beta k_5[E_0]$, [F] suddenly changes its value from $[F_0]$ to 0. This can be seen from Equation (A-7). The physical reason is that reduced species back up behind L causing F to be entirely converted to F^-.

In reality, we would not expect F^- to accumulate. Instead, we would expect species such as F^-, since they have very negative midpoint redox potentials, to start donating their electrons to molecular O_2. But the result is exactly the same; the net rate of electron transport cannot exceed $\beta k_5 [E_0]$. Thus, at light saturation:

$$R_{ET} = S'_A \qquad (A-13)$$

where $S'_A = \beta k_5[E_0]$ and is the light saturated rate of electron transport.

Discussion

Equation (A-10) says that the rate of electron transport, R_{ET}, varies directly with light intensity, I. This first-order behavior continues up until light saturation is reached, at which point Equation (A-13) governs. This behavior is of course dependent upon K_4/K_M approaching infinity; the smaller K_4/K_M is, the smoother is the transition between first-order and zero-order behavior.

Equation (6-15) gives the rate of electron transport below light saturation for the case of ATP control of the rate of photosynthetic electron transport. In contrast with Equation (A-10),

Equation (6-15) does not predict first-order behavior below light saturation, but instead predicts curvature, starting from zero intensity all the way up to light saturation. The experimental data given in Fig. 4, 14, and 17 seem to indicate some curvature at lower light intensities, but the data do not allow a clear preference for one model over the other.

Appendix III

THE RATE OF PHOTOCHEMICAL TRAPPING AS A FUNCTION OF THE CONCENTRATION OF PRIMARY PHOTOCHEMICAL TRAPS

The following model was developed by Joliot et al. (1966) and is a particular case of a more general model developed by Clayton (1967). The following assumptions are made.

1. Pigment units are separate, each with a single photochemical trap along with its share of harvesting pigment. For a given photosystem all such units are identical.
2. A quantum absorbed by a unit may undergo three possible fates: it may be trapped, it may be dissipated as heat or fluorescence, or its excitation energy may be transferred to another unit. It is assumed that all three of these competitive processes are first-order with respect to concentration of excitation quanta and may be described by the rate constants, k_{trap}, k_{diss}, and k_{trans}, respectively.
3. A quantum absorbed in a unit with an open trap is caught by that trap with 100 per cent efficiency. This assumption of perfect trapping is tantamount to the assumption that k_{trap} is much larger than k_{diss} or k_{trans}. If a quantum is absorbed by a unit with a closed trap, this quantum has a chance of being transferred to another unit; consecutive search of units continue until it has been trapped or dissipated. A closed trap is defined as one that has undergone chemical change by virtue of a recently absorbed quantum, rendering it incapable of absorbing another quantum until it has been regenerated to its open form.

In Fig. 40 an incoming quantum of light is absorbed by a unit in a region where a fraction, f, of the traps are open. The probability of the quantum being trapped in this unit is equal to the probability of that trap being open, f, since trapping is assumed perfect

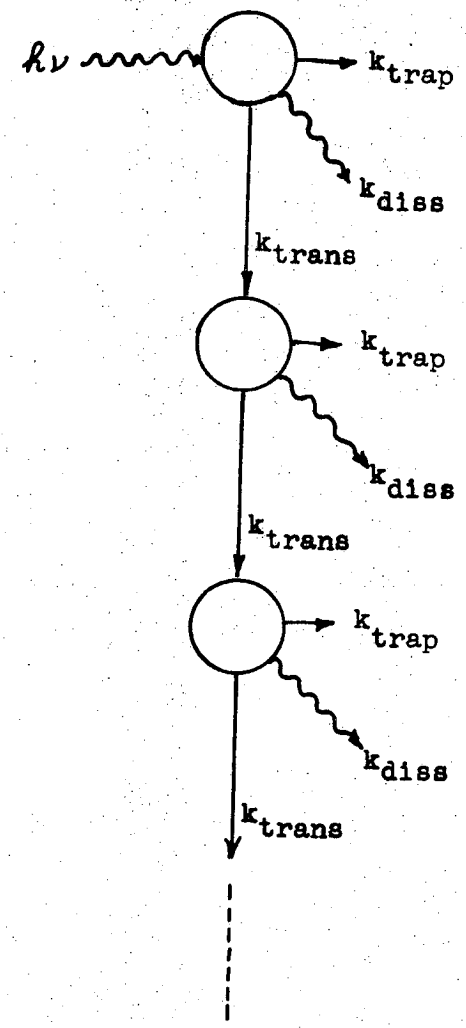

Probability of Trapping When the Average Fraction of Open Traps = f

$$f$$

$$f\left\{(1 - f)\frac{k_{trans}}{k_{trans} + k_{diss}}\right\}$$

$$f\left\{(1 - f)^2\left(\frac{k_{trans}}{k_{trans} + k_{diss}}\right)^2\right\}$$

XBL 709-6495

Fig. 40. The probability a quantum harvested by the top pigment aggregate has of being trapped by any given pigment aggregate. This system is discussed in Appendix III.

for units with open traps. The probability of the excitation energy being transferred to another unit is equal to the probability that the first unit is closed times the probability of the quantum being transferred rather than dissipated: $(1 - f)\,k_{trans}/(k_{trans} + k_{diss})$. In order to determine the probability of this transferred quantum being harvested by this second unit, the above term must be multiplied by f. Figure 40 shows the probability of trapping by each unit along the path of a migrating quantum. All of these terms must be added together to obtain the total probability of the quantum being trapped, P_{trap}:

$$P_{trap} = f\left\{1 + (1 - f)\frac{k_{trans}}{k_{trans}+k_{diss}} + (1 - f)^2\left(\frac{k_{trans}}{k_{trans}+k_{diss}}\right)^2 + \cdots\right\}. \qquad (A\text{-}14)$$

The above infinite series may be re-expressed:

$$P_{trap} = f\left\{\frac{1}{1 - \frac{k_{trans}}{k_{trans}+k_{diss}}(1 - f)}\right\}. \qquad (A\text{-}15)$$

Let $a = k_{trans}/(k_{trans} + k_{diss})$, the probability of transfer between units. Joliot's equation (Joliot et al., 1966) results:

$$P_{trap} = \frac{f}{1 - a(1 - f)}. \qquad (A\text{-}16)$$

Joliot's equation may be modified to give the rate of trapping:

$$\text{Rate of trapping} = \frac{\psi f}{1 - a(1 - f)} \qquad (A\text{-}17)$$

where ψ is equal to the light absorbed times the quantum efficiency when all traps are open.

Appendix IV

EXPERIMENTAL PROCEDURES

A. DRY WEIGHT DETERMINATION

1. Pipette 10 ml samples of recently resuspended algae into 10 ml centrifuge tubes of known weight.
2. Centrifuge cells at 5000 g (at 0-3° C) for 10 minutes, decant liquid, and resuspend the cells in distilled water using a small metal spatula (make sure to lose no cells). Centrifuge once again.
3. Decant water from the centrifuge tubes and place them in a 90° C oven for 18-22 hours.
4. After drying, place the centrifuge tubes in a $CaCl_2$ dessicator for about 1 hour. After removing the tubes from the dessicator they must receive a minimum of handling; they must not be rubbed, static electricity will cause the weighings to be wrong. The scale zero should be checked each time.

B. CHLOROPHYLL ASSAY

1. Follow steps 1 and 2 of the dry weight determination (preceding page). All subsequent steps in this analysis must be carried out in very subdued light.
2. After decanting the water, add about 5 ml of methyl alcohol to each of the centrifuge tubes and resuspend the cells with a small metal spatula, spinning the spatula until no cells are stuck to it.
3. Pour each cell suspension into a 50 ml beaker, making sure to wash the centrifuge tube and spatula several times, thus insuring transfer of all cells to the beaker. Each beaker should end up with about 15 ml of cell - MeOH solution.
4. Place the beaker on a hot plate (in a hood) at a temperature just sufficient to cause the MeOH solution to boil. Do not let

the beakers evaporate to dryness on the hot plate. Remove the beaker from the hot plate while there is still a small amount of liquid in it, and let it evaporate to dryness at room temperature.

5. When all beakers are dry, resuspend the dried material in an 80:20 (v:v) acetone-water mixture with the aid of a metal spatula. Pour this liquid carefully into a graduate cylinder. Rinse the beaker and spatula several times with the acetone-water mixture, making sure that all extracted cellular material is transferred into the graduate cylinder. Add more acetone-water mixture to the graduate cylinder until a dilution is reached sufficient to give an absorbance of 0.5 - 0.8 at 663 nm with a 1.0 cm path length cuvette.
6. Let the cellular remains equilibrate with the acetone-water mixture for at least 15 minutes.
7. Centrifuge a sample of this mixture at 5000 g for 10 minutes. Place the supernatant in a 1.0 cm path length cuvette and read the absorbance at 645 nm and 663 nm, using as a blank the acetone-water solvent. The following equations for the concentrations of chlorophyll a and chlorophyll b are due to Arnon (1949) and use the extinction coefficients of MacKinney (1941).

$$C_T = 20.2 \quad D_{645} + \quad 8.02 \; D_{663} \qquad \text{(A-18)}$$

$$C_A = -2.69 \; D_{645} + 12.7 \; D_{663} \qquad \text{(A-19)}$$

$$C_B = 22.9 \quad D_{645} - \quad 4.68 \; D_{663} \qquad \text{(A-20)}$$

where C is the concentration of chlorophyll in the acetone-water solvent (mg/l) (the subscripts T, A. B stand for total chlorophyll, chlorophyll a, and chlorophyll b, respectively), D_{645} is the absorbance at 645 nm, and D_{663} is the absorbance at 663 nm.

8. The chlorophyll a/chlorophyll b ratio is equal to C_A / C_B.

9. The weight per cent total chlorophyll may be determined by the equation:

$$\text{wt.\% Chl}_T = \frac{C_T \times \text{D. F.}}{\text{D. W.} \times 10} \qquad \text{(A-21)}$$

where D. F. is the dilution factor, the ratio of the volume of acetone-water solvent to the volume of cell suspension originally used; D. W. is the concentration of the original cell suspension (grams dry weight/l).

C. RESPIROMETER TECHNIQUES

The respirometer used was a Gilson GP-14 Photosynthesis Model. This instrument is a constant pressure device, as opposed to the Warburg-type constant volume respirometer. The advantage of the constant pressure respirometer is that no correction need be made for the gas (in this case oxygen) dissolved in the liquid phase, since the quantity of this dissolved gas does not change with time after initial induction effects.

In all cases two 50 watt tungsten filament reflector flood lamps were used to illuminate the number 8 and 12 position flasks in the respirometer. These two lamps (and the respirometer flasks that they illuminated) were not in adjacent positions, but were separated by one intervening unused position. The flasks were separated in this manner so that essentially all of the light reaching a flask would be from its own lamp.

Changes in light intensity were made by interposing stainless steel wire mesh screens between the lamps and the respirometer flasks. Calibration of light transmitted by these screens was carried out *in situ*. In some runs a copper sulfate solution (0.043 M, path length 2.8 cm) was placed between the lamps and the respirometer flasks. This gave a spectrum virtually identical to the spectrum of incident illumination under which the algae were grown (see Figs. 6 and 13). In other runs the copper sulfate solution was not used, in order to achieve higher light intensities. The saturated

rates of photosynthesis were found to be identical for both types of illumination. Indeed, no differences in curve shapes could be distinguished, when the initial slopes of the light response curve of photosynthesis were matched up. This conversion factor, to convert unfiltered light intensities to the equivalent light intensities for copper sulfate filtered light (both types of light with the same set of screens), was found experimentally to be 1.95.

Photosynthetic Rate with Carbonate-Bicarbonate Buffer

The carbonate-bicarbonate buffer system consisted of 0.19 M $KHCO_3$ and 0.01 M Na_2CO_3 dissolved in distilled water. This system gives a pH of about 9.0. The advantage of this system is that the carbon dioxide concentration in the gas phase (and also in the liquid phase) remains fairly constant. However, the carbon dioxide concentration in the gas phase changes with time, necessitating a small correction. How this correction is made will be shown later in this section. First, the experimental procedure will be given.

1. Freshly collected cells are kept chilled (0 - 3° C) and in subdued light during the following steps.
2. Centrifuge 10 ml of cell suspension at 5000 g for 10 minutes, decant the supernatant, and resuspend the cells in chilled carbonate-bicarbonate buffer using a small metal spatula (make sure to lose no cells).
3. Centrifuge the above cell suspension and repeat the rinsing with chilled buffer once again (as given in the above step 2).
4. Centrifuge the cell suspension for a third time. Decant the supernatant, and resuspend the cells in sufficient chilled carbonate-bicarbonate buffer to give 13.33 γ of total chlorophyll per ml.
5. Pipette 3 ml of this algal suspension into a clean dry respirometer flask (Gilson GME-140 with 9.6 cm^2 of illuminated area). Also prepare a control flask with 3 ml of plain carbonate-bicarbonate buffer.

6. Place the respirometer flasks in the respirometer, which has been allowed to equilibrate to its operating temperature. Let the flasks equilibrate for one hour, agitating at 160 rpm, before taking any readings.
7. The atmospheric pressure is noted before the readings. Respirometer readings are taken over a 20 minute interval for each intensity. Allow 5 minutes after switching light intensities to ensure a steady state rate of oxygen evolution is reached. In general, light intensities are run from low to high to prevent problems of solarization (impairment of the photosynthetic apparatus by high light intensities). Readings are corrected for changes in the control flask.

As previously mentioned, there is some change in the concentration of carbon dioxide in the gas phase as carbon dioxide is consumed by the photosynthesizing algae. No buffer has an infinite buffering capacity. Initially, the carbon dioxide concentration in the gas phase is about 0.90% at 25° C, but after 500 µl of oxygen have evolved it has dropped to about 0.52%. This effect causes the measured oxygen evolution to be less than the actual oxygen evolution.

The manner of making this correction will now be described. The initial concentration of carbonate and bicarbonate ions are known. Carbon dioxide in the liquid and in the gas phases, as well as H_2CO_3 in the liquid phase, are formed from the stoichiometric relation: $2HCO_3^- \rightarrow CO_3^{--} + H_2CO_3$. Knowing the volume of the liquid phase, the volume of the gas phase, the dissociation constants for H_2CO_3 and HCO_3^- (the values used were from McInnes and Belcher (1933)), and the Henry's law constant for carbon dioxide, material balances may be set up. These may be solved giving the carbon dioxide concentration in the gas phase as a function of the amount of the carbon dioxide consumed by the algae in photosynthesis. It is also assumed that one mole of oxygen is evolved for each mole of carbon dioxide consumed. The resultant graphs, which show the corrections to be added to the measured amounts of oxygen evolved, are shown in Fig. 41 for both 25° C and 10° C.

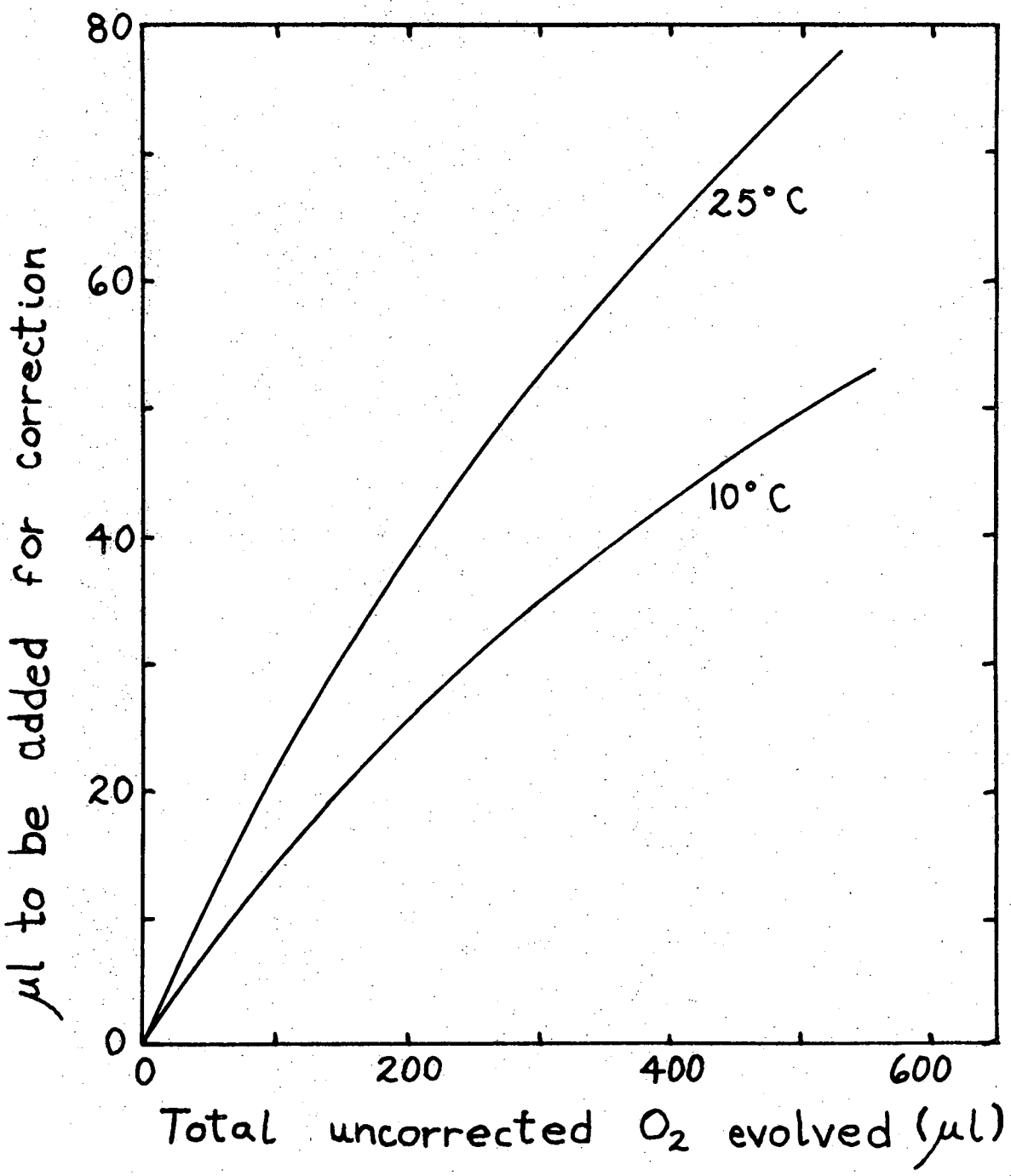

XBL 709-6507

Fig. 41. Gas phase correction for the carbonate-bicarbonate buffer system used in the respirometer. This correction is to be added to the measured quantity of evolved oxygen.

After adding the above corrections for gas phase contraction, the amount of gas evolved under the conditions of the experiment must be corrected to standard temperature and pressure. The manometer correction is:

$$\text{Manom. Corr.} = \frac{(P_T - P_{H_2O} - \delta)(273)}{(760)(T)} \qquad \text{(A-22)}$$

where P_T is the barometric pressure (mm Hg), P_{H_2O} is the vapor pressure of water at the temperature of the experiment (mm Hg), T is the temperature of the experiment (°K), and δ is a correction to account for the thermal expansion of mercury in the barometer (3 mm Hg if the barometer is at room temperature).

In plotting the light response curves, the dark respiration rates were added to the net rates of photosynthesis measured by the above procedure.

Dark Respiration Rate with Phosphate Buffer

Chilled phosphate buffer (0.035 M, pH = 7.4) was used to suspend a quantity of Chlorella cells that had previously been rinsed twice with this buffer (steps 1 - 3 of the previous procedure were used, but with substitution of the phosphate buffer for the carbonate-bicarbonate buffer). The cell concentration was several times higher than that used for determining photosynthetic rates, since dark respiration rates are small in Chlorella.

Three ml of this cell suspension were placed in a respirometer flask. The flask also contained 0.2 ml of 20% KOH along with a filter paper wick in its center well. The KOH consumes carbon dioxide as it is evolved by respiration. The manometer correction is given by Equation (A-22).

Respiration rates were also determined with the carbonate-bicarbonate buffer system. Dark respiration rates were measured in the same flasks used to determine photosynthetic rates, and these rates were determined prior to any illumination of the flasks.

Respiration rates determined with the carbonate-bicarbonate buffer were similar to the rates determined with the phosphate buffer.

Quinone Hill Reaction

The quinone Hill reaction in whole cell algae relies on the ability of para-bensoquinone to penetrate cell membranes. This reaction, like all Hill reactions, uses the photosynthetic electron transport system (at least System II) and results in the transport of electrons from water to the electron acceptor. In this case the electrons convert quinone to hydroquinone:

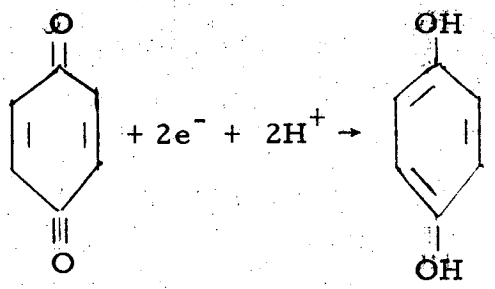

The ability of quinone to penetrate the cell membrane, an ability not possessed by other Hill oxidants such as potassium ferrocyanide, stems from the fact that it carries no net charge. Ionic molecules are generally excluded by cell membranes. The quinone Hill reaction in whole cell algae was discovered by Clendenning and Ehrmantraut (1950) and was further investigated by Ehrmantraut and Rabinowitch (1952). The following is based on the procedure given in the above references, but is modified in several important respects. The most important of these modifications is the additional inclusion of NH_4Cl, mannitol, and serum albumin to the reaction mix. These additions were all found to have a beneficial effect on the rate of oxygen evolution.

Reagents. 0.05 M potassium phosphate buffer (pH = 6.5), 20% KOH, bovine serum albumin (Calbiochem, grade A), mannitol, parabenzoquinone (Eastman Chemicals), and 0.3 M NH_4Cl.

The experimental procedure takes two days. The first day's activities follow. As usual the cells are kept in subdued light and only chilled solutions (0-3° C) are used in suspending the algae.

1. Centrifuge 10 ml of fresh cell suspension at 5000 g (at 0-3° C) minutes, decant supernatant, and resuspend the cells in chilled phosphate buffer (0.05 M, pH = 6.5) using a small metal spatula (make sure to rinse spatula with buffer).
2. Centrifuge the above cell suspension and repeat the rinsing with chilled buffer once again (as given in the above step 1).
3. Centrifuge the cell suspension for a third time. Store the cells in the centrifuge tube at 0° C and in the darkness until the next day (18-24 hours).

On the following day observe the following procedure, making sure the cells are kept in very subdued light and at 0-3° C.

1. Place about 100 mg of quinone in the bottom of a large test tube, insert a cold finger, and gently heat the test tube over a bunsen burner until sufficient quinone sublimes on the cold finger (30 mg or so). This resublimed quinone must be kept in very subdued light.
2. Dissolve 24 mg of the resublimed quinone in 20 ml of the chilled phosphate buffer (1.2 mg/ml). Keep this solution at 0° C.
3. Weigh out sufficient mannitol and bovine serum albumin to give a solution of the following composition when these are dissolved in chilled phosphate buffer: 0.3 M mannitol, 0.33 wt. % serum albumin, and 0.05 M phosphate buffer (pH = 6.5). Keep at 0°C.
4. Decant the supernatant from the cells centrifuged the previous day and suspend them in sufficient of the above mannitol-albumin-phosphate solution to give 22.2 γ of total chlorophyll per ml.
5. Place filter paper wicks into the center wells of two respirometer flasks. Place 0.2 ml of 20% KOH on the wicks. Place 0.2 ml of 0.3 M NH_4Cl in one sidearm of each flask. Chill the flasks in the refrigerator if the experiment is to be run at 10° C.
6. Add 1.0 ml of the chilled quinone-phosphate solution to the remaining sidearm of each flask. Add 1.8 ml of the chilled cell

suspension to the main compartment of one flask, and 1.8 ml of the same solution without any cells to the other flask, which will be used as a control.

7. Place the flasks in the respirometer and let them equilibrate for 10 minutes (15 minutes if at 10° C) before tipping the sidearms. After the sidearms are tipped, the reaction mix should contain 1.2 mg quinone, 40 μg of total chlorophyll, 0.54 mM mannitol, 0.14 mM phosphate, 6 mg serum albumin, and 0.06 mM NH_4Cl in a total of 3 ml.

8. After the sidearms are tipped, take readings at 5 minutes intervals over a period of 10 minutes (15 minutes if at 10° C) before turning on the illumination of the desired intensity.

9. Take readings on the flasks at two minute intervals for a period of at least 20 minutes after the illuminating lights are turned on.

Appendix V

CALCULATION OF QUINONE HILL REACTION INITIAL RATES

The rate of O_2 evolution, as measured in a respirometer, for the quinone Hill reaction is a function of time as well as light intensity. The rate of O_2 evolution decreases with time.* The rate of this decrease is a function of light intensity; at higher intensities the rate of decrease is more rapid.

Another factor also complicates raw data: the liquid and vapor phases are not at equilibrium with respect to O_2 concentration. In spite of shaking the respirometer flasks, a considerable mass transfer resistance exists between the liquid phase, where O_2 is evolved, and the vapor phase, where the evolved O_2 is measured.

Figure 42 shows a typical quinone Hill reaction run, where the accumulated amount of O_2 evolved is plotted as a function of time. Figure 43 shows the same data, but instead is plotted to show the differential rate of O_2 evolution. The data points plotted are the differences between the data points shown in Fig. 43.

The first data point shown plotted in Fig. 43 is low because a transient is caused by the high mass transfer resistance. But a steady state rate of O_2 evolution is never reached; at times greater than 4 minutes the rate of oxygen evolution declines. This decline in rate appears to be first-order with respect to remaining activity. First-order behavior would result in a straight line in Fig. 43, which is a semi-logarithmic plot. The initial (maximum) rate of O_2 evolution may be found simply by extrapolating the data back to origin. We did not use this technique, however, since the scattering of the data and the initial transient make hand-fitting the data difficult. Instead we fit the data by a non-linear least squares

*The back reaction, hydroquinone + O_2 → quinone, did not appear to be an important factor in the decrease of O_2 evolution rate with time. After the quinone Hill reaction had proceeded for some time, turning off the illumination resulted in little O_2 uptake.

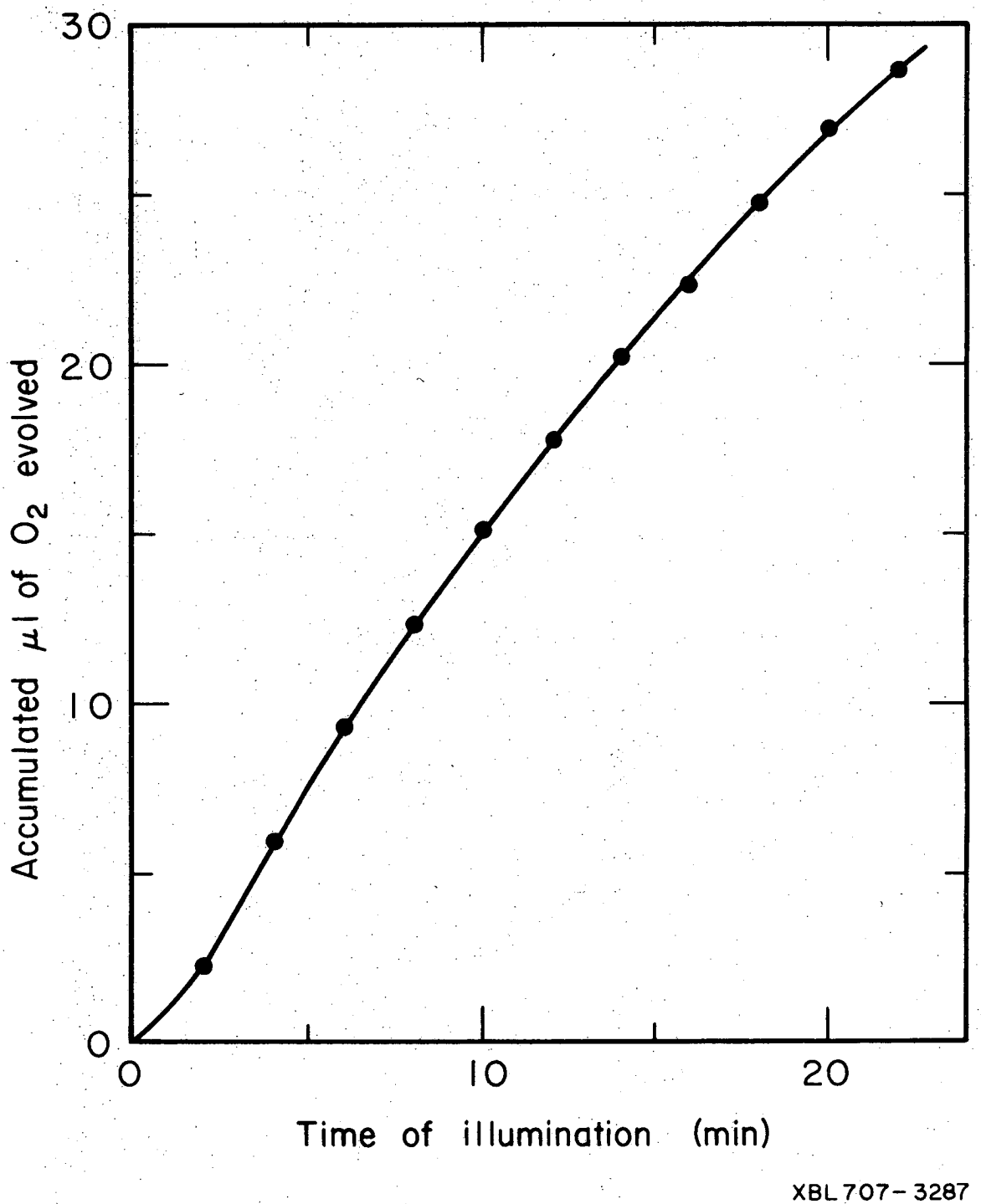

Fig. 42. Accumulative amount of oxygen evolved (uncorrected) as a function of time for a typical quinone Hill reaction respirometer run, Run D-43.

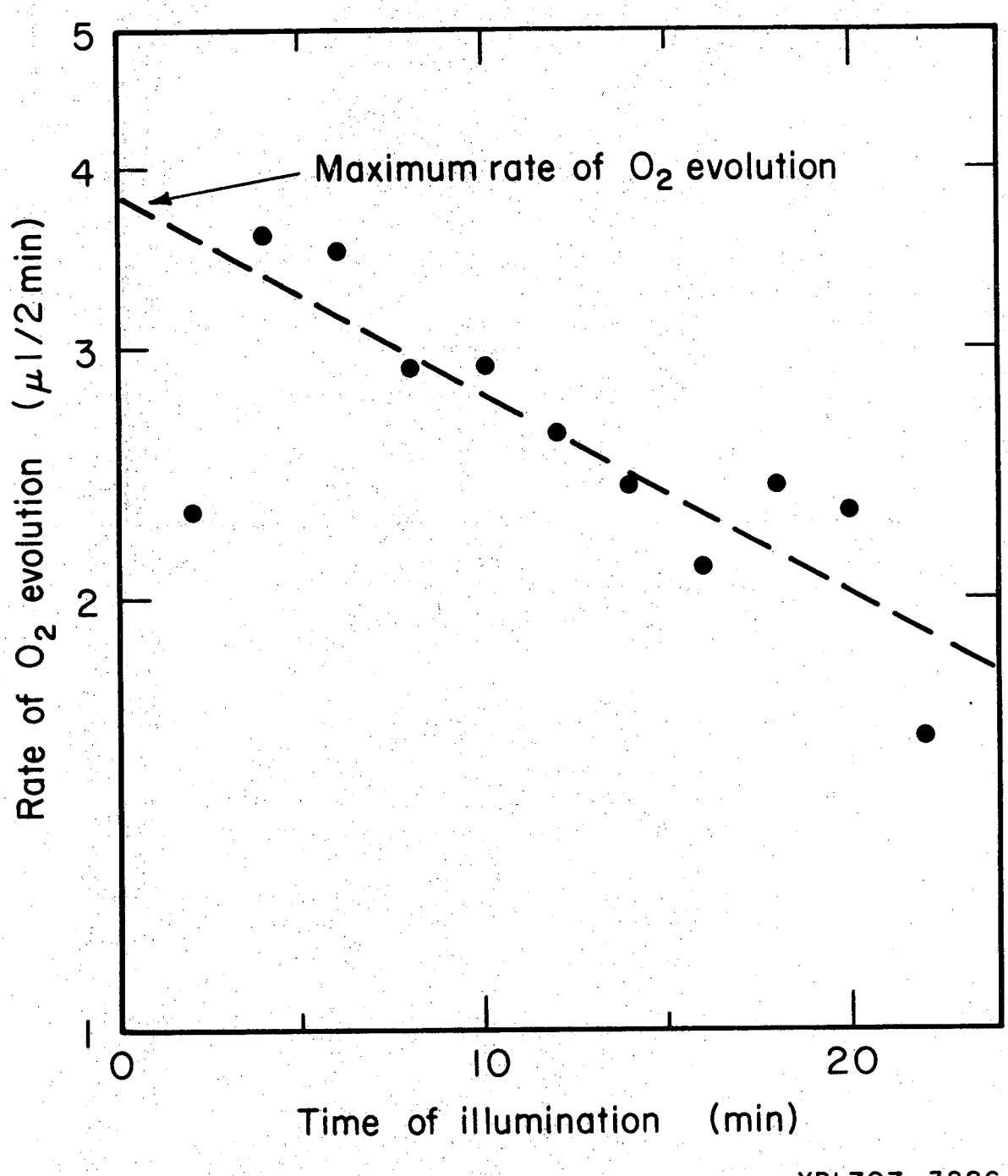

XBL707-3286

Fig. 43. The rate of oxygen evolution for the quinone Hill reaction as a function of time. These data points were obtained by taking differences between the data points shown in Fig. 42. After an initial transient caused by the mass transfer resistance between the liquid and gas phase of the respirometer flask, the typical first-order decay in oxygen evolution rate can be seen.

computer technique.

The following equation is from Briggs (1959):

$$\frac{dg}{dt} = \frac{k_L a}{v_L}\left(\rho - g\left\{\frac{v_G + \sigma v_L}{v_G}\right\}\right), \qquad \text{(A-23)}$$

where

g = rate of appearance of the evolved gas in the gas phase (μl/min)

ρ = rate of production of gas in the liquid phase (μl/min)

$k_L a$ = mass transfer coefficient between the liquid and gas phases (ml/min)

v_L = volume of liquid phase (ml)

v_G = volume of gas phase (ml)

σ = Henry's law constant, defined to be the concentration in the liquid phase divided by the concentration in the gas phase.

Since the rate of production of gas appears to decay in a first-order manner with respect to remaining photosynthetic activity:

$$\rho = Ae^{-kt} \qquad \text{(A-24)}$$

where

A = the initial rate of O_2 evolution (μl/min)

k = Parameter that describes the first-order decrease in activity (min^{-1})

It is the determination of A, the initial quinone Hill reaction rate, that is our objective.

By substituting Equation (A-24) into Equation (A-23) and integrating with respect to time, the following equation is obtained:

$$g = \frac{DA}{DB - k}(e^{-kt} - e^{-DBt}) \qquad \text{(A-25)}$$

where

D = $k_L a/v_L$ (1/min)

B = $(v_G + \sigma v_L)/v_G$ (very close to 1.00 in our case).

In obtaining Equation (A-25) use was made of the initial condition, at $t = 0$, $g = 0$.

The above equation could be used to fit rate data such as shown in Fig. 43. But we will carry the integration one step further so that accumulative data of the type shown on Fig. 42 can be described. Integrating Equation (A-25) yields:

$$y = \frac{DA}{DB-k}\left(\frac{1}{k}\left\{1 - e^{-kt}\right\} - \frac{1}{DB}\left\{1 - e^{-DBt}\right\}\right), \qquad \text{(A-26)}$$

where

y = the accumulative amount of O_2 evolved; note that $g = dy/dt$ (μl).

Equation (A-26) was obtained by making use of the second initial condition, at $t = 0$, $g = 0$.

Equation (A-26) was used to fit all quinone Hill reaction respirometer runs. Use was made of LSQVMT, a Lawrence Radiation Laboratory Computer Library program that may be used to fit nonlinear equations by a least squares procedure.

Appendix VI

PROGRAM ALGAE: PREDICTING THE PERFORMANCE OF OPTICALLY DENSE CULTURES OF ALGAE

```
      PROGRAM ALGA (INPUT,OUTPUT)

C EPSCAT = 10.

      REAL MU, INCINT, LAMDA, MUINC, MUCALC, INTTOT, MICWAT, MICTOT,
     1INTATS
      INTEGER SSTEP, QSTEP
      DIMENSION EPS(37), INCINT(37), LAMDA(37), CHAR(12), ZMU(300),
     1C(300), B(300), U(300), SA(300),ZX(300),ZP(300), ZS(1000), ZRPS(10
     200), ZRPSTT(300), ZMUCLC(300), MICWAT(37), TRANS(300)

      READ 50, (CHAR(I), I = 1,12)
   50 FORMAT (12A6)
      PRINT 60, (CHAR(I), I = 1,12)
   60 FORMAT (1H1, 12A6)

      READ 100, (EPS(L), INCINT(L), L = 1,35)
  100 FORMAT (2E10.0)
      DO 150 L = 1,35
      LAMDA(L) = 10.*(L + 37)
      MICWAT(L) = INCINT(L)/(3.E 11*LAMDA(L))
  150 CONTINUE
      PRINT 200
  200 FORMAT (1H0, 10X, 8HLAMDA, 13X, 7HEPSILON, 17X, 18HINCIDENT INTENS
     1ITY, 6X, 15HINCIDENT ENERGY)
      PRINT 210
  210 FORMAT (12X, 2HNM, 7X, 26HCM**2/MG TOTAL CHLOROPHYLL, 3X, 24HEIN
     1STEINS/HR/CM**2/10 NM, 3X, 22HMICROWATTS/CM**2/10 NM//)
      PRINT 220, (LAMDA(L), EPS(L), INCINT(L), MICWAT(L), L = 1,35)
  220 FORMAT ( 9X, F6.0, 10X, E13.5, 16X, E13.5, 14X, E13.5)
      MICTOT = 0.
      INTTOT = 0.
      DO 250 L = 1,35
      MICTOT = MICTOT + MICWAT(L)
      INTTOT = INTTOT + INCINT(L)
  250 CONTINUE
      PRINT 260, INTTOT
  260 FORMAT (1H0, 39HTHE TOTAL INCIDENT INTENSITY, INTTOT, =, E13.5,
     119H EINSTEINS/HR/CM**2)
      PRINT 270, MICTOT
  270 FORMAT (1H0, 36HTHE TOTAL INCIDENT ENERGY, MICTOT, =, E13.5,
     117H MICROWATTS/CM**2)

      READ 300, BS, V, PHI, SM
  300 FORMAT (4E10.0)
      PRINT 400, BS
  400 FORMAT (1H1, 36HTHE THICKNESS OF CULTURE UNIT, BS, =, F8.2, 3H CM)
      PRINT 410, V
  410 FORMAT (1H0, 32HTHE VOLUME OF CULTURE UNIT, V, =, F8.2, 6H CM**3)
      AREA = V/BS
      PRINT 420, AREA
  420 FORMAT (1H0, 33HTHE AREA OF CULTURE UNIT, AREA, =, F8.2, 6H CM**2)
      PRINT 430, PHI
  430 FORMAT (1H0, 33HTHE MAXIMUM QUANTUM YIELD, PHI, =, F8.5, 16H O(2)
     1PER QUANTA)
      PRINT 440, SM
  440 FORMAT (1H0, 71HTHE MAXIMUM RATE OF THE UNCOUPLED PHOTOELECTRON TR
     1ANSPORT SYSTEM, SM, =, F8.6, 35H MOLES O(2)/HR/MG TOTAL CHLOROPHYL
```

```
     2L)
      READ 500, MUINC, MUSTEP
  500 FORMAT (F10.0, I10)
      PRINT 510, MUINC, MUSTEP
  510 FORMAT (1H0, 23HMU INCREMENTS, MUINC, =, F8.3, 47H 1/DAY AND THE N
     1UMBER OF STEPS OF MU, MUSTEP, =, I4)
      READ 600, SSTEP
  600 FORMAT (I10)
      SINC = BS/SSTEP
      PRINT 610, SINC, SSTEP
  610 FORMAT (1H0, 21HS INCREMENTS, SINC, =, F8.5, 42H CM AND THE NUMBER
     1 OF STEPS OF S, SSTEP, =, I4)

C START OF MU (OUTERMOST) DO LOOP
      MU = 0.0
      DO 2000 M = 1,MUSTEP
      MU = MU + MUINC
C ZMU(M) NEEDED FOR PRINTING
      ZMU(M) = MU
C C(M) = MG TOTAL CHLOROPHYLL/MG DRY WT
      C(M) = 0.0261*MU + 0.0743
C B(M) = MG DRY WT/MOLE O(2)
      B(M) = 1.44E4 + 0.0654*MU
C U(M) = RESP RATE, MOLES O(2)/HR/MG DRY WT
      U(M) = 7.81E-8 + 2.18E-7*MU
C SA(M) = MOLES O(2)/HR/MG TOTAL CHLOROPHYLL
      SA(M) = 1.174E-4 + 1.334E-4*MU
      X = 2.8/(MU*BS)

C START OF S (MIDDLE) DO LOOP
      QSTEP = SSTEP + 1
      ICOUNT = 0
  900 S = -SINC
      ICOUNT = ICOUNT + 1
      DO 1100 K = 1,QSTEP
      S = S + SINC
C ZS(K) NEEDED FOR INDEXING
      ZS(K) = S

C START OF L (INNERMOST) DO LOOP FOR LIGHT ABSORPTION AT S
      ABSS = 0.
      INTATS = 0.
      DO 1000 L = 1,35
      ABSS = 2.303*INCINT(L)*(EPS(L) + 10.)*EXP(-2.303*X*S*(EPS(L) +
     110.)*C(M)) + ABSS
      INTATS = EXP(-2.303*X*S*(EPS(L) + 10.)*C(M))*INCINT(L) + INTATS
 1000 CONTINUE

C CALCULATION OF PHOTOSYNTHETIC RATE AT S, RPS
      ZA = SQRT(ABS(2.*PHI*ABSS*SM + (PHI*ABSS)**2))
      ZB = 2.*SM + PHI*ABSS + ZA
      RPS = 2.*PHI*ABSS*SM/ZB
      IF (RPS .GT. SA(M)) RPS = SA(M)
C ZRPS(K) NEEDED FOR INDEXING
      ZRPS(K) = RPS
 1100 CONTINUE

C START OF THE CUTE LITTLE ITSY-BITSY RPSTOT DO LOOP
```

```
      RPSTOT = 0.5*(ZRPS(1) + ZRPS(QSTEP))/SSTEP
      DO 1200 K = 2,SSTEP
      RPSTOT = RPSTOT +ZRPS(K)/SSTEP
 1200 CONTINUE
      MUCALC = 24.*(RPSTOT*C(M)*B(M) - U(M)*B(M))
      IF (ABS(MUCALC - MU) .LE. 1.E-3) GO TO 1900
      X = ABS(X*MUCALC/MU)
      IF (X .LE. 1.E-2) GO TO 1900
      IF (X .GE. 1.E+2) GO TO 1900
      IF (ICOUNT .GE. 200) GO TO 1800
      GO TO 900
 1800 X = 0.
 1900 ZX(M) = X
      ZP(M) = X*MU*BS
      TRANS(M) = 100.*INTATS/INTTOT
      ZRPSTT(M) = RPSTOT
      ZMUCLC(M) = MUCALC
 2000 CONTINUE

      PRINT 2100
 2100 FORMAT (1H1, 8X, 3HZMU, 13X, 1HC, 15X, 1HB, 15X, 1HU, 15X, 2HSA,
     117X, 2HZX, 15X, 2HZP)
      PRINT 2110
 2110 FORMAT (4X, 12HSPEC GR RATE, 4X, 12HFRACT CHL(T), 4X, 12HCONVERS F
     1ACT, 5X, 11HRESPIR RATE, 5X, 11HSAT PS RATE, 7X, 12HCELL CONC DW,
     24X, 12HPRODUCTIVITY)
      PRINT 2120
 2120 FORMAT (7X, 5H1/DAY, 8X, 12HMG CHL(T)/MG, 4X, 12HMG/MOLE O(2), 3X,
     114HMOL O(2)/HR/MG, 2X, 18HMOL O(2)/HR/MG CHL, 5X, 8HMG DW/ML, 6X,
     212HMG/CM**2/DAY)
      PRINT 2130,(ZMU(M), C(M), B(M), U(M), SA(M), ZX(M), ZP(M), M = 1,M
     1USTEP)
 2130 FORMAT (1H0, 5X, F8.3, 8X, F8.6, 7X, F10.1, 5X, F12.10, 6X, F12.10
     1, 8X, F8.4, 8X, F8.4)
      PRINT 2400
 2400 FORMAT (1H1, 8X, 3HZMU, 11X, 6HZRPSTT, 10X, 6HZMUCLC, 11X, 5HTRANS
     1)
      PRINT 2410
 2410 FORMAT (4X, 12HSPEC GR RATE, 4X, 12HAVRG PS RATE, 4X, 12HCALC GR R
     1ATE, 3X, 14HPER CENT TRANS)
      PRINT 2420
 2420 FORMAT (7X, 5H1/DAY, 5X, 18HMOL O(2)/HR/MG CHL, 5X, 5H1/DAY)
      PRINT 2430, (ZMU(M), ZRPSTT(M), ZMUCLC(M), TRANS(M), M = 1,MUSTEP)
 2430 FORMAT (1H0, 5X, F8.3, 6X, F12.10, 5X, F8.5, 6X, F8.5)
 3000 CONTINUE
      END
```

DEFINITION OF VARIABLES IN PROGRAM ALGAE

ABSS	= Light absorption at S, einstein/mg chlorophyll/hr
AREA	= Illuminated area of the culture unit, cm^2
B(M)	= Factor for converting photosynthetic rate from O_2 production to cell dry weight production, mg dry wt./mole O_2
BS	= Thickness of culture vessel, cm
C(M)	= Chlorophyll content of cells, mg chlorophyll/mg dry wt.
CHAR(I)	= Storage for A-field information
EPS(L)	= Epsilon, the extinction coefficient of the photosynthetic pigments, cm^2/mg chlorophyll
I	= Indexing value for A-field storage
ICOUNT	= Number of iterations in S (middle) DO loop
INCINT(L)	= Incident intensity of light on culture vessel surface, einsteins/cm^2/hr/10 nm
INTATS	= Light intensity at S, einsteins/cm^2/hr
INTOT	= Total incident intensity of light on culture vessel surface, einsteins/cm^2/hr
K	= Indexing value for S
L	= Indexing value for LAMDA
LAMDA	= Wavelength of light, nm
M	= Indexing value for MU
MICTOT	= Total incident energy of light on culture vessel surface, microwatts/cm^2
MICWAT(L)	= Incident energy of light on culture vessel surface, microwatts/cm^2/10 nm
MU(M)	= Actual specific growth rate, 1/day
MUCALC(L)	= Calculated specific growth rate, 1/day
MUINC	= Incremental change in MU, 1/day
MUSTEP	= Number of values of MU examined

PHI = Quantum yield, moles O_2/einstein

QSTEP = SSTEP + 1

RPS = Photosynthetic rate at S, moles O_2/hr/mg chlorophyll

RPSTOT = Average photosynthetic rate in culture unit, moles O_2/hr/mg chlorophyll

S = Distance into the culture unit from the front, cm

SA(M) = The actual saturated rate of oxygen evolution, moles O_2/hr/mg chlorophyll

SINC = Incremental change in S, cm

SM = The saturated rate of oxygen evolution intrinsic to the photoelectron transport system, moles O_2/hr/mg chlorophyll

SSTEP = Number of incrments of S

TRANS(M) = Per cent transmission of light intensity through the culture unit

U(M) = Uptake of oxygen due to dark respiration, moles O_2/hr/mg dry wt.

V = Volume of culture unit, cm^3

X = Concentration of algal cells, mg dry wt./ml

ZA = Defined term in photosynthetic rate equation

ZB = Defined term in photosynthetic rate equation

ZMU(M) = A particular indexed value of MU

ZMUCLC(M) = A particular indexed value of MUCALC

ZP(M) = Productivity, mg dry wt/cm^2/day

ZRPS(K) = Photosynthetic rate at a particular value of S

ZRPSTT(M) = A particular indexed value of RPSTOT

ZS(K) = A particular indexed value of S

ZX(M) = A particular indexed value of X

REFERENCES

Aiba, S., Humphrey, A. E., and Millis, N. F. (1965) Biochemical Engineering, Academic Press, New York, p. 88.

Arnold, W. and Kohn, H. (1934) J. Gen. Physiol. 18, 109.

Arnon, D. I. (1949) Plant Physiol. 24, 1.

Arnon, D. I. (1951) Nature 167, 1008.

Arnon, D. I., Allen, M. B., and Whatley, F. R. (1954a) Nature 174, 394.

Arnon, D. I., Allen, M. B., and Whatley, F. R. (1954b) J. Am. Chem. Soc. 76, 6324.

Arnon, D. I., Whatley, F. R., and Allen, M. B. (1957) Nature 180, 182.

Arnon, D. I., Whatley, F. R., and Allen, M. B. (1959) Biochim. Biophys. Acta 32, 47.

Avron, M. and Ben-Hayyim, G. (1969) Progress in Photosynthesis Research, H. Metzner, Ed., H. Laupp, Jr. Publ., Tubingen Germany, Vol. III, p. 1185.

Bach, M. K. and Fellig, J. (1958) Nature 182, 1359.

Bassham, J. A. and Calvin, M. (1957) Path of Carbon in Photosynthesis, Prentice-Hall, Englewood Cliffs, New Jersey.

Bassham, J. A. and Krause, G. H. (1969) Biochim. Biophys. Acta 189, 207.

Belyanin, V. N. and Kovrov, B. G. (1968) Doklady Biophys. (Eng. Trans.) 178, 31.

Bjorkman, O. (1968a) Physiol. Plantarum 21, 1.

Bjorkman, O. (1968b) Physiol. Plantarum 21, 84.

Blackman, F. F. (1905) Ann. Bot., Lond. 19, 281.

Bonaventura, C. and Myers, J. (1969) Biochim. Biophys. Acta 189, 366.

Bonner, J., (1962) Science 137, 11.

Bradley, D. F. (1953) Ph. D. Thesis, University of California, Berkeley.

Brannon, M. A. and Bartsch, A. F. (1939) Am. J. Bot. 26, 271.

Briggs, G. E. (1959) Plant Physiol. 34, 222.

Brody, M. and Emerson, R. (1959) Am. J. Bot. 46, 433.

Brown, A. H. and Weis, D. (1959) Plant Physiol. 34, 224.

Burlew, J. S., Ed. (1953) Algal Culture from Laboratory to Pilot Plant, Carnegie Inst. of Wash. Publ. 600.

Cahn, M. (1970) personal communication (Ph. D. Thesis) in preparation).

Clayton, R. K. (1967) J. Theor. Biol. 14, 173.

Clement, G., Giddy, C., and Menzi, R. (1967) J. Sci. Food Agric. 18, 497.

Clendenning, K. A. and Ehrmantraut, H. C. (1950) Arch. Biochem. Biophys. 29, 387.

Conrad, H. M. and Saltman, P. (1962) In Physiology and Biochemistry of Algae, R. A. Lewin, Ed., Academic Press, New York, p. 663.

Cramer, M. and Myers, J. (1949) Plant Physiol. 24, 255.

Darwin, C. (1859) On the Origin of Species by Means of Natural Selection, or the Preservation of Favored Races in the Struggle for Life, Everyman, London, sixth edition, 1928.

Denbigh, K. G., Hicks, M., and Page, F. M. (1948) Trans. Faraday Soc. 44, 479.

Duysens, L. M. N. (1952) Ph. D. Thesis, University of Utrecht, The Netherlands.

Duysens, L. N. M., Amesz, J., and Kamp, B. M. (1961) Nature 190, 510.

Ehrmantraut, H. C. and Rabinowitch, E. (1952) Arch. Biochem. Biophys. 38, 67.

Eley, J. H. and Myers, J. (1967) Plant Physiol. 42, 598.

Emerson, R. and Arnold, W. (1931) J. Gen. Physiol. 16, 191.
Emerson, R. and Arnold, W. (1932) J. Gen. Physiol. 16, 191.
Emerson, R., Chalmers, R., and Cederstrand, C. (1957) Proc. Nat. Acad. Sci. 43, 133.
Emerson, R. and Green, C. F. (1938) Plant Physiol. 13, 157.
Emerson, R. and Lewis, C. M. (1939) Am. J. Bot. 26, 808.
Emerson, R. and Lewis, C. M. (1941) Am. J. Bot. 28, 789.
Emerson, R. and Lewis, C. M. (1943) Am. J. Bot. 30, 165.
Englemann, T. W. (1883) Bot. Zeit. 41, 1.
Englemann, T. W. (1894) Arch. Ges. Physiol. (Pfluger's) 57, 375.
Englemann, T. W. (1884) Bot. Zeit. 42, 81, 97.
Eyster, H. C. (1967) USAF School of Aerospace Medicine Publ. No. SAM-TR-67-40.

Forbush, B. and Kok, B. (1968) Biochim. Biophys. Acta 162, 243.
Fredrickson, A. G., Brown, A. H., Miller, R. L., and Tsuchiya, H. M. (1961) J. Amer. Rocket Soc. 31, 1429.

Ghosh, A. K. and Govindjee (1966) Biophys. J. 6, 611.
Golueke, C. G. and Oswald, W. J. (1965) J. Water Pollution Cont. Fed. 37, 471.

Haldane, J. B. S. (1930) Enzymes, Longmans Green, London, p. 80.
Hearon, J. F. (1952) Physiol. Rev. 32, 499.
Hill, R. (1937) Nature 139, 881.
Hill, R. (1939) Proc. Roy. Soc. London B124, 192.
Hill, R. and Bendall, F. (1960) Nature 186, 137.
Hind, G. and Jagendorf, A. T. (1963) Proc. Natl. Acad. Sci. 49, 715.
Hind, G. and Olsen, J. M. (1968) Ann. Rev. Plant Physiol. 19, 249.
Hoch, G., Owens, O. H., and Kok, B. (1963) Arch. Biochem. Biophys. 101, 171.

Izawa, S., Connally, T. N., Winget, G. D., and Good, N. E. (1966) Brookhaven Symposia in Biology 19, 169.

Joliot, A, and Joliot, P. (1964) Compt. Rend. 258, 4622.

Joliot, P. (1965a) Biochim. Biophys. Acta 102, 116.

Joliot, P. (1965b) Biochim. Biophys. Acta 102, 135.

Joliot, P. (1966) Brookhaven Symposia in Biology, 19, 418.

Joliot, P., Delosme, R., and Joliot, A. (1966) in Currents in Photosynthesis, J. B. Thomas and J. C. Goedheer, Eds., Ad. Donker: Rotterdam, p. 359.

Joliot, P., Joliot, A., and Kok, B. (1968) Biochim. Biophys. Acta 153, 635.

Jones, L. W. and Myers, J. (1964) J. Phycol. 1, 6.

Katoh, S. and Takamiya, A. (1963) Plant and Cell Physiol. 4, 335.

Kelly, J. and Sauer, K. (1965) Biochemistry 4, 2798.

Kelly, J. and Sauer, K. (1968) Biochemistry 7, 882.

Knaff, D. B. and Arnon, D. I. (1969) Proc. Nat. Acad. Sci. 64, 715.

Kok, B. (1952) Acta Botan. Neerl. 1, 446.

Kok, B. (1956) Biochim. Biophys. Acta 21, 245.

Kok, B. (1957) Acta Botan. Neerl. 6, 316.

Kok, B. (1959) Plant Physiol. 34, 184.

Kok, B. (1961) Biochim. Biophys. Acta 48, 527.

Kok, B., Joliot, P., and McGloin, M. P. (1969) Progress in Photosynthesis Research, H. Metzner, Ed., H. Laupp, jr. Publ. Tubingen, Germany, Vol. II, p. 1042.

Lumry, R., Mayne, B., and Spikes, J. D. (1959) Disc. Faraday Soc. 27, 149.

Lumry, R. and Rieske, J. S. (1959) Plant Physiol. 34, 301.

Maaloe, O. and Kjeldgaard, N. O. (1966) Control of Macromolecular Synthesis, W. A. Benjamin, Inc., New York, p. 72.

MacKinney, G. (1941) J. Biol. Chem. 140, 315.

Mahler, H. R. and Cordes, E. H. (1966) Biological Chemistry, Harper and Row, New York, Chapter 10, p. 408.

Malkin, S. (1969) Biochim. J. 9, 489.

McInnes, D. A. and Belcher, D. (1933) J. Am. Chem. Soc. 55, 2630.

Miller, R. L., Fredrickson, A. G. Brown, A. H., and Tsuchiya, H. M. (1964) Ind. Eng. Chem., Proc. Des. Devel. 3, 134.

Miller, R. L., Smith, D. W., Ward, C. H., Dyer, D. L., and Gafford, R. D. (1968) USAF School of Aerospace Medicine Publ. No. SAM-TR-68-66.

Miller, R. L. and Ward, C. H. (1966) USAF School fo Aerospace Medicine Publ. No. SAM-TR-66-11.

Miller, S. F. (1971) Ph.D. Thesis in preparation.

Monteith, J. L. (1965) Ann. Bot. Lond. N.S. 29, 17.

Muller, A., Lumry, R., and Walker, M. S. (1969) Photochem. and Photobiol. 9, 113.

Murata, N., Tashiro, H., and Takamiya, A. (1970) Biochim. Biophys. Acta 197, 250.

Myers, J. (1963) In Encyclopedia of Chemical Technology, Interscience Publishers, New York, Second Edition, Vol. I, p. 653.

Myers, J. (1964) In Life Sciences and Space Research II, M. Florlnin and A. Dollfus, Eds., North Holland Publ. Co., Amsterdam, p. 323.

Myers, J. and Graham, J. R. (1959) Plant Physiol. 34, 345.

Myers, J. and Graham, J. R. (1961) Plant Physiol. 36, 342.

Myers, J. and Graham, J. R. (1963a) Plant Physiol. 38, 1.

Myers, J. and Graham, J. R. (1963b) Plant Physiol. 38, 105.

Ng, K. S. and Bassham, J. A. (1968) Biochim. Biophys. Acta 162, 254.

Oorschot, J. L. P. van, (1955) Mededel. Landbouwhogeschool te Wageningen 55, 225.

Oswald, W. J. and Golueke, C. G. (1964) Ann. Rev. Plant Physiol. 15, 387.

Oswald, W. J. and Golueke, C. G. (1968) Personal communication.

Park, R. B. (1962) J. Chem. Ed. 39, 424.

Park, R. B. and Biggins, J. (1964) Science 144, 1009.

Park, R. B. and Pon, N. G. (1961) J. Mol. Biol. 3, 1.

Pickett, J. M. and Myers, J. (1966) Plant Physiol. 41, 90.

Pratt, R. (1937) Am. J. Bot. 25, 498.

Rabinowitch, E. (1945) Photosynthesis and Related Processes, Interscience Publishers, New York, Vol. I.

Rabinowitch, E. (1951) Photosynthesis and Related Processes, Interscience Publishers, New York, Vol. II, Part 1.

Rabinowitch, E. (1956) Photosynthesis and Related Processes, Interscience Publishers, New York, Vol. II, Part 2.

Racker, E. (1965) Mechanisms in Bioenergetics, Vol. 3, Academic Press, New York, p. 193.

Ruben, S., Randall, M., Kamen, M., and Hyde, J. L. (1941) J. Am. Chem. Soc. 63, 879.

Sachs, J. V. (1890) History of Botany, Clarendon Press, Oxford, p. 453.

Sauer, K. and Biggins, J. (1965) Biochim. Biophys. Acta 102, 55.

Schmid, G. H. and Gaffron, H. (1967) J. Gen. Physiol. 50, 563.

Schwartz, M. (1967) Biochim. Biophys. Acta 131, 559.

Shelef, G., Oswald, W. J., and Golueke, C. G. (1968) Sanit. Eng. Res. Lab., University of California, Berkeley, SERL Report No. 68-4.

Shugarman, P. M. and Appleman, D. (1967) Anal. Biochem. 18, 193.

Sinclair, J. (1969) Biochim. Biophys. Acta 189, 60.

Steemann Nielsen, E. and Jorgensen, E. G. (1968) Physiol. Plantarum 21, 401.

Tamiya, H. (1959) Proc. UNESCO Symp. Algology, New Delhi, Indian Council of Agri. Research, Kanpur.

Tamiya, H., Hase, E., Shibata, K., Mituya, A., Iwamura, T., Nihei, T., and Sasa, T. (1953a) in Algal Culture from Laboratory to Pilot Plant, J. S. Burlew, Ed., Carnegie Inst. of Wash. Publ. 600.

Tamiya, H., Iwamura, T. Shibata, K., Hase, E., and Nihei, T. (1953b) Biochim. Biophys. Acta 12, 23.

Tolmach, L. J. (1951) Nature 167, 946.

Trebst, A. V., Tsujimoto, H. Y., and Arnon, D. I. (1958) Nature 182, 351.

Treharne, K. J. and Stoddart, J. L. (1968) Nature 220, 457.

Vallentyne, J. R. (1966) in Primary Productivity in Aquatic Environments, C. R. Goldman, Ed., University of California Press, p. 309.

Van Niel, C. B. (1931) Arch. Mikrobiol. 3, 1.

Vincent, W. A. (1969) Process Biochem. June, 1969, p. 45.

Vishniac, W. and Ochoa, S. (1951) Nature 167, 768.

Vishniac, W. and Ochoa, S. (1952) J. Biol. Chem. 198, 501.

Warburg, O. (1948) Am. J. Bot. 35, 194.

Wareing, P. F., Khalifa, M. M., and Treharne, K. J. (1968) Nature 220, 453.

Weis, D. and Brown, A. H. (1959) Plant Physiol. 34, 235.

Wild, A. and Egle, K. (1968) Planta 82, 73.

Witt, H. T. (1967) Nobel Symposium No. 5, Fast Reactions and Primary Processes in Chemical Kinetics, S. Claeson, Ed., Interscience, p. 261.

Witt, H. T., Doring, G., and Rumberg, B. (1961) Nature 192, 967.

Yin, H. C. (1937) Proc. Nat. Acad. Sci. 23, 174.

Yocum, C. F. and San Pietro, A. (1969) Biochem. Biophys. Res. Commun. 36, 614.

LEGAL NOTICE

TECHNICAL INFORMATION DIVISION
LAWRENCE RADIATION LABORATORY
UNIVERSITY OF CALIFORNIA
BERKELEY, CALIFORNIA 94720